Properties of the nuclear medium

M. Baldo and G.F. Burgio

Instituto Nazionale di Fisica Nucleare,
Sez. di Catania,
Via S. Sofia 64
95123 Catania, I

E-mail: `marcello.baldo@ct.infn.it, fiorella.burgio@ct.infn.it`

Abstract. We review our knowledge on the properties of the nuclear medium that have been studied, along many years, on the basis of many-body theory, laboratory experiments and astrophysical observations. Throughout the presentation particular emphasis is put on the possible relationship and links between the nuclear medium and the structure of nuclei, including the limitations of such an approach. First we consider the realm of phenomenological laboratory data and astrophysical observations and the hints they can give on the characteristics that the nuclear medium should possess. The analysis is based on phenomenological models, that however have a strong basis on physical intuition and an impressive success. More microscopic models are also considered, and it is shown that they are able to give invaluable information on the nuclear medium, in particular on its Equation of State. The interplay between laboratory experiments and astrophysical observations are particularly stressed, and it is shown how their complementarity enriches enormously our insights into the structure of the nuclear medium. We then introduce the nucleon-nucleon interaction and the microscopic many-body theory of nuclear matter, with a critical discussion about the different approaches and their results. The Landau Fermi Liquid theory is introduced and briefly discussed, and it is shown how fruitful it can be in discussing the macroscopic and low energy properties of the nuclear medium. As illustrative example, we discuss neutron matter at very low density, and it is shown how it can be treated within the many-body theory. The general bulk properties of the nuclear medium are reviewed to indicate at which stage of our knowledge we stand, taking into account the most recent developments both in theory and experiments. A section is dedicated to the pairing problem. The connection with nuclear structure is then discussed, on the basis of the Energy Density Functional method. The possibility to link the physics of exotic nuclei and the astrophysics of neutron stars is particularly stressed. Finally we discuss the thermal properties of the nuclear medium, in particular the liquid-gas phase transition and its connection with the phenomenology on heavy ion reactions and the cooling evolution of neutron stars. The presentation has been taken for non-specialists and possibly for non-nuclear physicists.

1. Introduction

Nuclear Physics has so many facets that it looks impossible to find a common theoretical picture that is able to unify under a common view, at least to a certain extent, the whole realm of phenomena where nucleonic systems play a role. Indeed, the structure of nuclei, their excitations, nuclear collisions, the structure of Neutron Stars, Supernovae explosion, very many astrophysical phenomena and processes, are all directly connected to that area of Physics that can be called "Nuclear Physics". The possible unification can come from the fundamental theory of strong and weak interactions, Quantum Chromo Dynamics (QCD), and the so called Standard Model. However, besides the difficulty to solve QCD for multi-baryonic systems with the necessary accuracy, this would be hardly useful for the understanding on simple physical basis of the rich structure that nuclear systems display in different contexts.

From a semi-classical or macroscopic point of view, all nuclear systems can be considered as pieces of a quite particular matter, the nuclear medium. The hypothetical uncharged infinite and homogeneous system formed by the nuclear medium is usually called Nuclear Matter. Actually, as we will discuss, in first approximation, Supernovae and Neutron Stars contain macroscopic portions of nuclear matter. From this point of view, nuclei are considered as droplets of nuclear matter, and indeed this is the basis of the Liquid Drop Model of nuclei. The macroscopic view cannot of course exhaust all the numerous aspects of nuclear structure, where microscopic many-body effects are essential. It is however physically meaningful to ask for the properties of the nuclear medium, since this is a state of matter of fundamental relevance.

In this brief review paper we will present the status of our knowledge on the nuclear medium as can be extracted phenomenologically and established theoretically. On the other hand, we will discuss, on the basis of the works performed in the last few years, the possibility of using the properties of the nuclear medium, noticeably its Equation of State (EoS), to guide the nuclear structure theory of normal and exotic nuclei. Along the same lines it can be of great physical insight to try to establish, to the extent that this is possible, a link between the macroscopic view and the general properties of finite nuclei.

The style of the review is intended for non-specialists. We introduce each subject by reporting standard results, leaving formal arguments to textbooks or original papers, before going to more advanced developments and the discussion about on-going research works. The presentation is of course guided by the personal views of the authors as well as by their limitations.

2. The free Fermi gas of nucleons

Before going to the microscopic many-body theory of nuclear matter, we remind the elementary properties of a free Fermi gas of nucleons. This will serve as starting point when the nuclear interaction will be introduced and at the same time as reference for

comparison with the realistic treatments and results.

2.1. The Equation of State

If we assume that no interaction takes place between N nucleons inside a box of large volume, we have the simplest model of nuclear matter, the free fermion gas. We remind here some elementary results, that will be useful in the sequel. The total energy E of the system is the sum over the single particle energies

$$E = \sum_k \frac{\hbar^2 \mathbf{k}^2}{2m} = g \sum_{\mathbf{k}} \frac{\hbar^2 \mathbf{k}^2}{2m} = \frac{gV\hbar^2}{2m} \int_{|\mathbf{k}|<k_F} \frac{\mathbf{k}^2 d^3k}{(2\pi)^3} \ , \tag{1}$$

and the energy per particle e is given by

$$e = \frac{E}{N} = \frac{g\hbar^2}{2m\rho} \int_{|\mathbf{k}|<k_F} \frac{\mathbf{k}^2 d^3k}{(2\pi)^3} = \left(\frac{3\hbar^2 k_F^2}{10m} \right) = \frac{3}{5} E_F \ . \tag{2}$$

In equation (2) we have used equation (1) and introduced the Fermi energy $E_F = \hbar^2 k_F^2 / 2m$, the energy of the highest occupied level. From Eqs. (2) and (**??**), one gets

$$e = \frac{3}{5} \frac{\hbar^2}{2m} \left(\frac{3\pi^2}{2} \right)^{\frac{2}{3}} \rho^{\frac{2}{3}} \tag{3}$$

which relates the energy per particle e to the density ρ, and therefore it is the EOS (the simplest one) for a free symmetric nucleon gas at zero temperature. If one measures the energy in MeV, the length in femtometers fm (otherwise also called "fermi"), and adopts for the nucleon mass $mc^2 = 938.9$ MeV, an average value between neutron and proton masses, for simplicity, then $\hbar^2/2m = 20.74$, and

$$e = 75.03 \, \rho^{\frac{2}{3}} \ \text{MeV} \ . \tag{4}$$

This well-known result indicates that the energy of a free fermion gas increases monotonically with the density. If nuclear matter must be stable in mechanical equilibrium at a density $\rho = \rho_0 \approx 0.16 fm^{-3}$, the so-called saturation density, a net attractive potential energy must be present around this density. This attraction, coming from the nucleon–nucleon interaction, must produce a minimum in the EOS, namely in the curve $e = e(\rho)$, at $\rho = \rho_0$. This requirement originates from the phenomenological observation that the central density of medium and heavy nuclei (as extracted from e.g. electron scattering data) is pretty constant along the nuclear mass table and close to the above mentioned value of ρ_0. This is interpreted as being the mechanical equilibrium density of nuclear matter and it is the starting point for the development of the empirical mass formula in its different versions. The latter is discussed at the beginning of the next section. Before doing that, some considerations on the free gas model and some of its applications will be discussed.

2.2. The incompressibility

Another way of presenting the free gas EOS (at zero temperature) is to consider the pressure

$$p \,=\, -\left(\tfrac{dE}{dV}\right)_N \,=\, \tfrac{\rho^2}{N}\left(\tfrac{dE}{d\rho}\right)_N \,=\, \rho^2\left(\tfrac{de}{d\rho}\right) \,=$$

$$=\, \tfrac{2}{5}\tfrac{\hbar^2}{2m}\left(\tfrac{3\pi^2}{2}\right)^{\frac{2}{3}}\rho^{\frac{5}{3}} \,\approx\, 50.02\,\rho^{\frac{5}{3}}\ \ \mathrm{MeV}fm^{-3}\ , \tag{5}$$

which can be considered the "Pauli pressure", namely the pressure due to the exclusion principle, a typical quantal effect. From the pressure, the incompressibility K_0 can be derived according to the usual definition

$$K_0 \,=\, -V\left(\tfrac{dp}{dV}\right) \,=\, \rho\left(\tfrac{dp}{d\rho}\right) \,=$$

$$=\, \tfrac{2}{3}\tfrac{\hbar^2}{2m}\left(\tfrac{3\pi^2}{2}\right)^{\frac{2}{3}}\rho^{\frac{5}{3}} \approx 83.36\,\rho^{\frac{5}{3}}\quad . \tag{6}$$

The definition of equation (6) is in agreement with the usual one adopted in textbooks on basic mechanics and thermodynamics. For practical reasons, it is more customary among nuclear physicists to use the alternative definition

$$K \,=\, k_F^2\left(\frac{d^2e}{dk_F^2}\right)\quad , \tag{7}$$

which has the dimension of an energy. The following relationship can be easily checked

$$K_0 \,=\, \frac{4}{3}p \,+\, \frac{1}{9}\rho K\quad . \tag{8}$$

Equation (8) is not restricted to the free gas model, but it is valid in general. At saturation $p = 0$, and the two definitions have a very simple connection. If one drops the first term on the right hand side of equation (8) and adopts for K_0 the free gas value given by equation (6), one gets

$$K \,=\, 6E_F \,\approx\, 221\ \ \mathrm{MeV}\ , \tag{9}$$

where the numerical value is taken at $\rho \approx \rho_0$. This value is close to the values obtained in several phenomenological analysis of the data on the monopole frequency in heavy nuclei [1]. It is appreciably lower than the value of 240 MeV obtained in reference [2] on the basis of a Skyrme force fit to the properties of a wide set of medium-heavy nuclei. This approximate agreement must be considered essentially fortuitous. In fact, the monopole frequency is determined by the mechanical incompressibility K_0, but for the free Fermi gas the pressure term $4/3p$ of equation (8) is quite large at $\rho = \rho_0$. Therefore, the procedure we followed to extract K is clearly inconsistent. The agreement is the result of some "compensation of errors". Of course, one can always *define* the incompressibility as $K' = 9K_0/\rho$ instead of equation (7) for all densities, in which case for a free Fermi gas indeed $K' = 6E_F$. Anyhow, the connection between monopole frequency and incompressibility is less obvious than at first sight [3].

2.3. Momentum distribution

The ground state of the free fermion gas is characterized by the filling of the lowest single particle levels, i.e. the occupation number of the states k is one below the Fermi momentum k_F and zero above, as indicated in figure (1a). This picture is expected

Figure 1. Schematic representation of the momentum distributions in a free fermion gas (a) and in an interacting fermion gas (b).

to be modified by the nucleon–nucleon interaction, as shown in figure (1b). Here the discontinuity at the Fermi energy is assumed to persist despite the nucleon–nucleon correlations. The Fermi liquids that have this property are called "normal" Fermi liquid. The deviation of the discontinuity from one is a measure of the strength of the correlations. The persistency of the discontinuity at k_F is the basis of the Landau theory of Fermi liquid and of the concept of quasi-particle [4], to be discussed in section 5. If nuclear matter is superfluid, as it appears to be in a range of density, the discontinuity disappears. Apart from the possible onset of superfluidity, which affects only weakly the gross properties of the EOS, nuclear matter appears to be a normal Fermi liquid. Superfluidity changes of course dramatically the transport properties of nuclear matter.

2.4. The symmetry energy

If the proton number N_p is different from the neutron number N_n, with $N = N_n + N_p$, then the neutron and proton Fermi momenta are different, since the neutron and proton densities are different. Accordingly, the EOS of equation (3) has to be generalized. Defining

$$\beta \,=\, \frac{N_n - N_p}{N_n + N_p} \,=\, \frac{\rho_n - \rho_p}{\rho} \tag{10}$$

as the "asymmetry" parameter, one easily gets

$$\begin{aligned} E &= E_n \,+\, E_p \,=\, N_p \tfrac{3}{5} E_F^{(p)} \,+\, N_n \tfrac{3}{5} E_F^{(n)} \\ e &= \tfrac{E}{N} \,=\, \tfrac{3}{10}\tfrac{\hbar^2}{2m}\left(\tfrac{3\pi^2}{2}\right)^{\frac{2}{3}} \rho^{\frac{2}{3}} \left[(1+\beta)^{\frac{5}{3}} \,+\, (1-\beta)^{\frac{5}{3}}\right] \\ &\approx e(\beta = 0) \,+\, a_{sy}\beta^2 \,+\, \cdots\cdots \\ a_{sy} &= \tfrac{1}{3} E_F \quad . \end{aligned} \tag{11}$$

Thus, for a fixed value of the total density ρ, the energy per particle e has a minimum at $\beta = 0$. The coefficient a_{sy} is called the symmetry energy. At $\rho \approx \rho_0$, one finds $a_{sy} \approx 12$ MeV. From the systematics on the asymmetry dependence of the binding energy of medium–heavy nuclei, a_{sy} turns out to be more than twice larger than this value. Here the interaction must play a major role. The density dependence of a_{sy} is one of the most relevant issue in nuclear astrophysics, but also in nuclear structure.

2.5. The single particle density of states

For many physical phenomena the single particle density of states at the Fermi energy is a relevant quantity. For the free gas model one can readily get an explicit expression

$$D(E_F) = \sum_k \delta\left(E_F - \frac{\hbar^2 \mathbf{k}^2}{2m}\right) = \frac{V \cdot g}{(2\pi)^3} \int d^3k \delta\left(E_F - \frac{\hbar^2 \mathbf{k}^2}{2m}\right) =$$

$$= \frac{N}{\rho} \frac{g}{(2\pi)^3} 4\pi \frac{m}{\hbar^2} k_F = \frac{3N}{2E_F} \approx \frac{N}{23} \ \mathrm{MeV}^{-1} \quad , \qquad (12)$$

where the last equality holds at $\rho \approx \rho_0$. This elementary result is expected to be modified by the presence of the interaction [5]. The effect of the nucleon–nucleon correlations on $D(E_F)$ can be introduced by substituting the free nucleon mass with the so called nucleon "effective mass", which will be shortly discussed in the section on Landau theory. Another related useful quantity is the single particle level density per unit volume, that for symmetric matter can be written

$$d(E_F) = D(E_F)/V = \frac{2m}{\pi^2 \hbar^2} k_F \qquad (13)$$

It depends only on the nuclear matter density.

2.6. Other microscopic physical quantities

In order to characterize the properties of the nuclear medium other quantities are necessary. First of all the nuclear surface properties are characterized by the values of surface thickness and the surface tension. Bulk and shear viscosity are essential to describe the macroscopic dynamics of Neutron Stars. They are dominated by the nucleon-nucleon interaction, and therefore they will be discussed after the correlations among nucleons will be introduced and discussed. In finite nuclei viscosity must to be treated in a different scheme than in nuclear matter, since the presence of the nuclear surface plays a major role. This issue will be also discussed in the section on viscosity.

3. Basic phenomenology

3.1. Mass formula and saturation

Some of the basic phenomenological data on the nuclear medium come from the semi-empirical mass formula [6, 7]. The aim of the mass formula is to express the total binding energy $B(A, Z)$ of a nucleus as a smooth function of the mass number A and the atomic number Z. Several versions of the formula exist. In any case, the physical

basis is the Liquid Drop Model or the so-called Droplet Model. In these models, the nucleus is described as a drop of a quantal liquid, the nuclear medium, whose properties are derived as for a classical liquid, with the addition of some quantal corrections, typical of the nuclear systems. A set of parameters are introduced, some macroscopic in character, some other more connected to a Fermi liquid behavior. The refined versions of the purely phenomenological mass formula contain several terms and can be written

$$B(A,Z) = a_V A + a_S A^{\frac{2}{3}} + (a_I + a_{IS}/A^{\frac{1}{3}})(\frac{N-Z}{A})^2 + a_C \frac{Z^2}{A^{\frac{1}{3}}} - \delta_P + E_D \tag{14}$$

which, in the written order, contains the bulk contribution (parameter a_V), the surface correction (a_S), the bulk and surface symmetry energies (a_I and a_{IS} respectively), the coulomb energy (a_C), the pairing energy (δ_P), to be discussed in detail in section 7.4, and the deformation energy (E_D). The overall trend of the empirical binding energy of nuclei and the way it can be reproduced by this simple formula, by adjusting the set of parameters a, are discussed in basic books [8], where the meaning and possible forms of the different terms are discussed in more detail. The values of the parameters depend slightly on the particular form used for δ_P and E_D [9, 10, 11]. The value of the bulk energy a_V in all cases is very close to -16 MeV. This formula provides an excellent fit to the smooth part of the binding energy of nuclei throughout the nuclear mass table with few parameters. This fact supports the interpretation of each term as schematically indicated above. A partial justification of the mass formula can be obtained within the semi-classical scheme of approximation. In fact, it is possible to show [8] that the smooth function $B(A,Z)$ can be considered the first term of the expansion in $\hbar$ of a mean field estimate of the nuclear binding energy. The deviations, which are actually in percentage very small, are therefore interpreted as "shell corrections" [5], i.e. corrections coming from the quantal effects related to the finite size of nuclei. Systematic methods to estimate these effects have been devised by many authors, in particular by Strutinsky [12]. They will be discussed in the section 8.1.

The very fact that in the fitting procedure a constant term a_V can be well identified as one of the relevant term indicates that this term can be indeed interpreted most naturally as the bulk part of the binding energy, namely the energy per particle of the infinite symmetric nuclear matter. This can be also seen if one extrapolates the formula for $A \to \infty$, provided $N = Z$ and the Coulomb energy is neglected. Then, in this case, only the first term survives. Similarly the coefficient a_I can be identified with the nuclear matter symmetry energy per particle. However, it has been argued recently [13, 14] that these parameters could reach the asymptotic values only at exceedingly large value of the mass number A, and therefore along the nuclear mass table they still contain a smooth dependence on the mass and atomic number.

The Droplet Model [15, 16] includes additional contribution with respect to the Liquid Drop Model, in particular a curvature term and a term taking into account the possibility of a slight compression of the nuclear medium in the nucleus.

The appealing physical feature of these models is the direct relationship between each parameter and a definite property of the nuclear medium. In principle, the

phenomenological analysis based on these models can provide basic physical quantities which characterize the nuclear medium, both in its homogeneous macroscopic phase and in finite nuclei.

One has to mention a similar approach, the so called microscopic-macroscopic models [17]. In this case some hints are taken from a more microscopic treatment of the binding energy, like the Thomas-Fermi, see section 8.1.

Of course the mass formula contains information only at the saturation density ρ_0, and therefore the knowledge of the complete EOS goes well beyond the content of equation (14). As mentioned briefly in the introduction, information on the EOS at $\rho \neq \rho_0$, finite temperature and large asymmetry are expected to come from heavy ion collision experiments and astrophysical observations.

Finally, one has to mention that the notion itself of saturation is coming also from the observation that the central density of medium-heavy nuclei is pretty constant throughout the nuclear chart. This fundamental phenomenological result has been obtained mainly from elastic electron scattering, which provides the whole charge distribution in nuclei. The total density is then obtained by assuming that the neutron density scales as N/Z with respect to the proton density. For a recent analysis see references [18, 19]. The value of the density is around 0.16 fm^{-3} and it is interpreted as the density at which symmetric nuclear matter displays its minimal energy (saturation point). Till now asymmetry effects are within the overall phenomenological uncertainty on the saturation point.

3.2. Giant Resonances in nuclei

If nuclei are viewed as droplets of nuclear matter, it is natural to consider the possibility of their excitations. The quantization of these modes correspond to collective excitations of the nucleus as a whole. This is the physical basis of the Bohr-Mottelson model [5] for the nuclear modes of excitation. These collective modes have found a clear and extensive experimental evidence [5, 8]. The vibrational excitations are classified according to the multipolarity of the surface oscillations and their isospin character, i.e. if neutrons and protons oscillate with the same or opposite phase (for simplicity we neglect spin flip). They are universally called "Giant Resonances", since they usually carry a large fraction of the total strength of the corresponding spectral function.

The simplest oscillation is the isoscalar monopole vibration, corresponding to a compressional mode of the nucleus. The question that arises naturally is then if it is possible to extract from the study of the monopole excitation, in particular from its energy, the compression modulus of nuclear matter at saturation. This possibility has been explored extensively since many years [3, 8]. From a purely macroscopic point of view there are essentially two difficulties along this line : a) To calculate the excitation energy, as for an harmonic oscillator, not only the incompressibility is needed, giving the restoring force, but also the dynamical mass that should be used, and b) the surface tension of the nucleus should play some role, but there is not any obvious relationship

between surface tension and incompressibility. As for point a), microscopically there is a general method to estimate the collective mass of an excitation, the so-called "cranking mass" [5, 8]. At macroscopic level it can be estimated assuming a particular velocity flow, in particular the scaling hypothesis implies a radial velocity proportional to the radius, in which case the inertial parameter has an analytic expression and it is proportional to the radius square of the nucleus [3, 20]. It is difficult to handle point b) with a satisfactory accuracy at macroscopic level, and it is necessary to introduce some microscopic elements in the theory. The most successful semi-microscopic method is the Skyrme functional method, to be discussed with some detail in section 8.2. According to this well known method, an effective nucleon-nucleon interaction is introduced and the energy of the nucleus is assumed to be equal to the Hartree or Hartree-Fock energy calculated with such a force, i.e. minimizing the mean field energy functional calculated with the force. The effective force is semi-phenomenological in character and therefore it contains few parameters. With the same force it is possible to calculate also the nuclear matter EoS, and to tune the parameters in order to obtain the correct saturation point and a given incompressibility modulus. In this way it is possible to check if a correlation exist between the energy of the isoscalar monopole vibration and the nuclear matter incompressibility. All the parameters are fitted in any case to reproduce the binding energy of a large set of nuclei, as well as other phenomenological data. For an extensive application of this method, see e.g. reference [21, 22]. One finds indeed that a correlation exists between incompressibility and position of the monopole Giant Resonance, so that, in principle it is possible to extract from the experimental data the value of the incompressibility in nuclear matter. For the method to be reliable, the result should be essentially independent of the particular Skyrme force used in the calculations. Unfortunately this is not the case. It was shown more recently [23] that the relationship between the centroid of the monopole excitation and the value of the incompressibility is not unique, but it depends also on other details of the force, mainly it is correlated also to the density dependence of the energy density and symmetry energy of the force [23, 24]. This also explains, at least partially, the reason why the incompressibility extracted from relativistic mean field functional tends to be systematically higher than the one extracted for non-relativistic Skyrme functional. At present, the constraints on the value of the nuclear matter incompressibility from the monopole excitation are not so tight. It is fair to say that it can be approximately constrained between 210 and 250 MeV. More refined value can be expected to come out in the near future from additional analysis of phenomenological data.

The prototype of Giant Resonance is surely the dipole mode, where neutron and proton oscillates against each other. The restoring force in this case is the symmetry energy. Both volume and surface contribution can be present. In fact, recent analysis [25, 26] on the correlation between dipole resonance energy and symmetry energy indicates that such correlation can be obtained if the symmetry energy is taken at 0.1 fm $^{-3}$, about 2/3 the saturation density. In any case it is difficult to get a strong constraint on the nuclear matter symmetry energy at saturation from the Giant Dipole

Resonance.

The isoscalar quadrupole mode is more connected with the surface tension in nuclei, since, in first approximation, the mode occurs at constant volume. However, this correlation has not been explored, probably because in this case it is more difficult to estimate the collective mass term.

The other Giant Resonances do not involve only one or few characteristics of the effective forces, and therefore they can hardly be used to study definite physical properties of the nuclear medium.

Finally it has to be mentioned the study of the Giant Resonance damping, which is measured by their width. From a macroscopic point of view such a damping should be connected to some sort of viscosity of the nuclear medium. Unfortunately the physical situation is much more complicated. First of all, one should take into account that we are dealing with a quantal liquid, as discussed in section 5. Therefore Giant Resonances actually should be considered as zero sound modes, and, in principle, no hydrodynamical picture should be adopted. Furthermore, the presence of the nuclear surface introduces a different type of damping, the so called one-body dissipation [27, 28, 29, 30]. The applicability of such damping mechanism requires the onset of a certain degree of chaos in the single particle dynamics [31], and therefore it seems not suited to Giant Resonance of low multipolarity. Probably the octupole vibration can be partly affected by such a type of dissipation. Finally the damping can be produced by the emission of nucleons, the so called decay damping. At least for all these reasons the extraction from the width of any sort of viscosity is strongly hampered, and the study of the Giant Resonance width must rely completely on nuclear structure analysis [32, 33]. Shear and bulk viscosity in nuclear matter, as present in Neutron Stars, must be predicted only on purely theoretical basis when microscopic models of astrophysical phenomena are developed.

3.3. Heavy ions

In a period that includes at least the last two decades intensive studies of heavy ion reactions at energies ranging from few tens to several hundreds MeV per nucleon (hereafter indicated as MeV/A) have been performed in different laboratories throughout the world. One of the main goal, probably the principal one, has been the extraction from the data on suitable observable quantities the gross properties of the nuclear Equation of State. An enormous literature exists on the subject, and therefore we will focus on few items that, according to our personal view, are connected with established and insightful results.

3.3.1. Flows and differential flows It can be expected that in heavy ion collisions at large enough energy nuclear matter is compressed and that, at the same time, the two partners of the collisions produce flows of matter. In principle the dynamics of the collisions should be connected with the nuclear medium EoS and its viscosity.

However at low enough energy the cross section is dominated by deep inelastic

processes, where target and projectile keep their identity during the collision, stick together for a while and separate again. This reaction mechanism persists up to about 10 MeV/A. At increasing energy the so called "multifragmentation" regime is encountered, where after the collision numerous nucleons and fragments of different sizes are emitted. Usually, at non-central collisions, one distinguishes target-like and project-like fragments, the so called spectators, and the participant region, where matter is partly stopped and tends to form a partly equilibrated zone. In semi-classical simulations of heavy ion collisions two main ingredients are introduced, the single particle mean field U and the in-medium NN scattering cross section $\frac{d\sigma}{\Omega}$. A Boltzmann-like kinetic equation is assumed for the nucleons

$$\frac{\partial f}{\partial t} + \vec{\nabla}_p \epsilon \cdot \vec{\nabla}_r f - \vec{\nabla}_r \epsilon \cdot \vec{\nabla}_p f = I \Big\{ \frac{d\sigma}{\Omega} \Big\} \tag{15}$$

where $n = n(\mathbf{r}, \mathbf{p}, t)$ is the single particle density distribution in phase space, $\epsilon = p^2/2M + U(\mathbf{r}, \mathbf{p}, t)$ the local single particle energy and I the two-body collision integral that describes the loss and gain of particles, at a given phase space point, due to scattering of nucleons in the medium. The single particle potential U can be written

$$U(\mathbf{r}, \mathbf{p}, t) = \int d^3r' d^3p' \, v_{eff}(\mathbf{r}, \mathbf{p}; \mathbf{r}', \mathbf{p}') n(\mathbf{r}', \mathbf{p}', t) \tag{16}$$

where v_{eff} is the effective NN interaction in the medium. In general U is identified with the single particle potential in nuclear matter at the local density, e.g. the Brueckner potential.

In practice it is not possible to get directly from the data indications on the EoS and the scattering cross section in the medium. Even if 4π detectors, with which is possible an (almost) complete reconstruction of the collision dynamics, have been developed, the interpretation of the data is not unique. The usual procedure is to assume a set of possibility for the potential U and, more rarely, for $d\sigma/\Omega$, and to find which ones in the considered sets fit better the data. Once U is chosen, the EoS can be calculated, since the single particle potential fixes the interaction energy per particle. Analogously, the scattering cross section determines the transport properties of the nuclear medium. However, very often the NN scattering processes have only the effect of driving the system toward equilibrium, or quasi-equilibrium, at least in the participant zone, so that the information on the cross section is often too indirect to be accessible. In any case it is true that the results of the simulations depend in general on both quantities.

One of the quantity that is more often analyzed is the so called transverse momentum, also in its differential form. If the reaction plane is the (x, y) plane and the initial direction of the two colliding nuclei is along the y axis, one calculates the average momentum p^x along the x-axis of the nucleons as a function of their velocity y (or "rapidity") along the y-axis

$$F(y) = < p^x >_y \quad ; \quad F'(y) = d < p^x >_y / dy \tag{17}$$

At high enough energy the flow is strongly affected by the matter compression during the collision and dominated by the corresponding pressure. Then the initial flow undergoes a

strong repulsion from the interaction zone, which means that $F(y)$ turns from negative to positive values as y changes sign, with a well defined slope. In fact the negative and positive values of y label the target-like and projectile-like fragments or nucleons, at least for y around zero ("mid-rapidity" region). It was hoped that the slope $F'(0)$ could characterize sharply the nuclear matter EoS. Unfortunately in the simulations only a weak dependence on the EoS stiffness is observed, somehow obscured by the numerical uncertainty of the simulations themselves [34]. This is probably due to the competing effect of the NN collisions incorporated in the collision integral I. For the same reason, it is difficult to extract any solid information on the in-medium cross section. To complicate further the situation, different simulation methods, like the Quantum Molecular Dynamics [35, 36, 37, 38], give slightly different results in the same physical conditions, which increases the uncertainty on the EoS that can be extracted.

Despite all these difficulties, some gross constraints on the nuclear EoS can be extracted. In reference [39] this effort was summarized by plotting the region where any reasonable EoS should pass through in the pressure vs. density plane. The pressure was taken at the center of the interaction zone at the moment of maximal density during the collision, using all the simulations with different EoS compatible with different data and including the uncertainties. The plot is reproduced in figure (2), as taken from reference [40], in comparison with some microscopic calculations to be discussed in section 4. In particular the EOS labeled BBG is the one calculated win the Brueckner approximation including three-body forces, as presented in detail in section 4, that looks in agreement with the data in the full density range. It has to be stressed that the EoS employed in such a constructions have incompressibility that ranges from $K = 167$ MeV to $K = 380$ MeV. Only the densities above twice the saturation density were included, since this guarantees that quasi-equilibrium in the participant zone was reached. This shows that only the EoS at high density can be studied in heavy ion collisions. The values of the incompressibility do not characterize completely the EoS, since it is actually density dependent, but in any case the analysis indicates the broad constraints on the EoS that can be obtained from heavy ion collisions. Despite they are somehow a little loose, they are able to exclude some of the phenomenological EoS [41].

3.3.2. K-meson production Strange particles production in heavy ion collisions can probe the central part of the participant zone. In fact near threshold strange particles are mainly produced in the high density region and, once produced, they interact weakly with the matter. This is due to strangeness conservation in reactions produced by strong force, which implies that strange particles are always produced in pairs and they cannot be directly re-absorbed by nucleons. However this does not necessarily mean that the interaction can be completely neglected. In particular, let us consider the lightest strange particle, the K-meson (kaon). In this case one has to distinguish between K^- and K^+, since the negative kaon forms resonances with nucleons even at low energy and therefore their interaction with the nuclear medium cannot be neglected. Unfortunately the interaction potential felt by K^- in the medium is not so well known theoretically,

Figure 2. Different EoS in comparison with the phenomenological constraint extracted by Danielewicz et al. (shaded area), where $\rho_0 = 0.16$ fm^{-3}. Full line: EoS from the BBG method with phenomenological TBF [73]. Dashed line : modified variational EoS of Heiselberg and Hjorth–Jensen [74]. Dotted line : variational EoS of Akmal et al. [57]. Open circle : EoS from the BBG method with "ab initio" TBF [73]. Dash–dotted line : EoS from Dirac–Brueckner method (van Dalen et al. [75]).

and this introduces uncertainty in the analysis of the experimental data. The situation for K^+ is different, since no resonance with nucleons is present and the interaction can be treated almost perturbatively, and actually the uncertainty is much reduced. The main mechanism of K^+ production is through the excitations of a nucleon to a Δ, that in turn decays in a Λ and a K^+

$$NN \longrightarrow N\Delta \longrightarrow N\Lambda K^+ \tag{18}$$

It is then clear that the simulations must include nucleon excitations and must be relativistic. The uncertainty is mainly due to the not so well known potential of the Δ in the nuclear medium. Fortunately this does not affect too much the final results, which look to be under control also numerically and almost independent on the simulation method. An excellent and extensive review of the subject, both at experimental and theoretical level, can be found in [42, 34]. Here we restrict to some of the conclusions that can be drawn from this line of research, that was developed along several years.

The optimal energy for this type of investigation is close or even below two-body threshold, since then the only way to produce the kaons is by compression of the matter. Since at threshold the production rate increases steeply, there is a strong sensitivity to the value of the maximum density reached during the collision, and this is an ideal situation for studying the EoS and its incompressibility. The comparison of the simulations with the experimental data on K^+ production, noticeably the ones from the KaoS [43] and FOPI [44] collaborations, points in the direction of a soft EoS. More precisely, the interval of compatible incompressibility is narrower than the ones obtained from the analysis of flows

$$180 \;\leq\; K \;\leq\; 250 \;\; \mathrm{MeV} \tag{19}$$

These values are compatible with the ones obtained from the monopole oscillations, see Section 3. However it has to be kept in mind that, in the simulations, kaon production occurs at density about 2-3 times larger than saturation, $\rho \geq 2 - 3\rho_0$, and therefore the two sets cannot be fairly compared. In any case, a stiff EoS above saturation seems to be excluded from this analysis, as it is apparent from figure (3), taken from reference [42].

Figure 3. Excitation function of the K^+ multiplicity ratio between inclusive Au + Au over C+C reactions. The simulations are performed with hard/soft nuclear EoS and compared with the data from the KaoS collaboration [45]

3.4. Astrophysics

The nuclear medium is directly and massively involved in core-collapse supernova explosions, where nuclear matter is compressed at supra-saturation density and trigger the shock wave that is the main agent of the outflow. The properties of nuclear matter determine completely the structure of Neutron Stars and the phenomena that occur in their interior or at the surface. Indirectly, the peculiarities of the nuclear medium are relevant for many other processes, like nucleosynthesis.

3.4.1. Supernovae One of the major puzzle in Astrophysics is the mechanism that drives the explosion of core-collapse Supernovae. In the complex simulations of the after-bounce stage of the supernovae the shock wave is stalling due to the energy loss, mainly produced by the disintegration of nuclei in the envelope. It is common wisdom that only the revival of the shock by the blast of neutrinos, initially trapped, can produce the final explosion [46]. For a long time it was believed that a direct link should exist between the possibility of explosion and the value of the incompressibility in nuclear matter. Many years of effort on supernova event simulations have disproved this believing and the difficulty of getting a real explosion in the computer has indicated that only a detailed treatment of the different aspects of the phenomenon could lead to a definite solution of the puzzle [47]. It seems now [48, 49] that the key ingredient is

the 3-dimensional character of the process, that makes more tiny the structure of the turbulent flow of matter and renders more efficient (with respect to a 2-dimensional situation) the energy deposition of neutrinos on the matter close to the shock. The possibility of the explosion is therefore not determined by the details of the nuclear EoS. However many quantitative aspects of the explosion do depend on the EoS, like the total energy release, neutrino luminosity and the timing of the whole phenomenon as determined by the neutrino mean free path (for which nucleon correlations in nuclear matter is essential). Unfortunately we are not yet at a stage where detailed quantitative predictions and comparisons can be made in relation to phenomenology because of the enormous complexity of the supernova explosion.

It has to be kept in mind that the nuclear medium present in supernovae, as well as in Neutron Stars, is very asymmetric and in different physical conditions than in heavy ion collisions. In particular the time scale is different by several order of magnitude, so that many processes that the nuclear medium can undergo in supernovae cannot occur in heavy ion reactions because the time is too short.

3.4.2. Neutron Stars The compact remnant of a supernovae explosion, if the collapse does not end in a black hole, is a Neutron Star, (NS) an extremely dense object, that in the standard view is composed of nuclear matter, electron and muons. Leptons are necessarily present because initially the star is of course neutral. The structure of the NS is determined by the properties of the nuclear medium in an extremely wide range of density, from few times the saturation one at the center, down to values several order of magnitude smaller close to the surface. An old enough NS is virtually at zero temperature and its exterior part is actually formed by a Coulomb crystal of nuclei [50, 51]. Below this outer crust, an inner crust is present, where nuclei are surrounded by a gas of dripping neutrons. In this region the EoS of pure neutron matter at low density is relevant. At the same time nuclei are very exotic, challenging our knowledge of the nuclear medium at large asymmetry. Below the crust asymmetric homogeneous nuclear matter fills the whole space. Again the asymmetry is very large, and a direct link with nuclear structure and heavy ion reactions in terrestrial laboratories is not possible. The challenge for microscopic many-body theory is just to establish this link and try to test it by comparison with phenomenology. In this section we discuss the item of the NS maximum mass and few related issues, leaving other issues to sections 6-9. A NS is bound by gravity, and it is kept in hydrostatic equilibrium only by the pressure produced by the compressed nuclear matter. It is then apparent that the nuclear matter EoS is the main medium property that is relevant in this case, as can be seen in the celebrated Tolman-Oppenheimer-Volkoff [52, 53] equations, valid for spherically symmetric NS

$$\frac{dP}{dr} = -G\frac{\varepsilon\, m}{r^2}\left(1 + \frac{P}{\varepsilon}\right)\left(1 + \frac{4\pi P r^3}{m}\right)\left(1 - \frac{2Gm}{r}\right)^{-1} \tag{20}$$

$$\frac{dm}{dr} = 4\pi r^2 \varepsilon$$

(21)

where G is the gravitational constant, P the pressure, ε the energy density, and r the (relativistic) radius coordinate. To close the equations we need the relation between pressure and density, $P = P(\varepsilon)$, i.e. just the EoS. In the Newtonian limit the energy density is just the mass density and in each parenthesis the second term is neglected, and we get the equations of hydrostatic equilibrium in non-relativistic mechanics. The use of General Relativity (GR) is demanded by the strong gravitational field. Integrating these equations one gets the mass and radius of the star for each central density. Typical values are 1-2 solar masses ($M_{\odot}$) and about 10 Km, respectively. This indicates the extremely high density of the object. It turns out that the mass of the NS has a maximum value as a function of radius (or central density), above which the star is unstable against collapse to a black hole. The value of the maximum mass depends on the nuclear EoS, so that the observation of a mass higher than the maximum one allowed by a given EoS simply rules out that EoS. Up to now the best microscopic EoS are compatible with the largest observed masses, that are close to 1.7 solar mass [54]. It would be of course desirable to have some phenomenological data also on the radius of NS. Unfortunately this is quite difficult, but some tentative analysis look promising [55]. In particular a recent analysis of the data on six NS based on Bayesian statistical framework [56] has led to a tentative constraint on the nuclear EOS. Depending on the hypothesis made on the structure of the NS, the results are slightly different. The overall allowed region where the EOS should lie is reported in figure (4), where the theoretical EoS from the BHF calculations, to be discussed in the next section, is also reported. The theoretical EoS appears to be compatible with the extracted observational constraints. It turns out that other microscopic EoS do not show the same agreement, in particular the EoS of reference [57] looks too repulsive at high density [56]. These boundaries obtained from astrophysical data are complementary to the ones obtained from heavy ion reactions, see figure (2) in the previous sub-section. In fact, in heavy ion collisions the tested matter is essentially symmetric, while in NS the matter is highly asymmetric. Considered together, the two types of constraints probe the density dependence of the symmetry energy.

Unfortunately the theoretical situation for the EoS in NS and for the maximum mass is actually much more complicated. In fact, in NS weak processes have time to develop and, if energetically convenient, they can produce strange particles like hyperons, and then change the composition of the nuclear medium. This is clearly at variance with what can happen in heavy ion reactions, where the collision time is short and the multiplicity of strange particles is so small that a bulk strange matter cannot be formed. On the contrary in NS, at least above a certain density, the difference of the neutron and proton chemical potentials is so high to overcome the mass difference between hyperons and neutrons. This is indeed the case, according to microscopic calculations [58]. Above 2-3 times saturation density Σ^- or Λ hyperons appear. This soften so much the EoS that the maximum mass becomes smaller than the most established NS mass [59, 54]. This result seems to be quite robust and not dependent on the not so well known hyperon-

Figure 4. Comparison of the phenomenological allowed region (within the dotted-dashed lines) for the Neutron Star matter EoS with the corresponding microscopic EoS from the BHF method (full line). Phenomenological data are from reference [56].

nucleon or hyperon-hyperon interaction [60]. The only way out seems to be, up to now, a possible phase transition to quark matter. Indeed, calculations on the basis of simple models ([61]-[65]) can result in a maximum mass that is (marginally) compatible with the observed largest mass. Of course it could also be that the quark matter EoS is stiffer than assumed in simple models [66, 67], but in any case it seems that we are close to test our knowledge on the QCD deconfined phase at high density. All that makes clear that the NS physics connected with the central high density core is quite different from the ones in heavy ions, where in ultra-relativistic collisions at LHC the deconfined QCD phase is tested at zero baryon density and high temperature. However it is a basic challenge to the theory to be able to connect the transition to quark matter in this two extreme different physical situations. Advances both in phenomenological observations and theoretical methods are needed.

The maximum mass problem clearly can lead far from the physics of "nuclear medium", at least as it is considered in traditional nuclear physics. However the distinction between traditional nuclear physics and QCD physics is partly artificial, and they should considered as the two complementary aspects of the same physical realm.

Finally one has to observe that an observation of a maximum mass of 2 solar masses or higher would be a real breakthrough of our knowledge on high density nuclear medium, since it would question the simple models of quark matter. Recent observations [68] on the pulsar of the binary system PSR J1614-2230 seem to indicate such a possibility, and as anticipated in reference [61], it would imply the necessity of a

repulsive interaction in quark matter [69].

4. From the Nuclear Interaction to the Correlated Nuclear Medium

The properties of the nuclear medium are determined or strongly affected microscopically by the features of the nucleon-nucleon (NN) interaction. In particular, one of the main characteristics of the NN interaction is the presence of a hard repulsive core, whose relevance can be hardly overlooked. Furthermore, any realistic NN potential must include a complex structure of operators involving spin, isospin and orbital angular momentum. This non-trivial structure is one of the main reasons that renders the microscopic many-body theory of nuclear matter and nuclei so hard to be handled. Another characteristics of the NN interaction is the presence of a quasi-bound state ($^1S_0$ channel) and a bound state ($^3S_1 -^3 D_1$ channel) in the s-wave. This peculiar feature is probably unique in nature and strongly affects the structure of low density nuclear matter. At increasing density the effect of the bound and quasi-bound states tends to be reduced and this indicates that many properties of the nuclear medium should change strongly with density. Furthermore at very low density we know that nuclear matter at not too high temperature must form clusters, i.e. light nuclei, and this has a decisive role for the Neutron Star or proto-neutron star crust, as well as for heavy ion collision processes. In order to illustrate these fundamental features of the medium as a many Fermion system, in this section the NN interaction is introduced on the basis of the meson-nucleon model of the strong interaction in the baryon sector, and the many-body theory of nuclear matter is then schematically developed following the most established methods. Each microscopic many-body theory has a particular scheme to treat the hard repulsive core, that, implicitly or explicitly, introduces an effective NN interaction, more manageable than the original NN interaction.

4.1. Sketch of the nucleon-nucleon interaction

The nucleon-nucleon interaction was intensively studied when Nuclear Physics started developing. Along the years the phenomenological analysis has been more and more refined. Presently the phase shifts in different two-body channels are known with high precision up to an energy of about 300 MeV in the laboratory, even if discrepancies between the results of different groups still persist [70]. For future reference in the paper we remind very briefly the connection between the two-body interaction and the cross section, the quantity which is actually measured. If one assumes that the interaction can be described by a static non-relativistic potential v, the scattering process at the energy E can be described by the T-matrix, that here we take with the standing wave boundary conditions (often called R-matrix). It can be calculated solving the integral equation

$$T(E) = v + v\frac{P}{E - H_0}T(E) \tag{22}$$

where H_0 is the free kinetic energy hamiltonian and P indicates the principal value for the integral, which fixes the stationary wave boundary conditions. For a central potential, the phase shift in a given channel l is given by

$$\tan \delta_l \;=\; -q\mu(q|T(E)|q) \tag{23}$$

where q is the relative momentum and μ the reduced mass. The differential cross section is given by

$$\frac{d\sigma}{d\Omega} \;=\; \frac{1}{q^2}|\Sigma_l(2l+1)(e^{2i\delta_l}-1)P_l(\theta)|^2 \tag{24}$$

The nucleon-nucleon interaction, as we will see, contains not only a central interaction part but also more complex operators, and the summation is extended to single and coupled channels α, characterized by the total angular momentum J, total spin S, total isospin T and the orbital angular momenta l, l' ($l = l'$ for single channel). Fitting the data on the cross sections at different energy, the phase shifts δ_α for each channel can be extracted. For the NN interaction a particular form is assumed, as suggested by the meson-nucleon theory of strong interaction, that contains several parameters that are fitted to reproduce the phase shifts. In this way one can fix the nucleon-nucleon potential, which however partly remains model-dependent. For details, see e.g. reference [71]. Here we sketch the main ideas of the meson theory of the nucleon-nucleon interaction. For simplicity we use a non-relativistic treatment, as a first schematic introduction to the theory of nuclear forces. Of course, the correct framework is the relativistic field theory of the meson-nucleon system. Let us consider the simplest possible case, the coupling of nucleons with a spinless neutral meson. If we indicate by ${b^\dagger}_q$ (b_q) the creation (annihilation) operator of a meson with momentum q, the simplest coupling term is the scalar one

$$\begin{aligned} H_c \;&=\; G_s \int d^3x \psi^\dagger(x)\psi(x)\phi(x) \\ &=\; G_s \frac{1}{\sqrt{V}} \sum_{kq} \sqrt{\frac{\hbar}{2\omega(q)}} ({a^\dagger}_k a_{k+q} {b^\dagger}_q + {a^\dagger}_k a_{k-q} b_q) \;, \end{aligned} \tag{25}$$

which describes the processes of emission and absorption of a meson. The two processes are included together, with the same weight, as required by the hermiticity of the interaction H_c and of the scalar field $\phi(x)$. The momentum conservation has been explicitly worked out and the constant G_s is the meson-nucleon coupling constant. In equation (25) $\omega(q)$ is the meson energy and the factor in front $1/\sqrt{2\omega}$ comes from the usual quantization of the boson (meson) field in a set of harmonic oscillators [72]. The creation and annihilation meson operators satisfies the usual boson commutation relations

$$[b_{k'}, {b^\dagger}_k]_- \;=\; -[{b^\dagger}_k, b_{k'}]_- \;\equiv\; b_{k'}{b^\dagger}_k - {b^\dagger}_k b_{k'} \;=\; \delta_K(k-k') \quad . \tag{26}$$

In equation (25) the product $a^\dagger a$ includes a scalar product in the spin component, $a^\dagger a \;\equiv\; \sum_\sigma {a^\dagger}_\sigma a_\sigma$. The total Hamiltonian will include, besides the free nucleon

Hamiltonian, also the free meson part

$$h_0 = \sum_q \omega(q) b^\dagger{}_q b_{-q} \tag{27}$$

and we can take the relativistic expression $\omega(q) = \sqrt{(mc^2)^2 + q^2c^2}$ since the meson mass m is usually much smaller than the nucleon mass, and therefore its kinematics is surely relativistic. We will indicate by H_0 the non-interacting part of the Hamiltonian. The inclusion of the coupling term of equation (25) in a non-relativistic framework is somehow problematic. In fact, since it involves the creation or annihilation of a particle, the center of mass energy in such a process cannot be conserved and therefore Galilei invariance is manifestly broken. The breaking is proportional to the ratio between the meson and the nucleon masses, and therefore it vanishes in the limit of infinitely heavy nucleons. This is indeed the limit in which the concept of a static nucleon-nucleon potential has a meaning. Perturbation theory in H_c of different physical quantities can easily be developed and the different terms can be represented by diagrams. For our purposes only the lowest order has to be considered. In the framework of the meson-nucleon theory, the effective nucleon-nucleon interaction can be identified with the irreducible part of the two-nucleon scattering matrix $T^{(2)}$. By "irreducible" here we mean the set of (connected) diagrams which cannot be separated into two distinct parts by cutting two nucleon lines at any given level along the diagram. The general perturbation theory for $T^{(2)}$ can be obtained from the usual expansion for the scattering matrix

$$\begin{aligned} T^{(2)}(E) &= H_c + H_c \frac{1}{E - H_0} T^{(2)} \\ &= H_c + H_c \frac{1}{E - H_0} H_c + H_c(\frac{1}{E - H_0} H_c)^2 \ldots \end{aligned} \tag{28}$$

In this expansion we have to select the processes which indeed correspond to the scattering of two nucleons and are irreducible. The lowest order which can contribute is the second order, since to first order the coupling term H_c can describe only emission or absorption of a meson. Let us denote by $|kk'\rangle$ the free (antisymmetrized) state $a^\dagger_k a^\dagger{}_{k'}|0\rangle$ of two nucleons with momenta k and k'. The amplitude for the scattering from the state $|k_0 k'_0\rangle$ to the state $|k_1 k_1'\rangle$ can be extracted from the second order term of $T^{(2)}$

$$\langle k_1 k_1' | T^{(2)} | k_0 k_0' \rangle \approx \langle k_1 k_1' | H_c \frac{1}{E - H_0} H_c | k k' \rangle \quad . \tag{29}$$

If we insert the expression of equation (25) for H_c, since by definition H_0 is diagonal in the free state representation, we can use Wick' s theorem for the vacuum state in a straightforward way. For the meson operators this is trivial (they commute with the nucleon operators). The four contractions which can contribute can be depicted as in figure (5) which give four distinct contributions. The corresponding analytical expressions for the the two-body scattering matrix is given by

$$\langle k_1 k_1' | T^{(2)} | k_0 k_0' \rangle = \sum_q \frac{\hbar}{V} \frac{G_s^2}{2\omega_q} \delta_K(k_0 + k_0' - k_1 - k_1') \times$$

Figure 5. The four possible meson exchange processes. Dashed lines indicate mesons, full lines nucleons.

$$
\begin{aligned}
&\{(\delta_K(q-k_0+k_1)-\delta_K(q-k_0-k_1{}'))\frac{1}{E_0-E+E_{k_0-q}-E_{k_0}+\omega_q}+\\
&(\delta_K(q-k_1{}'+k_0)-\delta_K(q-k_1-k_0))\frac{1}{E_0-E+E_{k_0{}'-q}-E_{k_0{}'}+\omega_q}\} \quad , \qquad (30)
\end{aligned}
$$

where $E_0 = E_{k_0} + E_{k_0'}$ is the initial energy. If we interpret this matrix element as the matrix element of a two-body potential v between nucleons, this potential is clearly non-local and energy dependent. It is convenient to introduce the relative and total momenta of the initial and final two nucleon states

$$
\begin{aligned}
Q &= \frac{1}{2}(k_0{}'-k_0) \quad ; \quad P = k_0{}'+k_0\\
Q' &= \frac{1}{2}(k_1{}'-k_1) \quad ; \quad P' = k_1{}'+k_1 \qquad (31)
\end{aligned}
$$

Putting $E = E_0$, the matrix element of v can be written as

$$
\begin{aligned}
&\langle k_1k_1{}'|v|k_0k_0{}'\rangle = \frac{1}{2}\frac{\hbar}{V}G_s^2\delta_K(P-P')\times\\
&(-\frac{1}{\omega_{Q-Q'}}(\frac{1}{E_{Q'_+}-E_{Q_+}+\omega_{Q-Q'}}+\frac{1}{E_{Q'_-}-E_{Q_-}+\omega_{Q-Q'}})\\
&\quad+\frac{1}{\omega_{Q+Q'}}(\frac{1}{E_{Q'_-}-E_{Q_+}+\omega_{Q+Q'}}+\frac{1}{E_{Q'_+}-E_{Q_-}+\omega_{Q+Q'}})) \qquad (32)
\end{aligned}
$$

where $Q_\pm = \pm Q + P/2$. The fact that a dependence on the total momentum is still present is a consequence of the already mentioned breaking of Galilei invariance. In the limit of large nucleon mass, the terms corresponding to the nucleon recoil can be neglected, which is equivalent to put $E_k \approx M$ everywhere in the expression. In this approximation a very simple form is obtained

$$
\begin{aligned}
\langle k_1k_1{}'|v|k_0k_0{}'\rangle &= \frac{\hbar}{V}G_s^2\delta_K(P-P')(-\frac{1}{\omega^2_{Q-Q'}}+\frac{1}{\omega^2_{Q+Q'}})\\
&= \frac{\hbar}{V}G_s^2\delta_K(P-P')(-\frac{1}{(Q-Q)^2c^2+(mc^2)^2}+\frac{1}{(Q+Q')^2c^2+(mc^2)^2}) \qquad (33)
\end{aligned}
$$

where the explicit form for $\omega(q)$ has been used. The expression is now Galilei invariant, since it depends only on the relative momenta Q and Q'. The expression of equation (33) can be interpreted as the direct and exchange matrix elements of a local potential. In agreement with the scalar nature of the exchanged meson, the interaction is independent

from the spins of the nucleons. The form of such a potential in coordinate representation is the celebrated Yukawa potential

$$v(r) = -G_s^2 \frac{\hbar}{V} \sum_q \frac{1}{q^2c^2 + (mc^2)^2} e^{\imath \mathbf{q}\cdot\mathbf{r}/\hbar} = -\frac{G_s^2}{4\pi\hbar^2c^3}(mc^2)\frac{e^{-\mu r}}{\mu r}$$

The range $a = 1/\mu = \hbar/mc$ of this potential is the Compton wavelength of the meson. This means that heavier mesons produce shorter potential range. The limit of large nucleon mass is equivalent to neglect the recoil energy of the nucleons involved in the interaction. It is also equivalent to consider the exchange of the meson as instantaneous, and therefore the approximation is usually referred to as the static approximation. It is only in this limit that the very concept of potential can be introduced. For the validity of such an approximation it is essential that the ratio between meson and nucleon masses be small. Unfortunately not all the possible mesons which can be considered involved in the nucleon-nucleon interaction processes have indeed a mass small compared to the nucleon one. The potentials derived from heavier meson exchange processes have therefore to be considered as effective ones, and the corresponding parameters as effective ones. The latter can therefore differ from the phenomenological ones extracted from meson nucleon scattering. Equation (25) is schematic, since mesons and nucleons are not point-like particles, and therefore a more refined treatment must introduce vertex corrections in the interaction processes. Usually these corrections are described by phenomenological vertex form factors which multiply the expressions of the type of equation (33) for the NN potentials. The corresponding form in coordinate representation is modified accordingly. From the above results it turns out that the local potential mediated by a scalar meson is attractive. This is the case of the so-called σ meson, which is commonly believed to be responsible of the intermediate range attraction characteristic of the two nucleon interaction. The lightest known (strongly interacting) meson, the π meson, is known to be a pseudoscalar meson, i.e. a meson with negative internal parity, which is therefore described by a field which change sign under the parity operation. For the π meson the scalar coupling of equation (25) cannot be used, since the Hamiltonian of strong interaction must be parity invariant. In the non-relativistic limit the only possibility in this case is a pseudo-vector coupling. Furthermore the π meson has three charge states and it is therefore a vector in isospin space. The simplest non-relativistic coupling is of the form

$$H_c = G_{pv}\frac{1}{\sqrt{V}}\sum_{kq}\sqrt{\frac{\hbar}{2\omega(q)}}({a^\dagger}_k(\sigma\cdot\mathbf{q})\tau a_{k+q}{b^\dagger}_q + {a^\dagger}_k(\sigma\cdot\mathbf{q})\tau a_{k-q}b_q)$$

where now the b and $b^\dagger$ operators refer to the π meson. The quantities $\sigma \equiv \sigma_x, \sigma_y, \sigma_z$ are the usual Pauli matrices which act on the spin variables of the nucleon creation and annihilation operators. The particular form ensures rotational invariance. Since the Pauli matrices form a pseudo-vector, the expression for H_c is indeed a scalar. The matrices $\tau \equiv \tau_x, \tau_y, \tau_z$ are the Pauli matrices in isospin spaces and as such they act on the isospin variables of the nucleon operators. The expression includes a scalar product

of these three Pauli matrices, which form a three-vector, with the isospin variables of the meson operator, namely $\tau b \equiv \sum_i \tau_i b_i$ (and analogously for $b^\dagger$), where i labels the three possible isospin (charge) states of the π meson. The scalar product ensures that H_c is scalar in isospin space, and this is dictated by the charge independence of the nuclear forces, which is phenomenologically observed to a very high degree of accuracy. Following the same procedure as in the case of a scalar meson, one gets the following expression for the direct matrix element of the interaction in the static limit, with $k = Q - Q'$

$$\langle Q'P'|v|QP\rangle = -G_{pv}^2 \frac{\hbar}{V} \delta_K(P - P') \frac{(\sigma_1 \cdot \mathbf{k})(\sigma_2 \cdot \mathbf{k})}{k^2c^2 + (mc^2)^2} (\tau_1 \cdot \tau_2) \tag{34}$$

where the matrix elements between spin-isospin states of the corresponding Pauli matrices have to be taken, i.e. the expression has to be considered still an operator in spin-isospin space. It is customary to introduce the tensor operator

$$S_{12} \;=\; 3(\sigma_1 \cdot \mathbf{k})(\sigma_2 \cdot \mathbf{k}) - \sigma_1 \cdot \sigma_2 k^2$$

and the expression can be written

$$\begin{aligned}\langle Q'P'|v|QP\rangle = \; & -\frac{1}{12} G_{pv}^2 \frac{\hbar}{V} \delta_K(P - P') \cdot \\ & [\frac{S_{12}}{k^2c^2 + (mc^2)^2} - \sigma_1 \cdot \sigma_2 \frac{m^2c^2}{k^2c^2 + (mc^2)^2} + \sigma_1 \cdot \sigma_2] \tau_1 \cdot \tau_2 \end{aligned} \tag{35}$$

A pseudoscalar meson gives rise to a tensor-isospin interaction plus a spin-isospin interaction. The last term is a contact interaction (a delta function in coordinate space). A more complete treatment should include the vertex form factors also in this case. It has to be noticed that the coupling constant has a different definition here than in the relativistic treatment. More complex couplings are possible, and they naturally arise in a relativistic treatment, which is the framework in which the theory of nuclear forces has ultimately to be formulated. The interaction is attractive or repulsive according to the quantum numbers of the interacting nucleons, namely on the two-body channel (including isospin). It turns out that the tensor part is attractive in the s-wave channels. The π meson is responsible of the long range attractive part of the NN interaction. Another important case is the exchange of a vector meson, namely a meson of spin one. The treatment of this case is more complex and require a full relativistic treatment. It turns out that a vector meson produces mainly a repulsive interaction. Therefore, at least part of the repulsive core, characteristic of the NN interaction, can be described by the exchange of spin-one mesons, like the ω meson. However, at distances smaller than the typical core size ($\sim 0.4\ fm$) the structure of the nucleons, as described by QCD, starts to play a role and the meson picture cannot be any more maintained. The meson theory in this range can be regarded as an effective model for more complex processes and the corresponding coupling constants and cut-off have to be considered as parameters to be adjusted to fit the experimental data on NN scattering.

In all these considerations, one assumes that only one meson is exchanged at a time, so that the NN interaction is fully determined by the set of known mesons and by their

couplings with nucleons. This is the so-called one boson exchange potential (OBEP). It turns out, however, that the intermediate range attraction cannot be obtained in this way. As already mentioned, it is customary then to introduce a fictitious scalar meson, the σ meson, with suitable mass and coupling to reproduce the phenomenological intermediate range attraction. It is usually believed that the hypothetical σ meson simulates the simultaneous exchange of two pions both correlated and uncorrelated. The phenomenology on pion–pion scattering gives only a broad structure in the s-wave channel, and therefore a fully satisfactory theoretical basis for the introduction of the σ meson is still lacking. For a historical account of the OBEP theory, see reference [70].

The main features of the NN interaction, derived from the meson-nucleon model and the phenomenological analysis, can be summarized schematically as in figure (6). At large distance, $r \geq 1fm$, the interaction is attractive with an exponential tail. At intermediate distance, $0.4 \leq r \leq 1fm$, a stronger attraction is present, at least once an average is made over the different partial waves and quantum numbers (i.e., channels). At short distance, $r \leq 0.4fm$, a strong repulsive core is in any case present. The repulsion is so strong that in the early versions of the NN potential an infinite impenetrable barrier was assumed to exist below about $0.4fm$. In the more modern versions the repulsive core is taken finite but very large with respect to the usual nuclear physics energy scale. The details of the interaction depend on the specific model for

Figure 6. Schematic representation of the nucleon-nucleon interaction potential.

NN forces, but schematic picture of Fig. (6) is in any case valid and the nuclear matter EOS is strongly influenced by these simple properties.

4.2. Theoretical many-body methods

Once the interaction between two nucleons is established, one can try to solve the many-body problem for the nuclear matter. However, it is not obvious that the nuclear Hamiltonian includes only two-body forces. Since we know that the nucleon is not an elementary particle, we can expect that the interaction in a system of nucleons is not fully additive, namely that it is not simply the sum of the interactions between pairs of nucleons, but also three or more nucleon forces must be considered. This important issue is discussed later. For the moment we restrict the treatment to the case of two-body forces, which are expected anyhow to be dominant around saturation or slightly above.

4.2.1. The Brueckner-Bethe-Goldstone expansion The Brueckner-Bethe-Goldstone (BBG) many-body theory is based on the re-summation of the perturbation expansion of the ground state energy. The original bare NN interaction is systematically replaced by an effective interaction that describes the in-medium scattering processes. The in-vacuum T-matrix of the general equation (22) is replaced by the so called G-matrix, that takes into account the effect of the Pauli principle on the scattered particles and the in-medium potential $U(k)$ felt by each nucleon. The corresponding integral equation for the G-matrix can be written

$$\langle k_1 k_2 | G(\omega) | k_3 k_4 \rangle \;=\; \langle k_1 k_2 | v | k_3 k_4 \rangle \, +$$

$$+ \sum_{k_3' k_4'} \langle k_1 k_2 | v | k_3' k_4' \rangle \, \frac{\big(1 - \Theta_F(k_3')\big)\big(1 - \Theta_F(k_4')\big)}{\omega - e_{k_3'} + e_{k_4'}} \, \langle k_3' k_4' | G(\omega) | k_3 k_4 \rangle \quad . \tag{36}$$

where the two factors $1 - \Theta_F(k)$ force the intermediate momenta to be above the Fermi momentum ("particle states"), the single particle energy $e_k = \hbar^2 k^2 / 2m + U(k)$ and the summation includes spin-isospin variables.. The G-matrix has not any more the hard core of the original bare NN interaction and is defined even for bare interaction with an infinite hard core. In this way the perturbation expansion is more manageable. The introduction and choice of the single particle potential are essential to make the re-summed expansion convergent. In order to incorporate as much as possible higher order correlations the single particle potential is calculated self-consistently with the G-matrix itself

$$U(k) \;=\; \sum_{k' < k_F} \langle k k' | G(e_{k_1} + e_{k_2}) | k k' \rangle \quad , \tag{37}$$

An account on the diagrammatic method, the degree of convergence of the BBG expansion and a summary of the results can be found in references [40, 76]. Here we restrict to indicate the expression of the correlation energy at the so called Brueckner level ("two hole-line" approximation)

$$\Delta E_2 \;=\; \frac{1}{2} \sum_{k_1, k_2 < k_F} \langle k_1 k_2 | G(e_{k_1} + e_{k_2}) | k_3 k_4 \rangle_A \quad , \tag{38}$$

where $|k_1 k_2\rangle_A = |k_1 k_2\rangle - |k_2 k_1\rangle$. At this level of approximation, that mainly includes two-body correlations, one can find that the corresponding ground state wave function Ψ can be written consistently as

$$|\Psi\rangle \;=\; e^{\hat{S}_2} |\Phi\rangle \quad , \tag{39}$$

where Φ is the unperturbed free particle ground state and $\hat{S}_2$ is the two-particle correlator

$$\hat{S}_2 \;=\; \sum_{k_1 k_2, k_1' k_2'} \frac{1}{4} \langle k_1' k_2' | S_n | k_1 k_2 \rangle a^\dagger(k_1') a^\dagger(k_2') \, a(k_2) a(k_1) \tag{40}$$

where the k ' s are hole momenta, i.e. inside the Fermi sphere, and the k' ' s are particle momenta, i.e. outside the Fermi sphere. The function $\hat{S}_2$ is the so called "defect function". It can be written in term of the G-matrix and it is just the difference

between the in-medium interacting and non interacting two-body wave functions [40, 76]. A recent systematic study of the dependence of the resulting EoS on the NN interaction can be found in reference [79].

One of the well known results of all these studies, that lasted for about half a century, is the need of three-body forces (TBF) in order to get the correct saturation point in symmetric nuclear matter. Once the TBF are introduced, the resulting EoS, for symmetric matter and pure neutron matter, is reported in figure (7) for the two-body interaction Av_{18} (squares). The TBF produce a shift in energy of about $+1$ MeV in energy and of about -0.01 fm $^{-3}$ in density. This adjustment is obtained by tuning the two parameters contained in the TBF, as in references [77, 78, 79] and was performed to get an optimal saturation point (the minimum). For comparison is also reported

Figure 7. Symmetric and pure neutron matter EOS from BHF scheme including TBF (squares). The full lines is a fit to the points. The circles indicate the EoS from reference [57].

the variational EOS of reference [57], that will be discussed in the next section. The connection between two-body and three-body forces within the meson-nucleon theory of nuclear interaction is discussed and worked out in references [80, 81, 82]. The possible interplay between two-body interaction and TBF for the resulting EoS is discussed in reference [83].

4.2.2. The Variational method In the variational method one assumes that the ground state wave function Ψ can be written in a form as in equation (39), i.e.

$$\Psi(r_1, r_2, ...) = \Pi_{i<j} f(r_{ij}) \Phi(r_1, r_2, ...) \quad , \tag{41}$$

where Φ is the unperturbed ground state wave function, properly antisymmetrized, and the product runs over all possible distinct pairs of particles. The correlation factor is here determined by the variational principle, i.e. by imposing that the mean value of the Hamiltonian gets a minimum (or in general stationary point)

$$\frac{\delta}{\delta f} \frac{\langle \Psi | H | \Psi \rangle}{\langle \Psi | \Psi \rangle} = 0 \ . \tag{42}$$

In principle this is a functional equation for the correlation function f, which however can be written explicitly in a closed form only if additional suitable approximations are introduced. The function $f(r_{ij})$ is assumed to converge to 1 at large distance and to go rapidly to zero as $r_{ij} \to 0$, to take into account of the repulsive hard core of the NN interaction. Furthermore, at distance just above the core radius a possible increase of the correlation function beyond the value 1 is possible.

For nuclear matter it is necessary to introduce a channel dependent correlation factor, which is equivalent to assume that f is actually a two-body operator $\hat{F}_{ij}$. One then assumes that $\hat{F}$ can be expanded in the same spin-isospin, spin-orbit and tensor operators appearing in the NN interaction. Momentum dependent operators, like spin-orbit, are usually treated separately. The product in equation (41) must be then symmetrized since the different terms do not commute anymore.

If the two-body NN interaction is local and central, its mean value is directly related to the pair distribution function $g(\mathbf{r})$

$$< V > = \frac{1}{2}\rho \int d^3 r v(r) g(\mathbf{r}) \quad , \tag{43}$$

where

$$g(\mathbf{r_1} - \mathbf{r_2}) \; = \; \frac{\int \Pi_{i>2} d^3 r_i |\Psi(r_1, r_2 ....)|^2}{\int \Pi_i d^3 r_i |\Psi(r_1, r_2 ....)|^2} \quad . \tag{44}$$

The main job in the variational method is to relate the pair distribution function to the correlation factors F. Again, in nuclear matter also the pair distribution function must be considered channel dependent and the relation with the correlation factor becomes more complex. In general this relation cannot be worked out exactly, and one has to rely on some suitable expansion. Furthermore, three-body or higher correlation function must in general be introduced, which will depend on three or more particle coordinates and describe higher order correlations in the medium. Many excellent review papers exist in the literature on the variational method and its extensive use for the determination of nuclear matter EoS [84, 85]. The best known and most used variational nuclear matter EoS is the one of reference [57], and it is reported in figure (7). A detailed discussion on the connection between variational method and BBG expansion can be found in reference [40].

4.2.3. The Relativistic approach One of the deficiencies of the Hamiltonian considered in the previous sections is the use of the non-relativistic limit. The relativistic framework is of course the framework where the nuclear EoS should be ultimately based. The best relativistic treatment developed so far is the Dirac-Brueckner approach. Excellent review papers on the method can be found in the literature [86] and in textbooks [87]. Here we restrict the presentation to the main basic elements of the theory.

In the relativistic context the only NN potentials which have been developed are the ones of OBE (one boson exchange) type. The starting point is the Lagrangian for

the nucleon-mesons coupling

$$\mathcal{L}_{pv} = -\frac{f_{ps}}{m_{ps}}\overline{\psi}\gamma^5\gamma^\mu\psi\partial_\mu\varphi^{(ps)} \tag{45}$$

$$\mathcal{L}_s = +g_s\overline{\psi}\psi\varphi^{(s)} \tag{46}$$

$$\mathcal{L}_v = -g_v\overline{\psi}\gamma^\mu\psi\varphi_\mu^{(v)} - \frac{f_v}{4M}\overline{\psi}\sigma^{\mu\nu}\psi(\partial_\mu\varphi_\nu^{(v)} - \partial_\nu\varphi_\mu^{(v)}) \tag{47}$$

with ψ the nucleon and $\varphi_{(\mu)}^{(\alpha)}$ the meson fields, where α indicates the type of meson and μ the Lorentz component in the case of vector mesons. For isospin 1 mesons, $\varphi^{(\alpha)}$ is to be replaced by $\boldsymbol{\tau}\cdot\boldsymbol{\varphi}^{(\boldsymbol{\alpha})}$, with τ^l ($l = 1, 2, 3$) the usual Pauli matrices. The labels ps, pv, s, and v denote pseudoscalar, pseudovector, scalar, and vector coupling/field, respectively.

The one-boson-exchange potential (OBEP) is defined as a sum of one-particle-exchange amplitudes of certain bosons with given mass and coupling. The main difference with respect to the non-relativistic case is the introduction of the Dirac-spinor amplitudes. The six non-strange bosons with masses below 1 GeV/c^2 are used. Thus,

$$V_{OBEP} = \sum_{\alpha=\pi,\eta,\rho,\omega,\delta,\sigma} V_\alpha^{OBE} \tag{48}$$

with π and η pseudoscalar, σ and δ scalar, and ρ and ω vector particles. The contributions from the isovector bosons π, δ and ρ contain a factor $\boldsymbol{\tau_1}\cdot\boldsymbol{\tau_2}$. In the so called static limit, i.e. treating the nucleons as infinitely heavy (their energy equals the mass) the usual denominator of the interaction amplitude in momentum space, coming from the meson propagator, is exactly the same as in the non-relativistic case (since in both cases meson kinematics is relativistic). This limit is not taken in the relativistic version, noticeably in the series of Bonn potentials, and the full expression of the amplitude with the nucleon relativistic (on-shell) energies is included. As an example, let us consider one pion exchange. In the non-relativistic and static limit the corresponding local potential is reported in equation (34). This has to be compared with the complete expression of the matrix element between nucleonic (positive energy) states [71]. In the center of mass frame it reads

$$V_\pi^{full} = -\frac{g_\pi^2}{4M^2}\frac{(E'+M)(E+M)}{k^2c^2+(mc^2)^2}\left(\frac{\sigma_1\cdot\mathbf{q}'}{E'+M} - \frac{\sigma_1\cdot\mathbf{q}}{E+M}\right)\times\left(\frac{\sigma_2\cdot\mathbf{q}'}{E'+M} - \frac{\sigma_2\cdot\mathbf{q}}{E+M}\right)$$

where E, E' are the initial and final nucleon energies. One can see that in this case some non-locality is present, since the matrix element depends separately on $\mathbf{q}$ and $\mathbf{q}'$. Putting $E = E' = M$, one gets again the local version. Notice that in any case the two versions coincide on-shell ($E = E'$), and therefore the non-locality modifies only the off-shell behaviour of the potential. The matrix elements are further implemented by form factors at the NN-meson vertices to regularize the potential and to take into account the finite size of the nucleons and the mesons. In applications of the DBHF method usually one version of the relativistic OBE potential is used, which therefore implies that a certain degree of non-locality is present. The fully relativistic analogue of the two-body

scattering matrix is the covariant Bethe-Salpeter (BS) equation. In place of the NN non-relativistic potential the sum $\mathcal{V}$ of all connected two-particle irreducible diagrams has to be used, together with the relativistic single particle propagators. Explicitly, the BS equation for the covariant scattering matrix $\mathcal{T}$ in an arbitrary frame can be written

$$\mathcal{T}(q',q|P) = \mathcal{V}(q',q|P) + \int d^4k \mathcal{V}(q',k|P)\mathcal{G}(k|P)\mathcal{T}(k,q|P) \ , \tag{49}$$

with

$$\mathcal{G}(k|P) = \frac{i}{(2\pi)^4} \frac{1}{(\frac{1}{2}\ \not{P} + \not{k} - M + i\epsilon)^{(1)}} \frac{1}{(\frac{1}{2}\ \not{P} - \not{k} - M + i\epsilon)^{(2)}} \tag{50}$$

$$= \frac{i}{(2\pi)^4} \left[\frac{\frac{1}{2}\ \not{P} + \not{k} + M}{(\frac{1}{2}P + k)^2 - M^2 + i\epsilon} \right]^{(1)} \left[\frac{\frac{1}{2}\ \not{P} - \not{k} + M}{(\frac{1}{2}P - k)^2 - M^2 + i\epsilon} \right]^{(2)} \tag{51}$$

where q, k, and q' are the initial, intermediate, and final relative four-momenta, respectively (with e. g. $k = (k_0, \mathbf{k})$), and $P = (P_0, \mathbf{P})$ is the total four-momentum; $\not{k} = \gamma^\mu k_\mu$. The superscripts refer to particle (1) and (2). Of course all quantities are appropriate matrices in spin (or helicity) and isospin indices. The use of the OBE potential as the kernel $\mathcal{V}$ is equivalent to the so-called ladder approximation, where one meson exchanges occur in disjoint time intervals with respect to each other, i.e. at any time only one meson is present. Unfortunately, even in the ladder approximation the BS equation is difficult to solve since $\mathcal{V}$ is in general non-local in time, or equivalently energy dependent, which means that the integral equation is four-dimensional. It is even not sure in general if it admits solutions. It is then customary to reduce the four-dimensional integral equation to a three-dimensional one by approximating properly the energy dependence of the kernel. In most methods the energy exchange k_0 is fixed to zero and the resulting reduced BS equation is similar to its non-relativistic counterpart. In the Thompson reduction scheme this equation for matrix elements between positive-energy spinors (c.m. frame) reads

$$\mathcal{T}(\mathbf{q}',\mathbf{q}) = V(\mathbf{q}',\mathbf{q}) + \int \frac{d^3k}{(2\pi)^3} V(\mathbf{q}',\mathbf{k}) \frac{M^2}{E_{\mathbf{k}}^2} \frac{1}{2E_{\mathbf{q}} - 2E_{\mathbf{k}} + i\epsilon} \mathcal{T}(\mathbf{k},\mathbf{q}|\mathbf{P}) \tag{52}$$

where both $V(\mathbf{q}',\mathbf{q})$ and $\mathcal{T}$ have to be considered as matrices acting on the two-particle helicity (or spin) space, and $E_{\mathbf{k}} = \sqrt{\mathbf{k}^2 + M^2}$ is the relativistic particle energy. In the alternative Blankenbecler-Sugar [71] reduction scheme some different relativistic kinematical factors appear in the kernel. This shows that the reduction is not unique. The partial wave expansion of the $\mathcal{T}$–matrix can then be performed starting from the helicity representation. The corresponding amplitudes include single as well as coupled channels, with the same classification in quantum numbers JLS as in the non relativistic case and therefore their connection with phase shifts is the same. In the intermediate states of momentum $\mathbf{k}$ only the positive energy states are usually considered (by the proper Dirac projection operator). As in the case of the OBEP potential, again the main difference with respect to the non-relativistic case is the use of the Dirac spinors.

The DBHF method can be developed in analogy with the non-relativistic case. The two-body correlations are described by introducing the in-medium relativistic G-matrix.

The DBHF scheme can be formulated as a self-consistent problem between the single particle self-energy Σ and the G-matrix. Schematically, the equations can be written

$$\begin{aligned} G &= V + i\int VQggG \\ \Sigma &= \; -i\int_F (Tr[gG] - gG) \end{aligned} \tag{53}$$

where Q is the Pauli operator which projects the intermediate two particle momenta outside the Fermi sphere, as in the BHF G-matrix equation, and g is the single particle Green' s function. The self consistency is entailed by the Dyson equation

$$g = g_0 + g_0\Sigma g$$

where g_0 is the (relativistic) single particle Green's function for a free gas of nucleons. The self-energy is a matrix in spinor indices, and therefore in general it can be expanded in the covariant form

$$\Sigma(k, k_F) = \Sigma_s(k, k_F) - \gamma_0\Sigma_0(k, k_F) + \boldsymbol{\gamma}\cdot\mathbf{k}\Sigma_v \tag{54}$$

where γ_μ are the Dirac gamma matrices and the coefficients of the expansion are scalar functions, which in general depend on the modulus $|\mathbf{k}|$ of the three-momentum and on the energy k_0. Of course they also depend on the density, i.e. on the Fermi momentum k_F. The free single particle eigenstates, which determine the spectral representation of the free Green' s function, are solutions of the Dirac equation

$$[\ \gamma_\mu k^\mu \ - \ M \ ]\, u(k) \ = \ 0$$

where u is the Dirac spinor at four-momentum k. For the full single particle Green's function g the corresponding eigenstates satisfy

$$[\ \gamma_\mu k^\mu \ - \ M \ + \ \Sigma \ ]\, u(k)^* \ = \ 0$$

Inserting the above general expression for Σ, after a little manipulation, one gets

$$[\ \gamma_\mu k^{\mu *} \ - \ M^* \ ]u(k)^* \ = \ 0$$

with

$$k^{0*} \ = \ \frac{k^0 + \Sigma_0}{1 + \Sigma_v} \quad ; \quad k^{i*} \ = \ k^i \quad ; \quad M^* \ = \ \frac{M + \Sigma_s}{1 + \Sigma_v} \tag{55}$$

This is the Dirac equation for a single particle in the medium, and the corresponding solution is the spinor

$$u^*(\mathbf{k}, s) = \sqrt{\frac{E^*_{\mathbf{k}} + M^*}{2M^*}} \begin{pmatrix} 1 \\ \frac{\boldsymbol{\sigma}\cdot\boldsymbol{k}}{E^*_{\mathbf{k}} + M^*} \end{pmatrix} \chi_s \quad ; \quad E^*_{\mathbf{k}} = \sqrt{\mathbf{k}^2 + {M^*}^2} \ . \tag{56}$$

In line with the Brueckner scheme, within the BBG expansion, in the self-energy of equation (53) only the contribution of the single particle Green' s function pole is considered (with strength equal one). Furthermore, negative energy states are neglected

and one gets the usual self–consistent condition between self–energy and scattering G–matrix. The functions to be determined are in this case the three scalar functions appearing in equation (54). However, to simplify the calculations these functions are often replaced by their value at the Fermi momentum.

In any case, the medium effect on the spinor of equation (56) is to replace the vacuum value of the nucleon mass and three–momentum with the in–medium values of equation (55). This means that the in–medium Dirac spinor is "rotated" with respect to the corresponding one in vacuum, and a positive (particle) energy state in the medium has some non–zero component on the negative (anti–particle) energy state in vacuum. In terms of vacuum single nucleon states, the nuclear medium produces automatically anti–nucleon states which contribute to the self–energy and to the total energy of the system. It has been shown in reference [88] that this relativistic effect is equivalent to the introduction of well defined TBF at the non–relativistic level. These TBF turn out to be repulsive and consequently produce a saturating effect. The DBHF gives indeed in general a better SP than BHF. Of course one can wonder why these particular TBF should be selected, but anyhow a definite link between DBHF and BHF + TBF is, in this way, established. Indeed, including in BHF only these particular TBF one gets results close to DBHF calculations, see e.g. reference [79].

Despite the DBHF is similar to the non–relativistic BHF, some features of this method are still controversial. The results depend strongly on the method used to determine the covariant structure of the in–medium G–matrix, which is not unique since only the positive energy states must be included. It has to be stressed that, in general, the self–energy is better calculated in the matter reference frame, while the G–matrix is more naturally calculated in the center of mass of the two interacting nucleons. This implies that the G–matrix has to be Lorentz transformed from one reference frame to the other, and its covariant structure is then crucial. Formally, the most accurate method appears to be the subtraction scheme of reference [89]. Generally speaking, the EoS calculated within the DBHF method turn out to be stiffer above saturation than the ones calculated from the BHF + TBF method.

4.2.4. The V_{low} approach The main effect of the hard core in the NN interaction is to produce scattering to high momenta of the interacting particles. It is possible to soften the hard core of the NN interaction from the start by integrating out all the momenta larger than a certain cutoff Λ and "renormalize" the interaction to an effective interaction V_{low} in such a way that it is equivalent to the original interaction for momenta $q < \Lambda$. By construction V_{low} must give the same half of the energy shell scattering T-matrix or R-matrix $(q'|R(E_q)|q)$ as the original interaction, where E_q is the energy of the initial state at relative momentum q. This can be done in a variety of methods, among which one can mention the Renormalization Group, the low momenta Effective Theory and the Lee-Suzuky scheme. It is surely outside the scope of the present report to describe these methods and we refer to recent review and papers where they are extensively discussed and applied [90, 91]. All these possible V_{low} interactions are of course much

softer, since no high momentum components are present. The short range repulsion is replaced by the non local structure of the interaction. It has to be kept in mind that any V_{low} is a legitimate realistic NN interaction. In fact, due to the mentioned equivalence, they fit exactly the same phase shifts up to an energy corresponding to the cutoff. The latter is taken above 300 MeV in the laboratory, corresponding to relative momentum $q \approx 2.1\text{fm}^{-1}$, that is the largest energy where the data are established. This means that the data and the NN interaction are not sensitive to the details of the hard core behavior. Indeed, for the same reason, all the V_{low}, at least their diagonal matrix elements, are almost identical up to the cutoff, provided it is not taken too large above 2.1fm^{-1}. The fact that V_{low} is soft has the advantage to be much more manageable than a hard core interaction, in particular it can be used in perturbation expansion and in nuclear structure calculations in a more efficient way. Again, at purely phenomenological level, a non-local interaction at short distance is perfectly legitimate as an hard core, since the behavior of the potential at short distance is not experimentally accessible. In principle, it is only a question of representation. However, as strongly stressed in reference [90], the required equivalence implies that, even starting from a local two-body interaction , the renormalization procedure introduces necessarily three-body forces, which has to be handled in many-body calculations. This is more apparent if V_{low} is constructed directly in the medium, in which case the procedure has some similarities with the Brueckner G-matrix construction.

If for the in-vacuum V_{low} one takes only the two-body component, one finds that nuclear matter does not saturate and actually seems to collapse towards infinite negative energy. This can be ascribed to the missing three-body forces, which should provide saturation. According to reference [90] the off-shell effects are not the main responsible for the saturation mechanism present in the BHF theory. This is probably partly true, but one has to keep in mind that a BHF procedure without the single particle potential, which is responsible for the presence of an off-shell energy, would dramatically overestimate the binding energy in nuclear matter.

In any case, up to now the consistent three-body force in V_{low} has not be used in nuclear matter calculations or in nuclear structure. Furthermore the renormalization procedure for a possible three-body forces has not yet been worked out. Up to now the two-body part of V_{low} has been used in nuclear matter in conjunction with TBF fitted separately in three and four-nucleon systems. If the TBF are averaged over the quantum numbers of one of the three particles, this approximate scheme seems to produce a reasonable saturation point. This is line with the fact that in BHF the repulsive part of the same TBF has to be drastically reduced to get the correct saturation point, since the two-body interaction gives a saturation point not too far from the empirical one. If the saturation property of V_{low} and its good performance in few-body nuclear systems will survive to a more consistent treatment of the renormalization procedure and the corresponding TBF, this will open a new route to the microscopic many-body theory of the nuclear medium. This point needs still to be clarified.

4.2.5. Trying a link to QCD : the chiral symmetry approach One of the main ambition of nuclear physics is to connect the low energy nuclear physics phenomena with the underlying more fundamental theory of strong interaction, i.e. QCD and the standard model, based on quark and gluons degrees of freedom, together with the Weinberg-Salam-Glashow theory of weak interaction. This is quite difficult because all hadron sector is in the non-perturbative regime, due to confinement. A possible strategy is the systematic use of the symmetries embodied in the hadronic QCD structure. The main symmetry that still remains visible in the confined matter is the Chiral Symmetry, the symmetry that QCD possesses if the bare quark masses are put equal to zero. The symmetry is spontaneously broken in the confined phase, i.e in hadronic matter, but, according to the general theorem by Goldstone, a zero mass boson should be present. This is indeed the π meson, that in the limit of zero quark mass should have also zero mass. This is the main signature of the underling chiral symmetry. For non-strange matter, only u and d quarks are relevant, and they indeed are expected to have a mass of few MeV. This small explicit breaking of chiral symmetry results in the physical mass of the pion, that is the lightest meson, even if it is not small at the energy scale of many nuclear phenomena. All that suggests to treat the pion degrees of freedom explicitly and to describe the short range part by structureless contact terms. Along this line Weinberg [92, 93, 94] proposed a scheme for the expansion of the NN interaction in the ratio Q/M between the relative momenta and the nucleon mass. The pion exchange term is still treated explicitly, and is considered the lowest order (LO) term of the expansion. Then contact terms are added and a power counting scheme is introduced. These terms can be considered as expansion of the nucleonic loops, that are the ones that give the largest contributions. At the same time the contact terms can be considered as counter-terms to regularize and renormalize the divergences coming from the loop integrals appearing as the order of the expansion increases. This procedure of renormalization is common in Quantum Field Theory, like Quantum Electrodynamics (QED). In renormalizable field theory the number of counter-terms are finite and their strengths are fixed by demanding that some quantities have their physical values. In QED they are fixed by imposing the physical values of the electron charge and mass. Then the perturbation expansion terms are all finite. In the case of nuclear physics one demands that the phase shifts in some channels and specific energies are reproduced correctly. However in this case at any order new counter-terms must be introduced. This renormalized expansion, the Chiral Perturbation Expansion (ChPE), can be used to construct NN interactions that are of reasonably good quality [91, 95] in reproducing the two-body data. They contain a set of parameters, and therefore they are still models, whose connection with QCD is still a little loose. To tighten the QCD link a non-perturbative regularization and renormalization has been tried, where the results are shown numerically to be independent on the single cut-off used in the renormalization procedure. This property assures a clear-cut separation between the long range pion exchange processes and the unresolved short range part of the interaction. Along this line progress has been made recently [96], but still a reasonable realistic interaction has not been constructed.

To summarize, the ambitious program of connecting the NN interaction with the underlying QCD theory is still a work in progress, but the connection is becoming stronger and solid. It requires the development of a quite complex formalism, that is hoped will be able to shed light on the origin of the NN interaction, including few-body interactions.

5. Nuclear Matter as a Fermi liquid

The many fermion systems are characterized by a sharp Fermi surface. If the interaction is not too peculiar, this is a general result known as Migdal' s theorem [4]. The nuclear medium is not an exception, and many properties of both finite nuclei and nuclear matter are strongly affected by this feature. In particular, low energy excitations and low temperature thermal properties can involve only particles close to the Fermi surface. For the same reason transport phenomena are determined by the scattering processes that occur close to the Fermi surface.

Landau theory of (normal) Fermi liquids exploits systematically this feature to develop a semi-phenomenological treatment of most of the low energy phenomena in homogeneous Fermi systems. Nuclear matter can be treated along the same lines, provided the isospin degrees of freedom is properly included. Migdal and collaborators [4, 97] have extended the approach to finite systems, in particular nuclei, where the so called Finite Fermi System Theory (FFST) has been extensively applied. Excellent and pedagogical expositions of Landau theory can be found in textbooks [4, 98]. Here we limit to remind the main concepts and some basic applications. At the basis of the theory is the introduction of quasi-particle states. The suggestion comes form the so-called adiabatic switching on of the interaction in a many-body system. The Gell-Mann and Low [99] theorem states that if one evolves a many-particle system, starting from an independent particle eigen-state, by switching on the interaction adiabatically, i.e. with an infinitely slow variation, then one obtains a state of the interacting system. Since for independent particles eigen-states are identified by the values of the occupation number $n(p)$ for each single particle state $p \equiv (\vec{p}, \sigma, \tau)$, so will be the corresponding state of the interacting system. The statement is correct if no phase transition or cluster formation occur during the switching on of the interaction, and this is what we assume for the moment. It follows that the ground state of the interacting system will be characterized by a distribution of occupation numbers as the non-interacting one, i.e. a sharp Fermi distribution (zero temperature). If we consider the excitation of the non interacting system that is obtained by adding a particle or forming a hole (i.e. subtracting a particle) at the single particle state p, these excitations will be called quasi-particle and quasi-hole in the interacting system. The corresponding variation in energy of the interacting many-particle system is called quasi-particle or quasi-hole energy, denoted by $\epsilon(p)$. In general, if we vary the distribution of occupation numbers in a smooth way, or we average the distribution within neighboring states, the general variation in energy

δE of the system to first order in the variation $\delta n(p)$ of the occupations can be written

$$\delta E \;=\; \frac{1}{\Omega}\sum_p \epsilon(p)\delta n(p) \tag{57}$$

where Ω is the volume of the system. It is clear that the quasi-particles are Fermions. However, unlike in the non-interacting system, they do interact, since the variation of the total energy will be a complex function of the variation $\delta n(p)$ and not just an additive linear function. To second order the energy variation will be

$$\delta E \;=\; \frac{1}{\Omega}\sum_p \epsilon(p)\delta n(p) \;+\; \frac{1}{2}\frac{1}{\Omega^2}\sum_{p,p'} f(p,p')\delta n(p)\delta n(p') \tag{58}$$

where

$$f(p,p') \;=\; \Omega^2 \frac{\delta^2 E}{\delta n(p)\delta(p')} \;=\; \Omega \frac{\delta\epsilon(p)}{\delta n(p')} \tag{59}$$

is the quasi-particle interaction, since it describes the variation of a quasi-particle energy due to the presence of the other quasi-particles. More precisely, if the quasi-particle distribution is changed by the amount $\delta n(p')$ for each p', the energy of the quasi-particle of momentum p changes by an amount given by the expression

$$\delta\epsilon(p) \;=\; \sum_{p'} f(p,p')\delta n(p') \tag{60}$$

However, the Gell-Mann and Low theorem is valid only if the perturbative expansion is convergent, since its demonstration is developed by considering each term of the perturbation expansion. This is not necessarily a valid assumption, and the quasi-particle state so constructed can be at best only approximate eigen-states of the system. This is indeed what happens, and the quasi-particle states have a finite lifetime and they actually decay. This can be best seen in the Green' s function formalism, where the Landau theory can be more rigorously formulated [100, 4]. It can be seen that the quasi-particles has an infinite lifetime only exactly at the Fermi surface, while they have a decreasing lifetime as one moves away from the Fermi surface. This is a general property based only on phase space argument. In a perturbative picture, a single quasi-particle can decay into two particles - one hole state (for momenta above the Fermi momentum), or in a two hole - one particle state (below the Fermi momentum), and one can easily see that the possible phase space vanishes exactly at the Fermi momentum. This remains true if one considers more complicated decay states (multi particles - multi holes). Once the quasi-particles are introduced, these considerations hold for the scattering processes between quasi-particles, which are then responsible for the decay. If the quasi-particle have no decay width at the Fermi surface, it is reasonable to expect that close enough to the Fermi surface the width will remain small, and there will be a region around the Fermi surface where the quasi-particles can be considered as stable, provided the phenomena that are considered have characteristic time scales shorter than the lifetime of the quasi-particles involved.

Again in a more formal language, a quasi-particle corresponds to the singular part of the single particle Green's functions, i.e. a pole in the complex energy plane at

a given momentum. The non-singular part should give a negligible contribution in many dynamical processes, since it is expected to be highly incoherent. However the non-singular part has the effect of renormalizing the properties of the quasi-particles. In summary, it is the pole contribution that behaves like a particle, with properly renormalized physical parameters. In this sense a quasi-particle can be viewed as a particle dressed by the interaction with the other particles. The pole moves from one sheet of the complex energy plane to the other, when the momentum moves from below to above the Fermi surface. This means that the occupation number has a jump at the Fermi surface, a property anticipated at the beginning of this section. If we neglect the non-singular part, the quasi-particles distribution in the ground state has to be considered as an unperturbed Fermi distribution, i.e. with occupation number 1 and 0 (at zero temperature), so they are fermion particles.

In summary, the dynamical processes that involve excitations close to the Fermi surface can be described in terms of quasi-particles kinetics, whose dynamics can be treated as particles (fermions), but with renormalized properties. In the semi-classical regime, valid in the long wave-length limit, the kinetic equations for the quasi-particle distribution $n(\mathbf{r}, p, t)$ must follows equations (15,16), where the effective NN interaction, in the momentum representation, is just the Landau effective interaction $f(p, p')$ of equation (59).

One has to be aware that the distribution function $n(\mathbf{r}, p, t)$ that appears in the equations (15,16) is essentially the semi-classical limit of the quantal density matrix $< \psi^\dagger(r', t)\psi(r, t) >$ (to be precise, its Wigner transform) [101]. If we consider a perturbation with total momentum $\mathbf{q}$, one has to consider the Fourier transform of the distribution function, which is equivalent to the density matrix in momentum representation $< \psi^\dagger(p + q, t)\psi(p, t) >$. Therefore, the momenta $p + q$ and p must form a particle-hole pair, i.e. they must lie on opposite sides of the Fermi surface. In fact, any perturbation of a Fermi liquid must imply the promotion of a particle from below to above the Fermi surface, and if the particles are removed from a position slightly different from the position where they are promoted the process involves a *variation* $\delta n(\mathbf{r}, p, t)$ of the distribution function at each point $\mathbf{r}$ which satisfies the kinetic equations (15,16). In the long wave-length limit, i.e. when $|\mathbf{q}|$ is much smaller then the Fermi momentum, the quasi-particle momentum p must lie close to the Fermi surface. Since the effective interaction is expected to be a smooth function, it can be then calculated for values of the momenta just on the Fermi surface, i.e. for $|\mathbf{p}| = |\mathbf{p}'| = p_F$, where p_F is the Fermi momentum. For rotational invariance f must depend only on $|\mathbf{p} - \mathbf{p}'|$. The dependence on the angle θ between $\mathbf{p}$ and $\mathbf{p}'$ can be expanded in Legendre polynomials $P_l(\cos\theta)$. Of course one should include also the spin and isospin dependence, and the explicit expression for f is usually written, following Landau,

$$f(p, p') = f + g\sigma\sigma' + f'\tau\tau' + g'\sigma\sigma'\tau\tau' \tag{61}$$

and each coefficient can be now expanded, e.g.

$$f = \sum_l f_l P_l(\cos\theta) \tag{62}$$

and similar. This defines four sets of parameters, $\{f_l\}, \{g_l\}, \{f'_l\}, \{g'_l\}$. They are basic quantities in the Landau theory. One has not to confuse this expansion with the expansion in partial waves of the NN interaction (effective or not), but rather the different terms in l are connected with the range in non-locality of the particle-hole interaction, or, equivalently, to its momentum dependence. In most applications these parameters are multiplied by the single particle density of state N at the Fermi surface, and one then introduces the dimensionless parameters $F_l = Nf_l$ and similar. The other basic quantity of the Landau theory is the collision integral. It can be worked out [98] for two-body collisions, that are assumed to dominate for not too high density. The two-body collision probability must contain two factors $n(k)$ (Fermi functions) to weight the two occupied initial single particle states and two factors $1-n(k)$ for the Pauli blocking of the two unoccupied final single particle states. Explicitly, the collision integral that has to be included at the second member of the kinetic equations (15,16), reads [98]

$$\begin{aligned} I(p_1) \;=\; & \tfrac{2\pi}{\hbar^2} \textstyle\sum_{p_2,p_3,p_4} | < p_3 p_4 | T | p_1 p_2 > |^2 \\ & \delta(p_1 + p_2 - p_3 - p_4)\delta(\omega_1 + \omega_2 - \omega_3 - \omega_4) \\ & [n_3 n_4 (1-n_1)(1-n_2) - n_1 n_2 (1-n_3)(1-n_4)] \end{aligned} \qquad (63)$$

where T is the scattering T-matrix (in the medium !), $n_i = n(p_i)$ and ω_i is the single particle energy of momentum $\mathbf{p}_i$. Remind that in the adopted notation $p_i = (\mathbf{p}_i, \sigma_i, \tau_i)$. This collision integral gives the probability that a particle of a given momentum p_1 scatters with a particle of any momentum p_2 to all possible final momenta p_3, p_4 (first term in the square bracket) and the probability that two particles of momenta p_3, p_4 scatters to the final momentum p_1 and any other momentum p_2 (second term). The two terms correspond to the loss and gain processes, for the state of momentum p_1, that can occur in the medium. We have not indicated explicitly that actually all the distribution functions appearing in the collision integral are calculated at a given space-time point. This is justified if the range of the interaction producing the collisions is much smaller than the average distance between particles. In this sense the theory is valid for low density, which in this context means that the average number of quasi-particles must be not too large. The collision integrals is the key quantity that determines the different transport coefficients, because if the particle distribution is macroscopically perturbed by an external action, it is through collisions that the system reacts to bring back the distribution to the equilibrium one. The particles through collisions transport different physical quantities, like momentum, energy, and so on, and the frequency of collisions is the main features that fix the speed of this restoration and therefore the corresponding transport coefficients or related quantities.

On the other hand, the set of Landau parameters that characterize the interaction are more related to the mechanical properties of the medium or to the dynamical microscopic processes that can take place.

5.1. *Effective mass*

We have introduced the concept of quasi-particles, and we have anticipated that their physical parameters have to be renormalized. If the interaction $f(p, p')$ depends explicitly on momentum, it changes the relationship between energy and momentum of the quasi-particle due to the dragging effect, see equation (60). The standard result is that the quasi-particle velocity v_k for the momentum k can be written

$$v_k = \frac{d\epsilon(k)}{dk} = \frac{k}{m^*} \tag{64}$$

where the effective mass m^* is given by

$$\frac{m^*}{m} = 1 + \frac{F_1}{3} \tag{65}$$

Here m is the bare mass, and F_1 is the dimensionless constant previously introduced. Only the term $l = 1$ of the expansion (62) contributes. The relation (65) is a consequence of Galilei invariance [98]. The concept of effective mass can be extended also to finite nuclei. It is extensively used in Energy Density Functional schemes or Skyrme forces (see section 8.2) as a parameter, possibly density dependent. Physical quantities that are particularly sensitive to its value are the energy of different Giant Resonances, notably the monopole one, see section 3.2, and the single particle density of states. The latter is mainly proportional to the effective mass.

The canonical value of the effective mass at the saturation density that appears in most of the Skyrme forces is close to $0.7m$. However, the density of state close to the Fermi energy extracted phenomenologically in finite nuclei seems to require a value close to m. This discrepancy can be explained and understood if one introduces dispersive effects in the single particle spectrum [102]. In fact in the nuclear medium it is essential to distinguish between the so called k-mass m_k and ω-mass m_ω. If one considers the single particle self-energy $M(k, \omega)$, the total effective mass can be written [103]

$$\begin{aligned}
\frac{m_\omega}{m} &= \left(1 - \frac{\partial M}{\partial \omega}\right) \\
\frac{m_k}{m} &= \left(1 + \frac{m}{k}\frac{\partial M}{\partial k}\right)^{-1} \\
\frac{m^*}{m} &= \left(\frac{m_\omega}{m}\right)\left(\frac{m_k}{m}\right)
\end{aligned} \tag{66}$$

The ω-mass is due to the energy dependence of the self-energy. In the calculation of the ground state energy and wave function with Skyrme forces the mean field is directly related to the k-mass. In the density of states what is involved is the single particle dynamics, that must include also the ω-mass, and therefore the total mass must be used. Extensive calculations [102] of the single particle levels confirm that indeed the total effective mass around the Fermi energy is close to the bare mass m. Similar results are obtained in microscopic calculations of symmetric nuclear matter [104].

In a general treatment of nuclear structure based on Energy Density Functional method, to be discussed in section 8.2, the effective mass is a parameter to be fixed or fitted to the experimental mass table, and not necessarily the distinction between the

ω-mass and k-mass is apparent or displayed. Therefore the effective mass in nuclear structure is not a well defined concept, nor it can be given a well defined value. In other words, its value depends on the theoretical scheme and on the physical quantity that is considered.

5.2. Static and equilibrium properties

Since Landau theory introduces the interaction between quasi-particles, it can be used to calculate some static and equilibrium properties of an interacting Fermi liquid with respect to a free gas.

In particular the incompressibility of equation (6) is modified, as follows by simple arguments. If the system is compressed, the Fermi energy ϵ_F increases, but the quasi-particles filling the new available states interact among each other, so that, according to equation (60) the variation in the quasi-particle energy is

$$\delta\epsilon(p) \,=\, f_0 \frac{1}{V} \sum_p \delta n(p) \,=\, f_0 \delta n \tag{67}$$

where the spherical symmetry of the distribution has been used. Then the Fermi energy will get an additional variation, with respect to a free gas model, given by equation (67). Since $\delta P = n\delta\epsilon_F$, this means that the incompressibility is multiplied by the factor $(1 + F_0)$, where F_0 is the Landau dimensionless constant for $l = 0$. At the same time the mass should be substituted by the effective mass. Then, referring to equation (6), the incompressibility K is related to the free gas one K_0 by

$$K \,=\, K_0 \left(\frac{m}{m^*}\right) (1 \,+\, F_0) \tag{68}$$

Other bulk properties are the specific heath c_V and entropy s. They require the formulation of the Landau theory at finite temperature [98]. In the low temperature limit the standard result is

$$c_V \,=\, \frac{m^*}{m} c_V^0 \qquad\qquad s \,=\, \frac{m^*}{m} s^0 \tag{69}$$

where c_V^0 and s^0 are the corresponding values for a free gas. The interaction changes just the density of states at the Fermi surface. These quantities are relevant for the thermodynamic evolution of neutron stars. For supernovae the temperature is much higher, typically few tens of MeV. Then the Landau theory cannot be applied and other methods must be used, either phenomenological (e.g. Skyrme functionals) or microscopic, see section 9. The thermodynamical properties of nuclear matter is only partially known at such temperatures. A clarification of this subject will be of great value for the detailed description of supernovae evolution.

5.3. Transport coefficients and macroscopic dynamics

Transport coefficients are fundamental properties of a Fermi liquid in general and of the nuclear medium in particular. They are physical parameters that describe the dynamical behavior of the system at macroscopic level and as such their main interest for

the nuclear medium is mainly related to astrophysical phenomena in compact objects. Shear viscosity, that can be viewed as momentum transport coefficient, is essential for understanding the damping of neutron star oscillations and supernovae evolution. Heat diffusion coefficient determines the early cooling evolution of neutron stars. The evaluation of these physical parameters can be done within the Landau theory by assuming a macroscopic deviation from equilibrium and solving the kinetic equation in stationary condition. The (linear) relation between the quantity that describes the deviation from equilibrium and the corresponding flux of the quantity that is driven by the deviation. A temperature gradient drives a heath flux, a fluid velocity gradient produces a transmission of momentum perpendicularly to the gradient.

Generally speaking, if local thermodynamical equilibrium is established in a Fermi system of particles, the collision integral vanishes, see equation 63, no flux can flow and the driving quantity is the deviation from local equilibrium $\delta^{leq} n(\epsilon, r)$. However, in a system of interacting quasi-particles one has to consider the true quasi-particle energies, that depends in turn on the quasi-particle distribution itself, see equation (60). Therefore the collision integral is expanded with respect to the deviation of the quasi-particle distribution from the particle local equilibrium distribution. The profile of this deviation is then determined to first order by solving the kinetic equation that includes the collision term. In stationary conditions the kinetic equation becomes a linear integral equation for the quasi-particle local equilibrium deviation, where the kernel of the integral is determined by the collision integral under the specific physical situation. Along these lines various approximations to solve the integral equations have been developed, until the works by Brooker and Sykes [105] and Jensen, Smith and Wilkins [106, 107], who supplied the exact analytical solutions for both the viscosity η and the thermal conductivity $\mathcal{K}$, besides the spin diffusion coefficient. The details of the derivation can be found in the original work or in reference [98]. The results involve in all cases the same angular integral over the probability W for elastic scattering of two quasi-particles at the Fermi surface

$$I_W = \int \frac{d\Omega}{4\pi} \frac{W(\theta, \phi)}{\cos(\theta/2)} \tag{70}$$

where W is proportional to the square of the matrix element of the scattering T-matrix, see equation (63). Because of conservation of momenta and energy, W depends only on two angles, here taken according to the Abrikosov-Khalatnikov convention, see references [108, 98]. The results for the thermal conductivity and the shear viscosity read

$$\begin{aligned} \mathcal{K} &= \tfrac{1}{2\pi^2} C_V v_F^2 \tau A_K \\ \eta &= \tfrac{1}{5} p_F v_F^2 \tau A_\eta \end{aligned} \tag{71}$$

where v_F is the Fermi velocity, C_V the specific heath, A_K, A_η are numerical factor that can be expressed in terms of numerical series, and τ is related to I_W by

$$\tau = 8\pi^4 \hbar^6 / (m^{*3} I_W T^2) \tag{72}$$

that has the meaning of a relaxation time. Actually the factors A_K and A_η depend also on the probability W through an additional integral, characteristic of each one of them. This must be carefully considered when comparing different models for W.

Several estimates of the shear viscosity have been presented in the literature, based on different models for W and different approximation schemes. The most recent microscopic calculations [109, 110, 111], where references to previous works can be found, stress the necessity of a treatment consistent with the nuclear matter EoS. These microscopic calculations show a fair agreement. However, further studies are needed to establish on a firm basis the value of η and its density dependence. In addition, a complete treatment in the asymmetric matter present in neutron stars is still missing.

As already mentioned in section 3.2, the shear viscosity is not relevant in the dynamics of finite nuclei at low excitation energy. The use of dissipative hydrodynamics, that involves the value of η, in heavy ion collisions has been rather limited. Collision dynamics appears too complex to allow any study on the relevance of the shear viscosity, not to speak of its possible value.

The thermal conductivity in neutron stars is dominated by the electron component. The specific heath of baryon matter can play a role in the cooling process. Only recently microscopic calculations have been developed, but the superfluid properties of neutron matter must be included [112, 113]. Still much work has to be done in this field.

Finally, one should consider also the bulk viscosity of the nuclear medium. However, the main contribution to the bulk viscosity in the nuclear matter present in compact stars is coming from the weak processes, and therefore it falls outside the scope of the present review. In any case it has been extensively studied, with somehow controversial results to be clarified [114, 115]. Furthermore, the possible hyperon component can be of decisive relevance [116]

5.4. Collective excitations

One of the fundamental results of the Landau theory of Fermi liquid, and nuclear matter in particular, is the possibility of collective microscopic excitations. Indeed, since the foundation of the theory, it has been shown by Landau that at low excitation energy the quasi-particle interactions can produce a concentration of the excitation strength at a particular value of the energy, where the response function displays a pole, i.e. a resonant behavior, that physically corresponds to a coherent motion of quasi-particles. Microscopically, the collective excitation is produced by the particle-hole interaction, as displayed in equation (61). If we limit the interaction to such a form, the possible excitations can be classified according to the values of the total spin S and isospin T. The $S = T = 0$ excitations correspond to density oscillation of the system. In finite nuclei they correspond to the iso-scalar monopole giant resonance. The function f in equation (61) determines the position and strength of the excitation. If the interaction is zero range (contact interaction), then only the value of f_0, i.e. f_l for $l = 0$, is different from zero. The value of f_0 is therefore a fundamental constant that

characterizes the nuclear medium. The onset of this collective motion can be seen by linearizing the kinetic equation (15) with respect to the variation of the quasi-particle distribution function, since we are considering small oscillations of the system. We put then $n(p,r,t) = n_0(p) + \delta n(r,p,t)$, where n_0 is the ground state quasi-particle distribution, i.e. a sharp Fermi distribution, and neglect any quadratic term in δn. We also neglect the collision integral I, that is we assume that the collision frequency is small with respect of the oscillation frequency. This means also that the quasi-particles decay can be neglected. After Fourier transform of the equation at the momentum $\mathbf{q}$ and frequency ω and simple manipulations, one gets, in the long wave-length limit ($q \to 0$)

$$(\omega - \mathbf{q}\cdot\mathbf{v_p})\,\delta n(\mathbf{q},\mathbf{p},\omega) + \frac{\partial n_0}{\partial \epsilon_p}(\mathbf{q}\cdot\mathbf{v_p})\sum_{\mathbf{p}'} f(\mathbf{p}' - \mathbf{p})\delta n(\mathbf{q},\mathbf{p},\omega) \tag{73}$$

This is an eigenvalue equation for the frequency ω at the momentum $\mathbf{q}$. Actually the equation depends only on the ratio ω/q, which is the propagation velocity of the oscillatory wave. The corresponding distribution distortion δn can be obtained by noticing that the derivative $\frac{\partial n_0}{\partial \epsilon_p}$ equals $-\delta(\epsilon - \epsilon_F)$, since n_0 is just a sharp Fermi distribution. Then also δn is proportional to the delta function

$$\delta n(\mathbf{q},\mathbf{p},\omega) = \delta(\epsilon - \epsilon_F)\xi(\mathbf{q},\mathbf{p},\omega) \tag{74}$$

If the interaction has only the $l = 0$ term different from zero, then ξ depends only on the modulus of $\mathbf{p}$, and substituting equation (74) in equation (73) one gets an explicit eigenvalue equation for ω. Putting $s = \omega/qv_F$, it reads

$$1 + \frac{1}{2}F_0 \int_{-1}^{1} d(cos\theta)\frac{cos\theta}{cos\theta - s} = 0 \tag{75}$$

where $F_0 = Nf_0$. If $s > 1$, corresponding to a repulsive interaction $f_0 > 0$, the integral is non singular and one gets a dispersion relation for s

$$1 + \frac{1}{2}F_0\left(1 + \ln\frac{s-1}{s+1}\right) = 0 \tag{76}$$

This solution is called "zero sound". It is an excitation mode of purely quantal origin, typical of any Fermion liquid with a repulsive interaction. As F_0 increases from 0 to large values, much larger than 1, the solution s_0 of the dispersion relation varies from 1 to $\sqrt{F_0/3}$. As already anticipated, this mode has an analogous mode in finite nuclei in the isoscalar monopole giant resonance, that can be then considered as the zero sound in finite nuclei. In nuclear matter other types of zero sounds can exist, corresponding to different spin-isospin total quantum number. The $T = 1$ and $S = 0$ corresponds to the dipole giant resonance in nuclei, the $T = 0, S = 1$ to the spin magnetic mode, the $T = 1, S = 1$ to the Gamow-Teller resonance. They have been all extensively studied in nuclei. If one keeps the correspondence with finite nuclei, it is possible to have phenomenological indications on the Landau parameters from the positions of the giant resonances in nuclei. It turns out, following this line, that the Landau parameter F_0 must be slightly negative, approximately $-0.4 < F_0 < 0$. The analogous Landau parameter $G_0 = Ng_0$ should be very small, due to the observed lack of collectivity of the spin mode in nuclei. The value of F_0' for the dipole mode should be also slightly negative,

but the extrapolation from nuclear matter to nuclei is questionable, because in nuclei there is a substantial contribution of the surface to this mode. The Landau parameter for the Gamow-Teller mode is much less known due to the substantial contribution of the Δ excitation, not included in the usual Landau treatment. The Landau parameters characterize the nuclear medium at fundamental level, but they are only partially known.

Going back to the dispersion relation (76), let us consider the case $s < 1$, that should appear when $F_0 < 0$. The integral is then singular and one has to specify how to handle the singularity. Physically speaking, if $s < 1$ the possible eigenfrequency falls inside the unperturbed particle-hole continuum. In fact the unperturbed continuum, in the long wavelength limit, spans the excitation energy up to $+qv_F$. This means that the mode couples directly to the particle-hole continuum and can decay. This implies that one should look for a complex solution of the dispersion relation, whose imaginary part will provide an estimate of the damping decay time of the mode. This decay mechanism is called "Landau damping" and is a phenomenon characteristic of Fermi liquids in general. It is not related to the collisions between quasi-particles, and therefore it has no connection to any sort of viscosity, being a purely quantal effect. It has to be stressed that when Landau damping is active, the excitation mode is strongly damped and in practice it disappears.

One could ask if Landau damping occurs in finite nuclei. In general the main strength of the giant resonances falls in the single particle continuum, that is at excitation energy where particle can escape, and therefore where the unperturbed particle-hole spectrum is continuous. In principle the Landau damping can therefore be present, however at the same time also the so called spreading width is present, that is the coupling with more complex configurations, like two particles-two holes states. In nuclear matter the latter turns out to be very small with respect to the Landau damping, just due to phase-space restrictions. In finite nuclei Landau damping is not so strong as in nuclear matter, due to the relatively small density of states at the excitation energy where they are located. The width of giant resonances, as already mentioned, is therefore mainly a nuclear structure problem, not related to the gross properties of the nuclear medium.

The elementary excitations in the nuclear medium have relevance for the physics of neutron stars. In the homogeneous region of the star these excitations affect the emission and propagation of neutrinos and the specific heath of matter. They are expected to be present also in the crust region [117]. For illustration we report in figure (8), taken form reference [118], the spectral functions of neutrons, protons and electrons at a nucleonic density equal to the saturation one. The neutron density is much higher and therefore also the strength function is much larger. One can see that the neutron strength is quite spread, showing that the excitations are in the region of Landau damping. One distinguish the sharp electron peak corresponding to the plasma mode. Neutron and proton excitations are mixed, but their interaction can be considered weak, because the proton strength looks rather localized and not so much affected by the Landau damping. In this calculations three possible effective interactions have been taken, corresponding

Figure 8. Strength functions in Neutron Star matter from reference [118]. The thin line corresponds to the neutron component, the thick one to the proton component. The vertical dashed lines indicate the position of the excitation branches, in particular the highest in energy is the electron plasma excitation. For detail see the reference [118].

to the Landau parameter F_0. Since matter is asymmetric, in this case we have three different F_0 parameters, corresponding to neutron-neutron, proton-proton and neutron-proton interactions. The first choice was taken from BHF calculations, the other two from particular Skyrme forces. The matter was assumed to be normal. Superfluidity can change partly this picture [119]. In any case the overall picture that comes from these analysis characterizes some of the fundamental properties of the nuclear medium.

Finally, we mention that in nuclear matter, when the characteristic frequencies of the motion become very small, the number of quasi-particles collisions per period of the oscillations can become so large that local equilibrium can be reached and the hydrodynamical regime is then established. Density oscillations can be still present and we have in this case the "first sound" mode. This is virtually identical to the sound in classical fluid, like air, in the same dynamical limit. In the hydrodynamical regime macroscopic motion are determined just by the conservation laws and the EoS of the nuclear medium. Macroscopic physical parameters, as the ones discussed in sections (5.2,5.3), then play the central role.

5.5. Theoretical challenges

We have seen that the fundamental parameters of Landau theory of Fermi liquid, as applied to the nuclear medium, are only poorly known on the basis of laboratory experiments on nuclei. Astrophysical observations can also give information on their values, but the data are still scarce and difficult to interpret. They are associated mainly with observations on neutron star oscillation or supernova evolution. It would be therefore quite desirable to have theoretical evaluations of their values and behavior with density on the basis of sound microscopical many-body theories.

We have already discussed the scattering matrix terms which appear in the collision integral and the present state of the art. There is a vast literature on the theoretical evaluation of the Landau parameters $\{f_l, g_l, f'_l, g'_l\}$ of the quasi-particle interaction. Their *ab initio* theoretical determination is extremely difficult because of the hard core character of the bare NN interaction. Among the different schemes that have been employed we can mention the self-consistent Babu-Brown equations [120, 121], the self-consistent Green' s functions expansion [122, 123] and more recently the Renormalization Group method [124]. The main difficulty in all methods lies in the estimate of the role of the screening processes. The quasi-particles can exchange collective excitations, as the ones discussed in section 5.4, where again the quasi-particle interaction appears. This entails a self-consistent procedure to calculate the interaction itself. However the results are sensitive to the scheme and approximations employed in the procedure and conclusive results are not yet available. Furthermore, for asymmetric matter, as the one present in neutron stars, calculations are quite scarce.

6. Neutron Matter at very low density. An exercise in many-body theory.

The low density region of pure neutron matter, as present in the inner crust of Neutron Stars, is less trivial than one could expect at a first sight since the neutron-neutron scattering length is extremely large, about -18 fm, due to the well known virtual state in the $^1S_0$ channel, and therefore even at very low density one cannot assume the neutrons to be uncorrelated. These considerations have also stimulated a great interest in the so called unitary limit, i.e. the limit of infinite (negative) scattering length of a gas of fermions at vanishingly small density. A series of works [125, 126, 127] have been presented in the literature based on various approximations, and a recent Monte Carlo calculation [128] on a related physical system has shown that the unitary limit can present a quite complex structure, involving both fermionic and bosonic effective degrees of freedom, which has still to be elucidated. Variational [129] and finite volume Green's function Monte Carlo calculations [130] for neutron matter at relatively low density have shown that the EOS, in a definite density range, can be written as the free gas EOS multiplied by a factor ξ, which turns out to be close to 0.5. This is actually what one could expect in the unitary limit regime, since no scale exists in this case, except the Fermi momentum. Monte-Carlo calculations [125, 126, 127] with schematic

forces in a regime close to the unitary limit have found a factor $\xi \approx 0.44$. The connection between the variational results and the unitary limit has been studied in reference [131] by means of effective theory methods.

6.1. A single G-matrix problem

Since the scattering length a and effective range r_0 in the ${}^1S_0$ channel of the neutron-neutron interaction differ by about a factor 6, there is no density interval where the unitary limit can be considered strictly valid. However, in the range $r_0 < d < |a|$, where d is the average inter-particle distance, the physical situation should be the "closest" possible to the unitary limit. This range corresponds to Fermi momentum range 0.4 fm^{-1} $< k_F <$ 0.8 fm^{-1}, which corresponds to densities between about 1/50 and 1/5 of the saturation density. Let us choose as realistic nucleon-nucleon potential the Argonne v_{18} interaction [132]. The first finding is that the three-body forces of the Urbana model, adjusted to reproduce the correct saturation point [77], give a contribution which is less than 0.01 MeV, and therefore we can neglect three-body forces to a good approximation. The second finding is that the single particle potential is very small in this density range, and its effect can be neglected. It affects the energy per particle less than 0.1 MeV.

It is enlightening to compare the in-medium G-matrix with the free K-matrix in the ${}^1S_0$ channel, reported in figure (9), taken from reference [133], at selected values of the relative momentum k and total momentum P (in fm^{-1}) at the Fermi momentum $k_F = 0.4$ fm^{-1}. For sake of comparison the free K-matrix has been divided by 3. Due to Galilei invariance, the free K-matrix is independent of P. Despite the Fermi momentum is quite small, a drastic difference between the two scattering matrices is apparent, not only in shape but also in absolute value. The Pauli operator effect is enhanced in this particular channel since the virtual state is suppressed in the medium. This illustrates the dramatic difference that can exist between the in-medium effective interaction and the free bare interaction. The large enhancement at the Fermi momentum and for small total momentum P is due to the pairing singularity, to be discussed in section 7.4 The BBG expansion relies on the basic idea that the contributions of the diagrams of the expansion decrease with increasing number of hole-lines which are included. Although the BBG scheme is essentially a low density expansion, it has been found [135, 136] that the convergence is valid up to densities as high as few times saturation density in symmetric nuclear matter and even better in neutron matter. It is then likely that at the low densities we are considering this convergence should be even faster. This is indeed confirmed by explicit numerical calculations [133], and indeed the third finding is that the three hole-line contribution is at most 0.15 MeV at the highest density considered and rapidly decreasing to vanishingly small values as the density decreases. Finally, the fourth finding is that higher partial waves give a negligible contribution both at the two hole-lines (Brueckner) and three hole lines level. These four findings, all together, point out that the many-body problem of neutron matter at low density is reduced to a single G-matrix problem, i.e. to the calculation of the ${}^1S_0$ G-matrix.

Figure 9. Plots of the free K-matrix (T), divided by 3 for convenience, in comparison with the in-medium K-matrix (G), at the indicated Fermi momentum, for different total momentum p, as a function of the relative momentum k. All the momenta are in fm^{-1}. The results are for the $^1S_0$ channel in pure neutron matter. The arrow indicates the maximum momentum needed in the calculation of the EoS. See reference [133] for detail.

6.2. The "exact" EoS

The two EoS, one calculated within the full BBG expansion up to the three hole-lines contributions and the other calculated with the single $^1S_0$ G-matrix, are compared in figure (10), taken from reference [133]. They are mainly indistinguishable. The energy per particle is very close to 1/2 of the kinetic energy. It turns out that the G-matrix is fully determined by the scattering length and effective range. One can construct a rank-one separable interaction [133]

$$(k'|v|k) \,=\, \lambda\, \phi(k')\phi(k) \tag{77}$$

with a simple form factor

$$\phi(k) \,=\, 1/(k^2 \,+\, b^2) \tag{78}$$

where the parameters λ and β are determined by imposing that the scattering length and effective range are reproduced. Then the G-matrix can be obtained analytically and the corresponding EoS by simple numerical integration. The procedure is equivalent to an Effective Theory with smooth cut-off and its accuracy is shown in figure (10). The calculation can be extended to very small density, as reported in figure (11), where one can see that the EoS approaches the one for a free gas, as it must be for $k_F < 1/|a|$.

[hb]

Figure 10. Neutron matter EOS calculated within the BBG method (label G), within the variational method of ref. [129] (triangles), according to the estimate of ref. [134] (dotted line) and with the separable representation of the G-matrix (label G sep). The dash-dotted line is one half of the free gas EOS. The square represents the result of the Quantum Monte-Carlo calculation of reference [137].

Figure 11. Neutron matter EOS calculated with the separable representation of the G-matrix, in comparison with the free Fermi gas EoS and one half of it. The squares represent the results of the Quantum Monte-Carlo calculation of reference [137].

In both figures (10,11) the squares indicate the results of the Monte Carlo calculations of reference [137]. They agree fairly well with the BBG results up to the density where the Monte Carlo calculation can be performed.

What is missing in the BBG calculations is the pairing correlations. The contribution to the EoS of pairing is not expected to be relevant, but it is important to know the value of the gap for many phenomena in Neutron Stars and as an indication for finite nuclei. The subject will be taken in sections 8.3 and 7.4.

Figure 12. The symmetry energy at low density. The symbols correspond to the Brueckner calculations with realistic forces, Argonne v_{14} (diamonds), Argonne v_{18} (small open circles which correspond to the polynomial fit) and Paris potentials (open squares). The lines correspond to phenomenological nucleon-nucleon forces, the SkM* (solid line) and the Sly4 Skyrme forces (short dashed line), and the Gogny force (long dashed line

7. Bulk properties of Nuclear Matter

In this section we try to illustrate our knowledge on some of the physical parameters that characterize the properties of the nuclear medium. Some of them have been discussed in previous sections for matter close to saturation density, so we concentrate mainly on their density dependence. A subsection is devoted to the possible superfluid phases, that have not been discussed up to now.

7.1. Density dependence of the symmetry energy

Hints about the symmetry energy below saturation density have been claimed to come from experimental data on heavy ion reactions at intermediate energy. The isoscaling regularity [138, 139] appears to be present in many experiments on multi-fragmentation, from which an estimate of the density dependence of the symmetry energy can be deduced [140]. Another possibility has been advocated [141, 142] to be the data on the so called "isospin diffusion" in heavy ion reaction at moderate energy.

Microscopic calculations show a fair agreement with these "data" and among each other up to saturation and slightly above. Comparison with results from different Skyrme forces show that only few of them are compatible with this general behavior. In figure (12), taken from reference [143], is shown the symmetry energy in the low density region calculated in BHF scheme in comparison with the few Skyrme forces that show a fair agreement with the microscopic calculations. The most modern Skyrme forces are constructed in such a way to fit the microscopic results, and the agreement is therefore enforced. Above saturation the situation is less under control. One one

hand the microscopic calculations need to extend the use of three-body forces to density where they are not well known. On the other hand experimental data on heavy ion collisions can provide hints on the density dependence of the symmetry energy only very indirectly through extensive simulations. This approach is extensively reviewed in reference [144], where the prospectives in this line of research are presented in detail, in particular in connection with the development of the facilities for exotic nuclei.

Astrophysical observations on the mass of neutron stars are also indirectly testing the symmetry energy at high density, because the value of the symmetry energy can change the value of the incompressibility of the very asymmetric matter at the center of compact stars. As already mentioned, the interplay of the data extracted from heavy ion reaction at intermediate energy, that test the EoS of almost symmetric matter, and the analysis of the observational data on neutron stars, where the matter is highly asymmetric, can be of great help to clarify this difficult but fundamental issue.

7.2. Incompressibility

The incompressibility near saturation has been already discussed. Below saturation density usually the EoS of symmetric matter and neutron matter are assumed to be simple low order polynomial functions. This can be a delicate point, since the small detail of the EoS behavior at low density, especially for symmetric matter, can be relevant for the construction of accurate Energy Density functionals to be used in the calculations of the mass table. Microscopic calculations look in close agreement in this density region, see figure (7). At higher density, well above saturation, the microscopic theories face the problem, already mentioned, of the three-body forces, that give a very large contribution but are not well known. As a reference density above which this problem can be serious, one can take a value around 3-4 times saturation density. Also in this case the interplay between theory and experiments is essential to make progress in this issue.

7.3. Viscosity

The notion of viscosity has been already discussed within the Landau theory of Fermi liquid. Here the effective interaction that enter, in a way or in another, in the calculation of the EoS must be the basic quantity to be used to calculate also the scattering probability W of section 5.3. For instance the G-matrix of the BHF scheme should be used as the basic quantity. Of course, at high density we meet the same problems as for the EoS.

7.4. Superfluidity

It has been argued a long ago [145, 146] that to explain the observed glitch phenomenon in several pulsars it would be natural to assume that nuclear matter is superfluid in the interior of neutron stars. In fact, the sudden increase of the rotational frequency and

the long time needed to recover the initial rotational frequency suggest the presence in the crust of an almost decoupled component with low viscosity. Since then a vast literature has developed on the subject, and different superfluid phases have been found theoretically at the physical conditions expected inside neutron stars. It is well known that theory of superfluidity, or better superconductivity, was first formulated by Bardeen, Cooper and Schiffrer [147]. In a more general formulation, the constitutive equation for the onset of a superfluid phase is the gap equation [100, 4]

$$\Delta(\mathbf{k}) \;=\; -\frac{1}{2}\sum_{\mathbf{k}'} \mathcal{V}(\mathbf{k},\mathbf{k}')\frac{\Delta(\mathbf{k})}{E_k} \tag{79}$$

Here the gap function Δ is related to the pairing correlation function, or "pair wave function" by

$$\frac{\Delta(\mathbf{k})}{2E_k} \;=\; < \psi^\dagger(\mathbf{k})\psi(-\mathbf{k}) > \tag{80}$$

For simplicity we assume pairing in the s-wave and the particles that form the Cooper pair have opposite momentum and spin. Then the so called quasi-particle energy is given by

$$E_k \;=\; \sqrt{e_k \,+\, \Delta_k^2} \tag{81}$$

where e_k is the single particle spectrum in absence of pairing interaction. In this case all quantities depend only on the modulus of $\mathbf{k}, \mathbf{k}'$. The kernel $\mathcal{V}$ is the irreducible particle-particle interaction. In the many-body language, it is the sum of all diagrams that describe the interaction of two particles and that cannot be divided into two disconnected parts by cutting two particle lines. For strong pairing correlation it also depends on the pairing gap Δ. The exact equation for the pairing gap is more complex than equation (79). It can be formulated in terms of single particle Green' s functions and it can be found in textbook [100, 4]. We will discuss later the possible modifications, but equation (79) already contains some of the main features of the pairing problem for the nuclear medium. For neutron-neutron or proton-proton pairing the only s-wave channel is the $^1S_0$ two-body channel, and we will first discuss this case. Equation (79) is a non-linear equation for the gap function $\Delta(k)$, due to its presence in E_k in the denominator. The onset of the superfluid phase of the nuclear medium is indicated by a non-zero solution for the gap. The zero solution $\Delta(k) = 0$ is always present, but it can be shown that the energy of the superfluid phase, if it exists, is always lower than the normal phase. This is of course a general feature. What characterizes the pairing correlation in the nuclear medium is the value of the gap, that is estimated to be a substantial fraction of the Fermi energy. Another feature is that the effective interaction is not concentrated around the Fermi surface, like in ordinary superconductor or in superfluid ^3He. Although a large contribution in the gap equation comes from the interaction at the Fermi momentum, also momenta that are far away from the Fermi surface are essential and the pairing gap function $\Delta(k)$ is momentum dependent. All that can be seen by considering the simplest approximation for the pairing interaction, the bare NN interaction. It turns out that the bare NN interaction is able to produce a substantial pairing gap at low

Figure 13. Different pairing gaps as a function of density in Neutron Star matter.

density, but, due to the hard core of the interaction, high momentum components must be taken into account. The approach can be extended to other channels, and the possible pairing gaps at the Fermi surface in this approximation as a function of density in neutron star matter is depicted in figure (13), taken from reference [148]. In this evaluation of the different pairing gaps the single particle spectrum has been taken form BHF calculations for the neutron star matter. Accordingly, the concentration of protons has been calculated at the beta equilibrium and the nuclear matter EoS from the BHF theory. Other microscopic EoS would give anyhow similar results. This is mainly equivalent to the use of the effective mass. In this case the effective mass is smaller than the bare one. This reduces the pairing gap because it increases the kinetic energy and reduces the density of states. The effect is larger at higher density, such as for the proton and the $^3PF_2$ neutron pairing, and it is almost negligible for the $^1S_0$ neutron pairing. The proton-proton pairing is shifted at higher density with respect to neutron-neutron one just because the fraction of proton is varying smoothly from few percents to about 10-15 %, according to adopted EoS. The p-wave neutron pairing is present only at high density because the phase shifts of the $^3PF_2$ channel becomes appreciable only at higher momentum, and so at higher Fermi energy.

This overall picture is very important for many phenomena that occur in neutron stars, in particular for the cooling process and the glitches events. However the quantitative description of the observational data requires an accurate prediction of all these pairing gaps. This turns out to be an extremely difficult task. First of all the pairing gap is a quite sensitive quantity and small variations of the interaction can change substantially its value. This can be seen in the so called weak coupling limit, that corresponds to assume the interaction independent of the momentum with a cutoff and approximate as constant the density of states, taken at the Fermi momentum. In this limit the pairing gap can be obtained from a simple integration and it is a constant.

Figure 14. Pairing gap in the ${}^3PF_2$ channel as a function of density in neutron matter.

It depends exponentially and non-analytically on the interaction strength

$$\Delta \;=\; E_0 \exp(1/\mathcal{V} k_F m) \tag{82}$$

where the factor E_0 is related to the cutoff, but it varies smoothly and has a logarithmic dependence on it. The non-analyticity is a manifestation that a phase transition takes place, for any small value of an attractive interaction at the Fermi surface.

Then the question arises if we know accurately enough the bare NN interaction that the pairing gap so calculated is essentially independent on the particular realistic NN interaction. This turns out to be true for the ${}^1S_0$ neutron and proton pairing gap, but it is invalid for the ${}^3PF_2$ channel at the higher density. This is because the phase shifts are known up to about relative momentum $k = 2\mathrm{fm}^{-1}$, above which any potential give essentially extrapolated values. This can be dramatically seen in figure (14), where the pairing gap in the ${}^3PF_2$ channel, calculated in the BCS approximation, is reported for different interactions. Above $k_f = 2\mathrm{fm}^{-1}$ the diverging results is a manifestation of this uncertainty. Further uncertainty is introduced at the higher density, where three-body forces start to play a role. Besides this basic uncertainty, not present for the lower density, the BCS approximation must be implemented by including the many-body effects in the gap equation. Correlations affect the single particle motion. As already mentioned, the momentum dependence of the normal part of the self-energy introduces the single particle potential, that can be approximated by substituting the bare mass with the effective mass. Besides that, the energy dependence introduces the so-called quasi-particle strength or Z-factor, that gives the weight with which the quasi-particles can take part to a Cooper pair. More generally, if one assumes that the effective pairing

interaction is energy independent, the gap equation can be written [4]

$$\begin{aligned}\Delta(k) &= -\sum_{k'} \mathcal{V}(k,k')\frac{\Delta(k)}{2\mathcal{E}(k)} \\ \frac{1}{2\mathcal{E}(k)} &= \frac{1}{\pi}\int d\omega' \mathrm{Im}(\frac{1}{D(k,\omega')}) \\ D(k,\omega) &= (\tilde{\epsilon}_k - \omega + M(k,\omega)) \cdot (\tilde{\epsilon}_k + \omega + M(k,-\omega)) + \Delta(k)^2 \end{aligned} \quad (83)$$

where $\tilde{\epsilon}_k = e_k - \mu$, being e_k the free spectrum and μ the chemical potential, and $M(k,\omega))$ is the normal component of the self-energy. It can be calculated in normal (non-superfluid) nuclear matter, e.g. within the BHF scheme, since the pairing gap is small with respect to the Fermi energy. It contains both a real and imaginary part. The factor $\mathrm{Im}(1/D(k,\omega'))$ appearing in this gap equation is the single particle strength function, that describes the distribution in energy of the single particle at momentum k inside the medium. The strength function is an even function of the energy and has two poles at positions symmetrical with respect to the imaginary axis. If one takes only their contributions to the energy integral, which corresponds to the quasi-particle approximation, the gap equation reduces to

$$\Delta(k) = -\sum_{k'} \mathcal{V}(k,k')Z_{k'} \frac{\Delta_{k'}}{2\sqrt{\left[\tilde{\epsilon}_k + \frac{1}{2}\mathrm{Re}(M(k,-E_k) + M(k,E_k))\right]^2 + \Delta(k)^2}} \quad (84)$$

where E_k and $-E_k$ are the real parts of the two poles energy, being E_k the quasi-particle energy in the superfluid nuclear medium, the factor $Z(k')$ is the anticipated residue at the poles, and Re means real part. In the weak coupling limit, the presence of the self energy can be approximated by introducing the effective mass, while the Z factor (always smaller than 1) reduces the strength of the interaction. Equation (82) becomes

$$\Delta = E_0 \exp(1/\mathcal{V}k_F Z(k_F)^2 m^*) \quad (85)$$

Due to the exponential dependence, the Z factor can substantially reduce the pairing gap. The total effective mass at the Fermi momentum, when dispersive effects are included, turns out to be close to 1 in the density range where neutron matter is expected to be superfluid. These effects have been studied by several authors, both using the more general equation (83) and the pole approximation [149, 150, 151, 152, 153] of equation (85). The reduction of the gap looks to be moderate, approximately 20-30%.

The estimate of the many-body effects on the pairing interaction $\mathcal{V}$ turns out to be the most difficult task. The main problem seems to be the inclusion of the medium polarization effects on the effective interaction. This problem has been approached by a variety of techniques and approximations. The results are summarized in reference [148]. They all display a strong reduction of the pairing gap in the neutron $^1S_0$ channel, but they do not agree on the size of the reduction, that has a value between 0.5 and 0.2 or even smaller. The discrepancy is again related to the extreme sensitivity of the pairing gap to the value of the effective pairing interaction, that requires an accuracy difficult to reach in this many-body problem. More recently the Renormalization Group method has been used [124]. The results look similar to the previous calculation in reference [122]. In

Figure 15. Weak coupling parameter λ (top panel) and gap Δ (bottom panel) in several approximation. Here $\Delta \sim \exp(1/\lambda)$, see equation (82). The solid curves show BCS results without any in-medium effects, the dashed curves include the modification of the effective mass m^*, and the dotted curves take account of the Z-factor and the polarization corrections in addition. The left panels show results with only two-body forces in the interaction kernel of the gap equation, and the right panels include also three-body forces.

the region of lowest density also Monte-Carlo calculations are available [137, 154, 155]. Despite some discrepancies among the results, they seem to indicate a much smaller reduction of the pairing gap for this channel. If this is due to some limitation of the Monte-Carlo calculations or to a drawback of the other microscopic many-body methods is a question that is waiting for an answer.

The ${}^1S_0$ proton pairing gap is more difficult to treat, because the much higher density of neutrons can have a dominant effect. The most recent calculation [156] indicates that the effect of the neutron component strongly enhance the effective pairing interaction through the tensor component of the NN interaction, but this effect is in competition with the strong reduction due to the effective mass and Z-factor. To illustrate how difficult is to control all these competing effects in figure (15) is reported the pairing gap when each one of these many-body contributions is introduced. Notice that without the neutron polarization effect the gap would be zero. The final gap turns out to be more concentrated at lower density with a smaller strength. Further studies are surely needed to confirm these results.

The $^3PF_2$ neutron pairing gap turns out to be much smaller and relevant only in a deeper region of a neutron star. Application [157] of the Renormalization Group method to this channel brings the gap to a very small value, in the range of few tens of KeV, even compatible with a vanishing one.

Observational data on neutron star cooling can indirectly give indications about the values of all these pairing gap. Analysis based on the assumption of pure nucleonic matter [158] constraints the gaps to values that are compatible with the theoretical predictions. In particular the $^3PF_2$ is seen to be necessarily quite small, of the same order as the theoretical results. The proton pairing gap is deduced to be indeed restricted to relatively lower baryon density, mainly outside the inner core. For the neutron $^1S_0$ the constraints are less stringent, but anyhow compatible with most of the theoretical predictions.

The possible onset of exotic matter components, like hyperons and quarks, complicates noticeably the analysis. These components can be also superfluid, but unfortunately their pairing gaps are even more uncertain than in the nucleonic case. From the observational data on glitches one can extract indications on the pinning energy of vortices, and therefore indirectly on the pairing gap. However this phenomenon needs still a complete dynamical theory, before any conclusion on both the pairing gap and the pinning energy can be deduced.

The possible link of these results with the pairing phenomenon in nuclei is discussed in section 8.3.

8. Connection with Nuclear Structure

One of the basic questions that was posed since the first developments of Nuclear Physics is to what extent the properties of the bulk nuclear medium can be transferred to finite nuclei or to what extent they influence the general trends that are observed in Nuclear Structure studies. Otherwise stated, is there a link between the nuclear medium properties and the structure of finite nuclei ? The simplest scheme where this link is exploited is the Liquid Drop Model, introduced in section 3.1. As explained, in this semi-classical model the assumed constant saturation energy per particle is corrected by the surface and Coulomb energy to explain the binding energy of finite nuclei. In more sophisticated variants of the model other terms are introduced, but in any case a set of parameters are introduced which cannot be derived from the theory. Furthermore, quantal characteristics like shell effects are not included. We will briefly describe some of the methods that have been used and developed to understand more deeply this possible link and, at the same time, to devise practical and general theoretical scheme for Nuclear Structure.

8.1. The Thomas-Fermi approximation and implementations

Historically, the first method to relate the properties of finite quantal systems to the corresponding homogeneous system was the semi-classical Thomas-Fermi scheme. It was devised to calculate the ground state properties of large atoms and molecules in the case of independent particle limit. In fact, even in this limit, the quantal calculations can become quite complex. The original form of the scheme is equivalent to take the zero order term in the expansion in $\hbar$ of the density matrix for the independent particle wave function, but it can be easily derived by assuming that the system is locally equivalent to a free Fermi gas at the local density and local potential. We remind here some features of the approximation that are useful for the development of the presentation. In its simplest version it can be formulated within the Density Functional method, i.e. assuming that the energy of the system can be written as a functional of the density $\rho(\mathbf{r})$

$$E_{TF} \,=\, T_F(\{\rho\}) \,+\, V_c(\{\rho\}) \,+\, V_{pp}(\{\rho\}) \tag{86}$$

where T_F is the kinetic energy contribution, V_c the external potential and V_{pp} the particle-particle interaction. In case of atoms, V_c is the energy due to the central Coulomb potential and V_{pp} is the electron-electron Coulomb interaction energy

$$\begin{aligned} T_F(\{\rho\}) \;&=\; \tfrac{3}{5}\int d^3r E_F(\rho(\mathbf{r}))\rho(\mathbf{r}) \quad ; \quad V_c(\{\rho\}) \,=\, -Z\int d^3r' v(r)\rho(\mathbf{r}') \\ V_{pp}(\{\rho\}) \;&=\; \int d^3r \int d^3r' v(|\mathbf{r}-\mathbf{r}'|)\rho(\mathbf{r})\rho(\mathbf{r}') \end{aligned} \tag{87}$$

with Z the charge of the nucleus, $v = 4\pi e^2/r$ the Coulomb potential between two electrons (of charge e) and E_F the Fermi energy for a free gas at the density $\rho(\mathbf{r})$. The Euler-Lagrange equation corresponding to the minimization of this functional with the constraint of a fixed number of particles is

$$E_F(\rho(\mathbf{r})) \,-\, Zv(r) \,+\, \int d^3r' v(|\mathbf{r}-\mathbf{r}'|)\rho(\mathbf{r}') \,=\, \mu \tag{88}$$

where μ is the Lagrange multiplier, that has the meaning of chemical potential. Notice that μ is a constant, independent of the position. The solution of this equation gives the density and then the energy of the ground state. A way of solving this equation is to apply the Laplacian differential operator and use the Poisson equation $\Delta V_C = -4\pi e^2\rho(\mathbf{r})$, where V_C is the last term at the left hand side of equation (88), that is the potential produced by all electrons at $\mathbf{r}$. This gives the familiar differential equation of the Thomas-Fermi scheme in its simplest form [159]. We will not discuss the many refinements of the approximation that have been developed, to include e.g. the exchange interaction, but rather we consider the Thomas-Fermi approximation in the nuclear case. The physical situation is rather different. There is no central interaction, and the binding must come from the NN interaction. The latter is not long range, like the Coulomb potential, but it is short range, even zero range if we adopt a Skyrme effective interaction. Then equation (88) has no solution, except in the trivial case of an homogeneous system. To get any sensible result for a nucleus one has to go to the

next order in the expansion in $\hbar$ of the kinetic energy term in the functional. This introduces gradient terms [8]. To order $\hbar$ only one term contributes, proportional to $(\nabla\rho)^2$. With the inclusion of this term, a surface can develop and the nuclear Thomas-Fermi approximation can describe the density profile of a nucleus.

This discussion makes clear that in the nuclear case the kinetic term must be treated at different order in the expansion in $\hbar$ and at a different level of approximation. The full quantal treatment of the kinetic term must be considered to construct any accurate nuclear energy functional.

Despite that, the Thomas-Fermi approximation, or more advanced expansions in $\hbar$ can be useful. In fact the Thomas Fermi approximation and its implementations are expected to describe the smooth part e.g. of the density of states, leaving outside of their possibility the description of the shell effects, that are a pure quantal effect. Indeed the expansion in $\hbar$ of many quantities is actually asymptotic, and the quantal effects depend non-analytically on $\hbar$. This property of the $\hbar$ expansions can be used to evaluate the shell effects in the so-called microscopic-macroscopic approach, introduced in section 3.1. The difference between the exact quantal calculations and the results of the expansion is taken as an estimate of the shell effects. Implicitly, it is assumed that shell effects are essentially the same in the independent particle model as in the fully correlated system. The smooth part, obtained from the liquid drop or droplet models, are expected to include in an effective way the correlation contribution. Along these lines, recently in reference [160] the Kirkwood $\hbar$ expansion to fourth order has been used to estimate the shell effects by comparing the results with the quantal calculations. This method, as similar ones based on $\hbar$ expansions, are methods alternative to the Strutinski smoothing method [12].

A step further along these lines is the construction of general effective Energy Density functionals that are devised to include all the correlations in an effective way and without any $\hbar$ expansion. Although they are necessarily in part phenomenological, i.e. they contain a certain number of parameters, the ambition is to relate their characteristics in terms of the properties of the nuclear medium. On the other hand, if they are treated at purely phenomenological level, they turn out to be extremely accurate. These items will be discussed in the next section.

8.2. The Density Functional Method

A fully quantal microscopic method to connect the nuclear medium properties and the structure of finite nuclei is to introduce an effective NN force, whose parameters are fitted, on one hand, to reproduce the nuclear matter EoS, as derived phenomenologically and microscopically, and on the other hand to reproduce binding energy and radii of a representative set of nuclei. This is the scheme of the Skyrme forces. These effective forces have been developed along the years with increasing success and have been widely used in nuclear structure and spectroscopic studies. It is surely not possible to review the enormous literature on the subject, and we limit here to sketch the main features

of the method. The simplest Skyrme force can be written, for symmetric system

$$V = t_0\rho(\mathbf{r})\delta(\mathbf{r}-\mathbf{r}') + t_3\rho(\mathbf{r})^2\delta(\mathbf{r}-\mathbf{r}')\delta(\mathbf{r}'-\mathbf{r}'') \tag{89}$$

where ρ is the nucleon number density at the point $\mathbf{r}$ and the parameters t_0 (negative) and t_3 (positive) are adjusted to reproduce the saturation point of Nuclear Matter, where the force depends only on the constant total density. They correspond to effective two-body and three-body interactions, respectively. Besides these parameters, an effective mass m^* is also usually introduced in the kinetic part, so that the total Hamiltonian can be written

$$H = T + V \quad , \quad T = -\frac{\hbar^2}{2m^*}\nabla\delta(\mathbf{r}-\mathbf{r}')\nabla \tag{90}$$

Then the force is used to calculate the ground state of nuclei in the Hartree-Fock (mean field) approximation, thus establishing an indirect link between nuclear matter and finite nuclei. Much more elaborated forces have been developed, in which density gradient terms and asymmetry dependent terms are introduced. Then the number of parameters increase, but the precision of the fit on the overall mass table can be really impressive, see e.g. references [21, 22]. More elaborated terms involving higher degrees of the density derivatives can be still introduced, and the accuracy of the fit can be astonishingly good [161, 162]. However, along this line, the connection with NN bare forces and nuclear matter EoS is gradually lost, since the additional terms have a form loosely connected with the NN interaction and are all vanishing in uniform matter.

Another method that tries to keep more closely the connection with the properties of the bulk nuclear medium is based on the Kohn and Sham (KS) [163, 164, 165, 166, 167, 168, 169] approach, first devised for atomic, molecular and solid systems and developed also for nuclear system. Let us consider the microscopic bulk EoS, as reported in figure (7), extended to asymmetric nuclear matter. This can be taken as the bulk contribution to the Energy Density Functionals (EDF). For numerical applications it can be written in a polynomial form. The functional must be then implemented mainly by three additional contributions. The first one is the Coulomb energy, that can be calculated with different degrees of sophistication, e.g. by including the exchange and short range parts. The second one must take into account the presence of the surface, that in nuclei is sharply localized, within a length of the order of 1 fm, and therefore cannot be described only by the bulk part. The additional contribution has to be localized at the surface, and the simplest way to do so is to introduce density gradient terms or non-local short range convolution terms. The surface terms are connected to the surface tension of nuclear matter, because, in the macroscopic limit, they modify the surface energy of the system. Finally, it is mandatory to add a spin-orbit term, since it strongly affects the single particle level scheme and it is mandatory in order to reproduce the shell sequence (i.e. the "magic numbers"). The spin-orbit interaction is roughly proportional to the gradient of the single particle potential, and therefore it is also localized at the surface. The strength of this term is severely constrained by phenomenology, but it has still some degree of uncertainty. It is desirable to keep the number of surface and spin-orbit

terms to a minimum, since they introduce additional phenomenological parameters. It is one of the ambition of the Energy Density Functional method to get these parameters from microscopic many-body theory, but in order to get a high precision fit to the wide set of nuclear binding and radii throughout the mass table, they must be finely tuned beyond the possibility in accuracy of any microscopic theory. The possibility still remains to have a guidance to their values within a reasonable accuracy and to get a deeper understanding of their microscopic origin. This program has still to be developed.

Following the above considerations, the EDF can be written

$$E = T_0 + E^{s.o.} + E_{int}^{\infty} + E_{int}^{FR} + E_C. \tag{91}$$

For the surface term, following reference [173], one can take a simple finite range term

$$\begin{aligned} E_{int}^{FR}[\rho_n, \rho_p] &= \frac{1}{2} \sum_{t,t'} \int \int d^3r d^3r' \rho_t(\mathbf{r}) v_{t,t'}(\mathbf{r} - \mathbf{r}') \rho_{t'}(\mathbf{r}') \\ &- \frac{1}{2} \sum_{t,t'} \gamma_{t,t'} \int d^3r \rho_t(\mathbf{r}) \rho_{t'}(\mathbf{r}) \end{aligned} \tag{92}$$

with t = proton/neutron and $\gamma_{t,t'}$ the volume integral of $v_{t,t'}(r)$. The substraction in (92) is made in order not to contaminate the bulk part, determined from the microscopic infinite matter calculation E_{int}^{∞}. Finite range terms have been used in e.g. [170, 171, 172], generalizing usual Skyrme functionals. In references [173, 174], for the finite range form factor $v_{t,t'}(r)$ a simple Gaussian ansatz: $v_{t,t'}(r) = V_{t,t'} e^{-r^2/r_0{}^2}$ was taken, so that a minimum of three open parameters was introduced : $V_{p,p} = V_{n,n} = V_L, V_{n,p} = V_{p,n} = V_U$, and r_0.

In equation (91), E_{int}^{FR} and E_C are the spin-orbit and Coulomb parts, respectively. More detail on their determination can be found in references [173, 174]. The first piece T_0 in equation (91) corresponds to the uncorrelated part of the kinetic energy and within the KS method it is written as

$$T_0 = \frac{\hbar^2}{2m} \sum_{i,s,t} \int d^3r |\nabla \psi_i(\mathbf{r}, s, t)|^2. \tag{93}$$

where the functions $\psi_i(\mathbf{r})$ form an auxiliary set of A orthonormal single particle wave functions , being A the number of particles, and the density is assumed to be given by

$$\rho(\mathbf{r}) \; = \; \Sigma_{i,s,t} |\psi_i(\mathbf{r}, s, t)|^2 \tag{94}$$

where s and t stand for spin and iso-spin indices. At each point $\mathbf{r}$ the bulk term equals the nuclear matter EoS at the corresponding local density (and asymmetry). Then, upon variation to minimize the EDF, one gets a closed set of A Hartree-like equations with an effective potential, the functional derivative of the interaction part with respect to the local density $\rho(\mathbf{r})$. Since the latter depends on the density, and therefore on the ψ_i's, a self-consistent procedure is necessary. The equations are exact if the exact EDF would be known. The existence of the latter is proved by the Hohenberg-Kohn (HK) theorem [175], which states that for a Fermi system, with a non-degenerate ground

Figure 16. (Color online) Energy differences as a function of mass number for a set of 161 spherical nuclei (diamonds, black points) and 306 spherical odd nuclei (full circles, red points).

state, the total energy can be expressed as a functional of the density $\rho(\mathbf{r})$ only. Such a functional reaches its variational minimum when evaluated with the exact ground state density. In practice of course a reliable approximation must be found for the otherwise unknown density functional, taking inspiration from physical considerations and microscopic input, as discussed above. It has to be stressed that in the KS formalism the exact ground state wave function is actually not known, the density being the basic quantity. It has also to be noticed that in the standard KS scheme, the kinetic energy term includes the bare nucleon mass, but variants with an effective mass are possible (to incorporate the correlated part of the kinetic energy).

As an illustration of the method, in figure (16), taken from reference [174], is reported the difference in total binding energy between the calculated and the experimental values for a wide set of spherical nuclei. The parameters of the functional have been fixed by fitting a set of deformed nuclei, both normal and super-heavy (functional BCP) . The choice of fitting first deformed nuclei is suggested by the consideration that these nuclei should be better described by mean field, while spherical nuclei need corrections due to zero-point motion in the ground state, e.g. RPA correlations in the ground state. The mean error in binding energy in the fit of deformed nuclei is about $\sigma_E = 0.52$ MeV, while the discrepancy for the spherical nuclei, where the functional was fixed and no fit was any more performed, is about $\sigma_E = 1.2$ MeV. In figure (17) the corresponding deviations for the root mean square radii are reported for the spherical nuclei.

The performance is comparable with the best Skyrme forces, like the Gogny D1S [176], but of lower quality than the one from HFB calculations of e.g. references [21, 22]. It must be stressed again that the functional of equation (91) has been developed by

Figure 17. (Color online) Differences of radii are shown as a function of mass number for a set of 88 spherical nuclei (diamonds, black points) and 111 spherical odd nuclei (full circles, red points)

introducing a minimal set of finite size terms, i.e. surface and spin-orbit terms, in addition to the bulk part fixed once for ever from microscopic nuclear matter EoS. In this way one can clearly separate the bulk and surface contribution to the binding and the radius in finite nuclei and establish a link between the properties of the nuclear medium (EoS and the bulk symmetry energy) and the structure of finite nuclei. It would be interesting to further analyze this link on the basis of an extended set of results.

Finally it is worth mentioning that an additional term in the functional should be included, the so called "Wigner term" [21], that introduces an additional binding for symmetric nuclei, but rapidly vanishes as the nucleus becomes asymmetric. In a purely phenomenological approach it has a parametrical form of the type [21]

$$E_W = V_W \exp\left[-\lambda\left(\frac{N-Z}{A}\right)^2\right] + V_W'|N-Z|\exp\left[-\left(\frac{A}{A_0}\right)^2\right] \tag{95}$$

and it can be ascribed to neutron-proton correlation/pairing, that indeed tends to disappear as soon as neutrons and protons occupy different shells. This is expected to produce a strong improvement in the overall quality of the fit. Again, it is an ambition of the microscopic approach to calculate, at least approximately, the values of the parameters appearing in this expression, following their physical interpretation [21, 22].

8.3. Pairing in nuclei

Soon after the formulation of BCS theory [147], it was shown [177] that pairing correlation is present in nuclei. Since then, pairing correlation has played a major role in the development of nuclear structure. Despite the enormous development in this field,

the main physical question that remains still unanswered is the origin of the attractive pairing interaction in nuclei in terms of the NN interaction. In most applications the pairing interaction is treated as a phenomenological force. This approach is quite successful, particularly with the Gogny force [176], but still the physical processes at the basis of these forces is not yet clarified. We will focus here only to pairing between like-particles, because the neutron-proton pairing is restricted mainly to symmetric or almost symmetric nuclei, where isospin symmetry is valid. We have seen that the bare NN potential is able to produce in nuclear matter a substantial pairing gap mainly at sub-saturation density. It is not trivial to relate these results to pairing in nuclei, since the bulk density is at saturation and the nuclear surface is too sharp to justify a local density approximation. Furthermore in nuclei surface modes can play a role in the physical processes responsible of the effective pairing interaction [178, 179, 180].

Besides the many-body aspects of the problem, at least two other features of the nuclear pairing have to be mentioned. One is related to the fact that the pairing phenomenon occurs close to the Fermi surface, while the bare nucleon-nucleon (NN) potential necessarily involves also scattering to high energy (or momentum) due to its strong hard core component, which is one of the main characteristics of the nuclear interaction. It looks therefore natural to develop a procedure which removes the high energy states and "renormalize" the interaction into a region close to the Fermi energy. This can be done in different ways, among which the most commonly used seems to be the Renormalization Group (RG) Method [124]. A second feature is the relevance of the single particle spectrum, not only because the density of states at the Fermi surface plays of course a major role, but also because the whole single particle spectrum has influence on the effective pairing interaction.

In the last few years relevant progress has been made in the microscopic calculations of pairing gap in nuclei [178, 179, 180, 181, 182, 183, 184, 185]. The main established result is that the bare NN interaction, renormalized by projecting out the high momenta, is a reasonable starting point that is able to produce a pairing gap which shows a discrepancy with respect to the experimental value not larger than a factor 2. In view of the great sensitivity of the gap to the effective interaction this result does not appear obvious. The effective pairing interaction constructed within this renormalization scheme [186] explains qualitatively also the surface relevance. Indeed, this interaction at the surface can exceed the value inside by one order of magnitude. Direct effect of the surface enhancement of the gap was presented in [187, 188] for semi-infinite nuclear matter and in [189] for a nuclear slab. Besides the renormalization of the bare interaction of the high momentum components, other physical effects should be included in a microscopic approach, like the ones related to the effective mass, or more generally, the single particle spectrum, and the many-body renormalization of the pairing interaction.

Let us first consider the problem of reducing the interaction to an effective one close to the Fermi energy. In general language this can be seen as a typical case that can be approached by an "Effective Theory", where the low energy phenomena are decoupled from the high energy components. In this procedure the resulting low

Table 1. the Argonne v_{18} potential.

λ	SLy4	Sly4-1	Sly4-2	Sly4-3
$3s_{1/2}$	1.23	1.10	0.83	0.56
$2d_{5/2}$	1.32	1.18	0.89	0.61
$2d_{3/2}$	1.34	1.20	0.92	0.63
$1g_{7/2}$	1.48	1.31	0.96	0.64
$2h_{11/2}$	1.27	1.13	0.85	0.57
Δ_{F}	1.34	1.19	0.89	0.60

energy effective interaction is expected to be independent of the particular form of the high energy components. However the procedure is not unique. The RG method has been particularly developed for the reduction of the general NN interaction keeping the deuteron properties and NN phase shifts up to the energy where they are well established. In this way a potential, phase equivalent to a known realistic NN potential, can be obtained, which contains only momenta up to a certain cut-off. The extension of this procedure to the many-body problem appears in general to require the introduction of strong three-body forces. It has been applied also to the pairing problem. To illustrate the difficulty of decoupling low and high momentum components for the pairing problem, we consider the simple case of nuclear matter in the BCS approximation discussed in section 7.4, see equation (79). Taking for the pairing interaction the bare NN interaction $V(k,k')$, it is possible to project out the momenta larger than a cutoff k_c by introducing the interaction $V_{\mathrm{eff}}(k,k')$, which is restricted to momenta $k < k_c$. It satisfies the integral equation

$$V_{\mathrm{eff}}(k,k') = V(k,k') - \sum_{k''>k_c} \frac{V(k,k'')V_{\mathrm{eff}}(k'',k')}{2E_{k''}} \, , \tag{96}$$

The gap equation, restricted to momenta $k < k_c$ and with the original interaction V replaced by V_{eff}, is exactly equivalent to the original gap equation. The relevance of this equation is that for a not too small cut-off the gap $\Delta(k)$ can be neglected in $E(k)$ to a very good approximation and the effective interaction V_{eff} depends only on the normal single particle spectrum above the cutoff k_c. As such V_{eff} contains necessarily some dependence on the in-medium single particle spectrum at high momenta. In the RG approach, if the procedure of constructing the low momenta interaction $\mathrm{V}_{low}(k,k')$, discussed in section 4.2.4, is carried out in vacuum, it implicitly assumes a free spectrum at high momenta. In the medium it faces the same uncertainty.

This procedure of projecting out the high momenta can be extended to finite nuclei, and the same uncertainty persists. To illustrate this point in table 1, taken from reference [190], are reported the values of the pairing gap for ^{120}Sn. The diagonal pairing gap matrix elements for the levels around the Fermi energy and the corresponding average values are compared for different types of calculations. For the mean field the Sly4 Skyrme force has been used. In the procedure of projecting out the high momenta the effective mass has been put equal to the bare one above a certain cut-off Λ. This can be

done within the so-called Local Potential Approximation (LPA) [191, 192], that has been proved to be a quite accurate approximation. In the first column the effective mass has been taken equal (and constant) to the original Sly4 value only inside the model space, i.e. within the states where the effective interaction is calculated after the projection of the high momentum components, according to equation (96). The model space corresponds to single particle energies $\epsilon_\lambda < 40$ MeV. For the second column $\Lambda = 3\text{fm}^{-1}$, for the third $\Lambda = 4\text{fm}^{-1}$ and for the fourth $\Lambda = 6.2\text{fm}^{-1}$. The original interaction is the Argonne v_{18} NN potential. In all cases the original density dependence of the effective mass was kept within the LPA scheme. The strong sensitivity of the pairing gap to the value of Λ indicates that the separation between small and high momenta components can be problematical.

We have seen in section 7.4 that in nuclear matter one of the main open questions is the role of the medium in screening the effective pairing interaction. It turns out [178, 179, 180] that the same processes of exchange of collective excitations between quasi-particles produce an overall attractive interaction, usually indicated as "induced interaction", and could contribute substantially to the strength of the effective pairing interaction. This striking difference could be due to the strong collectivity of the low lying surface modes in nuclei and to the corresponding small strength of the spin modes. The above described calculations that include only the bare NN interaction, on comparison with the experimental data, can put limits on the relevance of the induced interaction. Due to the mentioned uncertainties, it is not yet possible to draw any quantitative conclusions. In any case this is an active field of research and some answers, at least partial, could come form future works.

Finally it is important to mention one of the main issues that is involved when one tries to relate pairing in nuclear matter and finite nuclei. The size ξ of the Cooper pairs in nuclear matter can be estimated in the weak coupling limit

$$\xi \approx \frac{\hbar v_F}{\sqrt{8}\Delta_F} \tag{97}$$

In nuclear matter for the neutron pairing gap obtained with the free NN interaction one gets that $\xi > 5$ fm. If one extrapolates this expression to finite nuclei and takes a typical value for the gap of 1-2 MeV, then the value of ξ can exceed the size of the nucleus. It looks that we cannot describe pairing correlation in nuclei with a simple spacial picture. Also in this case the role of surface is essential. It has been found that the pairing correlation length ξ depends on the center of mass of the pair, and it shrinks just at the surface of the nucleus. In figure (18), taken from reference [193], is reported the case of a slab of nuclear matter. Here the Cooper pair size ξ_x in the direction x perpendicular to the slab is reported as a function of the center of mass position X. The minimum of ξ_x falls exactly at the surface of the slab, where $\xi_x \approx 2$ fm, independently of the pairing interaction used. This is in line with the results presented in references [194] for realistic cases, where the Cooper pair size was also found to be minimal at the surface and around 2 fm. References to previous works on this subject can be found in this paper. Even if this shrinking of the pair size at the surface could be a general effect,

Figure 18. Size of the Cooper pair in the direction perpendicular to a slab of nuclear matter. The surface of the slab is located at about X = 6 fm, very close to the position of the minimum.

not necessarily connected with the pairing interaction but rather just with the available phase space, it looks that pairing correlation has room mainly at the surface. This is in agreement with the already mentioned enhancement of the local pairing gap at the surface. Loosely speaking, one can imagine that the Cooper pairs are mainly formed around the surface, where the pairing correlation can develop.

8.4. Neutron and Proton Radii

It is not easy to establish at a formal level a direct connection of the properties of nuclei and nuclear matter. It has been then pursued a different strategy, that can be considered a semi-empirical theoretical method. One considers a wide set of Skyrme forces with different characteristics and one looks for a possible correlation between a specific nuclear matter property and a physical parameter in nuclei as the force is varied within the given set. This approach was followed in reference [206], where it was shown that the difference between the neutron and proton root mean square radii ("neutron skin") of Pb is linearly correlated to the slope of the neutron matter EoS at the density of 0.1 fm^{-3}. This linear correlation plot is shown in figure (19), taken from reference [143]. The linear correlation was shown to hold also for other nuclei and also if one considers, instead of the neutron matter EoS, the slope of the symmetry energy as a function of density in symmetric nuclear matter at approximately the same density [26]. Even if the approach is not formally microscopic, it is quite fruitful because it links in a direct way the nuclear EoS to the structure of nuclei. In other words, measuring a physical quantity in nuclei would give direct information on the nuclear EoS. Unfortunately it is not easy to measure the neutron radius, since the hadron probes are strongly interacting, at variance of electrons that provide the charge radius. There is a large expectation on the parity violation electron scattering experiment PREX that is going on at JLAB [207],

Figure 19. Linear correlations between the neutron and proton radii and the slope (Mev fm^3) of the symmetry energy at the density $\rho = 0.1\text{fm}^{-3}$. Squares from the top correspond to$NL1$ [195], $NL3$ [196], $G1$, $G2$ [197] and $Z271$ [198]. Triangles to Gogny forces $D280$, $D300$, $D250$, $D260$ $D1$ and $D1S$ [199]. Circles correspond to the Skyrme forces SV [200], SIV [200], SkM , SkM^* [201], $SLy4$, $SLy5$ [202], $T6$ [203], $SGII$ [204], SI [205], SII [205],$SIII$ and SVI [200]. The result for the BCP functional is labeled by a star.

because these measurements will give directly the difference between neutron and proton radii in ^{208}Pb. It has to be seen if the accuracy of the data will be enough to distinguish among different functionals. Partial justifications of some of these correlations have been presented in the literature [208], but further microscopic investigations are surely needed to clarify the field. As an illustration, in figure (20) is reported the results for the neutron skin value from one of the version of the functional BCP throughout the mass table. The set of results looks in overall agreement with the phenomenological data. It would be desirable to identify the main properties of the forces or functionals that determine the value of the radii difference [210, 26] (or other physical quantity), but this goal has still to be reached. This would be indeed a real progress in our understanding of the fundamental properties of the nuclear medium, from nuclear matter to finite nuclei.

8.5. Exotic Nuclei

The physics of exotic nuclei, i.e. nuclei far away from the stability valley that are not present on the Earth, is a field of rapid development where a large effort is concentrated in many laboratories throughout the world. Long term projects with large collaboration networks have been established in different countries or Continents (e.g. EURISOL, FIRB) to produce radioactive beams. They will allow to study systematically the properties of exotic nuclei that are not yet available, extending nuclear structure considerably along the asymmetry axis of the mass table. This is a challenge for the

Figure 20. Neutron skin calculated with the BCP functional throughout the mass table. The uppermost line and lowermost line are the phenomenological boundaries obtained in reference [209]. The middle line is just the average value of the phenomenological boundaries.

existing most sophisticated EDF, whose predictions for the forthcoming exotic nuclei often disagree. This line of research will provide invaluable information about the behavior of nuclei and the nuclear medium at increasing asymmetry. New phenomena are expected to occur at large enough asymmetry, like the onset of new nuclear shells. However, these phenomena depend on delicate nuclear structure features, and lie outside the scope of the present review.

8.6. The Neutron Star Crust

We have seen that the crust of Neutron Stars is the place in the Universe where the most asymmetric nuclei are present in a stable manner. The reason is of course the existence of the electron gas that is surrounding the nuclei and prevents their beta decay due to the Pauli blocking. In the inner crust also a neutron gas exists, but at not too high density it is possible to separate out, at least approximately, the nucleus at the center of the lattice cell. In this way one can picture the inner crust as a lattice of nuclei surrounded by a neutron gas (besides the electron gas). These nuclei are therefore unstable even with respect to the strong interaction (neutrons are "dripping" from them), but they are in equilibrium with the surrounding neutron gas. To illustrate this point, in figure (21) are reported the results of the calculations in reference [211], where the neutron density profile in the WS cell is compared, at different density, with the corresponding profile of a nucleus with the same atomic number and a mass number equal to the number of nucleons inside the radius of the "blob" (approximately estimated). They are evaluated with the same functional, and are stable with respect to strong interaction. One observes

the formation of the neutron gas outside the "nucleus" at the center of the WS cell as the density increases. Of course these nuclei would be strongly unstable with respect to weak interaction. Beyond the reported maximum density, it is not possible any more to

Figure 21. Neutron density profile of the nuclei at the upper edge of the inner crust of a neutron star. The dotted lines indicate the corresponding neutron density profile of a nucleus with the same atomic and mass numbers of the "cluster" of matter at the center of the Wigner-Seitz cell.

find finite nuclei corresponding to the "blob" at the center of the WS cell, because they are unstable even with respect to strong interaction. Then it is not any more possible to distinguish the "blob" as a nucleus separated from the surrounding neutron gas.

The structure of all these WS cells can be studied solely on the basis of a strong extrapolation of the theoretical methods, in particular of the various EDF, developed and checked along the available mass table. Unfortunately, despite all EDF must agree, within a certain accuracy, for the nuclei that can be produced in Laboratory, their predictions on the nuclei of such a large asymmetry are often diverging. This indicates that we are still far from having under control the microscopic theory of the asymmetry dependence of the nuclear medium properties. This uncertainty reflects into the uncertainty of the Neutron Star crust, and the discrepancy extends to the region of higher density, where it is not possible to separate any more a definite nucleus at the center of cell, until the transition to homogeneous matter occurs. As illustration in table (2) are reported the values of the atomic numbers of nuclei in the inner crust calculated in the classical paper by Negele and Vautherin [212] and with a different functional [213]. The latter includes also the pairing correlations with three different strengths (P1, P2 and P3). The reason of these type of discrepancies remain to be clarified, but it has to be stressed that the position of the minimum in the energy as a function of the atomic number is quite delicate, because it can often happen that

Table 2. Atomic number of the matter inside the Wigner-Seitz cell throughout the inner crust and corresponding cell radius. The calculations labeled P1, P2, P3 are for three different pairing strengths, reported in reference [213], in comparison with the results (NV) of reference [212].

k_F, fm^{-1}	Z				R_c, fm		
	P1	P2	P3	N&V	P1	P2	P3
0.6	58	56	56	50	37.51	36.85	36.92
0.7	52	46	46	50	32.02	30.31	30.27
0.8	42	40	40	50	26.90	25.97	25.97
0.9	24	20	20	40	20.26	18.34	18.39
1.0	20	20	20	40	16.69	16.56	16.56
1.1	20	20	20	40	14.99	15.05	15.05
1.2	20	20	20	40	13.68	13.73	13.74

different local minima are competing among each others. In the table are reported also the values of the Wigner-Seitz cell radius, that turns out to be a less sensitive quantity. It must be pointed out that these discrepancies persist at lower density, down to the drip point and slightly below, as systematically explored in reference [214] for a wide set of Skyrme forces and relativistic mean field functionals. To illustrate the difficulty and uncertainty in these calculations, in figure (22) are reported typical energy curves for the WS cell as a function of the atomic number [213]. Besides the apparent competition among different energy minima, it has to be noticed the tiny variation of the binding energy. The accuracy needed to predict the absolute minimum is of the order of 5-10 keV per particle, which is at the limit of the performance of the best EDF, and surely the extrapolation to so asymmetric matter is not yet under control. In any case, since the structure of these nuclei cannot be studied in laboratory, one has to look for observational data on Neutron Stars that are sensitive to their properties. The main physical parameters of the crust is the values of the atomic number of the nuclei in the lattice as a function of density and the lattice spacing. Other quantities, like the shear modulus or the incompressibility are functions of these parameters on the basis of well known properties of Coulomb lattices. In fact, even in the inner crust, the effect of the neutron gas on these quantities is negligible. The observation of NS oscillations during flares of X-ray or gamma ray emission in accreting processes or in magnetar quakes can be a possibility of studying the structure of the crust. These observations are now numerous [215, 216, 217, 218]. If in the oscillations the crust is decoupled from the core, the spectral analysis of these data can be used to constrain the shear modulus and, consequently, the density dependence of the symmetry energy [219]. This types of analysis are partly model dependent, but they open a window on the possibility of studying, even if in a very indirect way, the nuclear medium for very high asymmetry at and below saturation density. As illustration we report in figure (23) the luminosity

Figure 22. Energy per particle as a function of the atomic number in the Wigner-Seitz cell. The minimum corresponds to the actual configuration of the crust at the given density. The dotted lines indicate the results for a different choice of the boundary conditions at the edge of the cell, see reference [213]. The discrepancy between the full and dotted lines is a measure of the uncertainty in the Wigner-Seitz approximation.

oscillations discovered in reference [218] in the tail of an hyper-flare of SGR 1806-20. The three panels correspond to three different bands of the radiation frequencies [218].

9. Liquid-gas phase transition

In the latest stage of the supernovae collapse the EOS of asymmetric nuclear matter at finite temperature plays a major role in determining the final evolution. Microscopic calculations of the nuclear EOS at finite temperature are quite few. The variational calculation by Friedman and Pandharipande [220] was one of the first few semi-microscopic investigation of the finite temperature EOS. The results appear fairly close to the predictions based on Skyrme force models: symmetric nuclear matter undergoes a liquid-gas phase transition, with a critical temperature $T_c = 18 - 20$ MeV. This is a fundamental property of the nuclear medium. Different types of Skyrme forces

Figure 23. Light curves in the tail of the hyperflare from the SGR 1806-20. Observations and analysis of reference [218].

give different critical temperatures, but they lie all close to this range of values. Later, Brueckner-like calculations at finite temperature [221] confirmed these findings with very similar values of T_c. The full finite temperature formalism by Bloch and De Dominicis (BD) [222] was followed. In this section we sketch the main results and the method followed in the finite temperature case. We then discuss the connection with Laboratory experiments and data.

9.1. The critical temperature

The starting point in the many-body theory of finite temperature EoS is the calculations of the grand-canonical potential Ω. In the BD formalism,in line with the Brueckner scheme, a self-consistent single particle potential $U(\mathbf{k})$ is introduced and finally the grand-canonical potential is given by

$$\Omega = \Omega_0' + \Delta\Omega \tag{98}$$

where

$$\Omega_0' = -\frac{2V}{\pi^2}\int_0^{+\infty} k^2 dk[\ \frac{1}{\beta}\log(1 + e^{-\beta(e_k\mu)}) + U(k)n(k)\ ] \tag{99}$$

is the grand canonical potential for independent particles with hamiltonian

$$H_0' = \sum_k e_k a_k^\dagger a_k = \sum_k (\frac{\hbar^2 k^2}{2m} + U(k))a_k^\dagger a_k \tag{100}$$

and μ is the chemical potential. The interaction part $\Delta\Omega$ of the grand canonical potential is given by

$$\Delta\Omega \ = \ \frac{1}{2}e^{2\beta\mu}\int_{-\infty}^{\infty}\frac{e^{-\beta\omega}}{2\pi}d\omega Tr_2\left[\arctan\left(\mathcal{K}(\omega)\pi\delta(H_0' - \omega)\right)\right]. \tag{101}$$

Figure 24. (Color on line) Free energy of symmetric nuclear matter as a function of density at different temperatures. The lines are fits to the calculated points. The curves decrease systematically as the temperature increases.

The trace in the previous equation Tr_2 is taken in the space of antisymmetrized two-body states and the two-body scattering matrix $\mathcal{K}$ is defined by,

$$\langle k_1\ k_2|\mathcal{K}(\omega)|k_3k_4\rangle =$$

$$(n_>(k_1)n_>(k_2)n_>(k_3)n_>(k_4))^{\frac{1}{2}}\langle k_1k_2|K(\omega)|k_3k_4\rangle \tag{102}$$

where the scattering matrix K satisfies the integral equation,

$$\langle\ k_1k_2|K(\omega)|k_3k_4\rangle{=}\langle k_1k_2|v|k_3k_4\rangle{+}$$

$$\textstyle\sum_{k_3'k_4'}\langle k_1k_2|v|k_3'k_4'\rangle\ \frac{n_>(k_3')n_>(k_4')}{\omega-e}\ \langle k_3'k_4'|K(\omega)|k_3k_4\rangle. \tag{103}$$

In these equations $n_>(k) = 1 - n(k)$, with $n(k)$ the Fermi distribution function at a given temperature and for the single particle spectrum $e(k)$. Then equation (103) coincides with the Brueckner equation for the G matrix in the zero temperature limit. It has to be noticed, that only the principal part has to be considered in the integration, thus making K a real matrix. The appearance of the arctan in equation (101) looks peculiar, but it comes from a ladder summation similar to the one for the zero temperature G-matrix. More detail on the derivation and on the numerical treatment of the equations can be found in reference [221]. In this approach one calculates the free energy $F = \Omega + \mu N$ and then the pressure from the thermodynamical relationship

$$p = \rho^2\frac{\partial f}{\partial\rho} \tag{104}$$

where ρ is the total number density and f the free energy per particle F/N. A typical result is reported in figure (24), where the full lines are interpolations of the calculated points, suitable for differentiation. The resulting EoS at finite temperature, i.e. pressure vs. density, is reported in figure (25). One recognizes the familiar Van der Waals shape,

Figure 25. (Color on line) The isotherms of symmetric nuclear matter. The full diamond marks the critical point of the liquid-gas phase transition.

which entails a liquid-gas phase transition, with a definite critical temperature, i.e. the temperature at which the minimum in the Van der Waals isotherm disappears. This is clearly a fundamental property of the nuclear medium : it behaves macroscopically at finite temperature in a way similar to a classical liquid. The critical temperature turns out to be around $T_c = 18 - 20$ MeV.

A difficulty in this approach is the lack of thermodynamical consistency. In fact the thermodynamical relation $p = -f' + \mu\rho$, usually referred as the "Hughenoltz-Van Hove theorem", is not satisfied. Here f' is the free energy per unit volume F/V. In other words, the pressure calculated from equation (104) does not coincide with the pressure calculated from $p = -\Omega/V$. This point, that is not necessarily a too serious drawback, is discussed in the next section.

9.2. Theoretical uncertainties and challenges

We have seen that symmetric nuclear matter undergoes a liquid-gas phase transition. This is the result of calculations with microscopic calculations, but also with effective forces, e.g. Skyrme forces. The values of the critical temperature, however, depends on the theoretical scheme, as well as on the particular effective force adopted. In particular, it turns out that the critical temperature within Dirac-Brueckner scheme is definitely smaller [223, 224] than in the non-relativistic scheme, about 10 MeV against 18-20 MeV. This cannot be ascribed to relativistic effects, since the critical density is well below, about 1/3, the saturation density. Probably this is due to a different behavior of the Dirac-Brueckner EoS at low density. This point still needs clarification.

As anticipated in the previous sub-section, another uncertainty stems from the violation of the Hughenoltz-Van Hove (HVH) theorem within the extension to finite temperature of the non-relativistic Brueckner scheme, as implemented by Bloch and De

Dominicis [222]. In the applications, the pressure is calculated from the derivative of the free energy per particle and the theorem is actually automatically satisfied. The difficulty is then that the chemical potential determined by fixing the density in the Fermi distribution is not strictly the one extracted from the derivative of the free energy per unit volume, as it should be. In any case the procedure looks the most reliable within the Brueckner scheme, since the HVH theorem, as a thermodynamic relationship, is satisfied.

A general approximation scheme that strictly satisfies the theorem have been devised by G. Baym [225]. It is based on the self-consistent Green' s function method, where the single particle self-energy is approximated by a functional of the Green' s function itself, which is then calculated in a self-consistent manner. Numerical calculations have indeed [226] shown that the HVH is satisfied. The results at the two-body correlation level, at least when only two-body forces are used, in some cases are similar to the Brueckner ones, in some others they differ appreciably, according to the forces used [226, 227]. The main difference with the Brueckner scheme is the introduction in the ladder summation also of the hole-hole propagation. The expansion scheme is therefore at variance with the hole-line expansion, and actually it is not clear how to proceed to improve the approximation or if convergence has been reached. Therefore, on one hand we have the hole-line expansion at zero temperature that has some definite sign of convergence already at the two hole-line (Brueckner) level, on the other hand at finite temperature we have a different truncation scheme to satisfy the HVH theorem, that however is not proved to be a satisfactory approximation and does not reduce to the Brueckner scheme at zero temperature. It would be quite desirable to have a scheme that is able to have both requirements satisfied, i.e. to have a good degree of convergence and the fulfillment of the HVH theorem (at zero and finite temperature). Although this sort of dilemma is a challenge that requires further studies, the gross properties of nuclear matter at finite temperature appear well established.

9.3. Isospin dependence

If the nuclear matter is asymmetric, the existence of two components, neutrons and protons, complicate quite a bit the phase transition picture. The spinodal region is still well defined, the bulk incompressibility at a given asymmetry is negative in specific portions of the various possible thermodynamical planes. The coexistence line presents a new feature, the "distillation" phenomenon. The name is suggested by the analogy with the process used in the distillation of liquors. The chemical equilibrium between liquid and vapor requires the equality of the proton and and neutron chemical potentials. They are however different if matter is asymmetric, and therefore, in view of the density dependence of the symmetry energy, the fraction of neutrons and protons are different in the liquid and in the vapor. In general, it turns out that the vapor is expected to be more neutron rich. The effect is not dramatic, but it has been claimed that in heavy ion reactions, where the phase transition similar to the liquid-gas phase transition is

Figure 26. Isotherms of asymmetric nuclear matter at the indicated protons/nucleons ratio Z/A. Upper panel, neutron chemical potential. Lower panel, pressure. The points A and B indicate the endpoints of the coexistent region.

expected to occur, this effect should be seen [228]. The distillation has also the effect that the Maxwell construction for asymmetric matter is modified with respect to the symmetric case. The horizontal line that characterizes the construction in the pressure vs. density plane, within the coexistence region, is replaced by a non-horizontal line, see figure (26), taken from reference [229]. In fact, if the fractions of vapor and liquid are changed, while they have different compositions the overall asymmetry must be kept constant. This can be achieved only by changing the equilibrium pressure in order to shift properly the neutron and proton chemical potentials.

Both the spinodal decomposition [230] and the distillation phenomenon [229] in asymmetric matter at finite temperature have been studied within the Skyrme functional scheme. The line that marks the onset of the spinodal instability is now characterized not only by the values of the total density and temperature (at a given overall asymmetry) but also by the direction along which the instability can develop, i.e. the fractions of protons and neutrons. According to this direction, the curvature of the free energy in the plane of proton vs. neutron chemical potentials can vary. The direction where the curvature is minimal should indicate the most unstable direction and therefore the most probable composition of the liquid clusters that are produced due to the instability. This is illustrated in figure (27), taken form reference [230].

This can have direct relevance in astrophysics for the formation process of the NS crust, where however it is necessary to introduce the electron component and the Coulomb interaction.

Figure 27. (Color on line) Left panel. Coexistence (outer region) and spinodal (inner region) boundaries for three different Skyrme forces. In the right panel the arrows indicate the direction of minimal curvature of the free energy.

9.4. Phenomenology : the limiting temperature

We have seen that symmetric nuclear matter undergoes a liquid-gas phase transition. However, if this phase transition exists, it does not possess a direct correspondence in finite nuclei, due to the Coulomb interaction and finite size effects. In particular, the Coulomb force is long range and strong enough to modify the nature of the phase transition. However some authors [231, 232] have pointed out that the nuclear EoS can be linked to the maximal temperature a nucleus can sustain before reaching mechanical instability. This "limiting temperature" T_{lim} is mainly the maximal temperature at which a nucleus can be observed.

It has to be stressed that the reaction dynamics can prevent the formation of a true compound nucleus. The onset of incomplete fusion reactions can mask completely the possible presence of fusion or quasi-fusion processes. At higher energies, the heavy ion reaction can be fast enough that no (nearly) thermodynamical equilibrium can be reached, as demanded in a genuine standard fusion-evaporation reaction. However, combined theoretical and experimental analysis [233] indicate that a nearly equilibrium condition is reached in properly selected multi-fragmentation heavy ion reactions at intermediate energy. The main experimental observation is the presence of a plateau in the so-called "caloric curve", i.e. in the plot of temperature vs. total excitation energy [234, 235, 236, 237]. This behavior was qualitatively predicted by the Copenhagen statistical model [238] of nuclear multi-fragmentation. The relation between multi-fragmentation processes and the nuclear EoS was extensively studied by several authors within the statistical approach to heavy ion reaction at intermediate energy [239, 240, 241, 242, 243, 244, 245].

In different experiments, various methods were used to extract from the data the values of the temperature of the source which produces the observed fragments, but a careful analysis of the data [233] seems to indicate a satisfactory consistency of the results. In refs. [233, 246] an extensive set of experimental data was analyzed and it was

shown that the temperature at which the plateau starts is decreasing with increasing mass of the residual nucleus which is supposed to undergo fragmentation. Both the values and the decreasing trend of this temperature turn out to be consistent with its interpretation as limiting temperature T_{lim}. According to this interpretation, at increasing excitation energy the point where the temperature plot deviates from Fermi gas behavior and the starting point of the plateau mark the critical point for mechanical instability and the onset of the multi-fragmentation regime. The corresponding value of the critical temperature can be calculated within the droplet model, and indeed many estimates based on Skyrme forces are in fairly good agreements with the values extracted from phenomenology [233, 232]. Moreover, the relation between nuclear matter critical temperature T_c and T_{lim} appears to be quite stable and independent on the particular EoS and method used, which allows [246] to estimate T_c from the set of values of T_{lim}.

In general, one can expect that T_{lim} is substantially smaller than the critical one, T_c. In fact, both the Coulomb repulsion and the lowering of the surface tension with increasing temperature tend to destabilize the nucleus. Since the surface tension goes to zero at the critical temperature, T_{lim} is reached much before T_c. These predictions were checked in the seminal paper of reference [231], as well as in further studies based on macroscopic Skyrme forces [232], for which a simple relationship was established between T_{lim} and T_c. If microscopic EoS are used, then the relationship between T_{lim} and T_c is not so simple and the ratio T_{lim}/T_c depends on the detail of the EoS [247]. In principle the comparison with the phenomenological data can discriminate among different EoS. Indeed, most of the microscopic EoS reproduce the empirical saturation point, but their behavior at finite temperature can be quite different. This is mainly because the critical temperature, and therefore the limiting temperature, is very sensitive to the details of the EoS. In fact T_c is determined by the behavior of the derivative of the pressure with respect to the density, which in turn is the second derivative of the free energy. If the pressure is extracted directly from the grand canonical potential as a function of the chemical potential, still a strong sensitivity to the low density and high temperature properties of the EoS remains. In figure (28) is reported the pressure as a function of the chemical potential in symmetric nuclear matter, where one can recognize the liquid branch (the branch starting from the lowest cusp) and the vapor branch (the almost vertical one that starts from the upper cusp) [247]. Their intersection gives the coexistence point, while the smooth branch joining the two cusps is the unstable part of the EoS, corresponding to the Maxwell construction. The upward shifted liquid branch (dashed line) is the branch of a finite nucleus that takes into account the Coulomb interaction and finite size effects. Since the vapor branch is assumed almost unchanged, the shifted branch gives the shifted coexistent point between the nucleus and the vapor (assumed uncharged). If, as in the figure, the liquid branch touches the upper cusp, then the corresponding temperature is the searched limiting temperature [247], since at increasing temperature the cusp is lowered and no coexistence point exists anymore. In figure (29), taken from reference [247], are reported the results of a systematic calculation of T_{lim} for different nuclei and for different EoS in comparison with the values extracted

Figure 28. Chemical potential vs. pressure for symmetric nuclear matter (full line). The line starting from the lower cusp is the liquid branch, the one (almost vertical) starting from the upper cusp is the vapor branch. The intersection point is the coexistence point at that temperature. The line joining the two cusps is the unstable branch. The dashed line corresponds to a finite nucleus. It is obtained within a simplified Liquid Drop model. The figure corresponds to the case of a temperature equal to the limiting temperature.

Figure 29. Limiting temperature calculated with different EoS in comparison wit the experimental data (squares with error bars) From the bottom, full triangles corresponds to the Dirac-Brueckner EoS [223], full diamonds to EoS calculated within the finite temperature BHF and with the Bonn + TBF interaction, full circles to the same method but with the Av_{14} + TBF interaction [247], and finally full squares to the EoS from the chiral perturbation theory of reference [248].

from experimental data [233, 246]. One notices the strong dependence on the EoS derived from different microscopic schemes, and at the same time the relative small sensitivity to the NN force within the same scheme (BHF). It seems that the non-relativistic EoS based on the BHF approximation is the favored one.

9.5. The astrophysical link

The outer part of cold Neutron Stars is formed by a solid crystal of nuclei, while in a supernova, during the after bounce stage, the temperature is so high that nuclear matter is in the homogeneous fluid phase. During the cooling process medium-heavy nuclei are formed from the homogeneous matter, and this transition is quite similar to a liquid-vapor phase transition, where liquid droplets are formed in the mixed phase. The droplet formation is directly related to the so called "spinodal" instability, i.e. the region in the phase diagram where the incompressibility is negative. However, the presence of Coulomb interaction changes the nature of the transition [249]. It turns out that, despite it is of first order, the thermodynamical potentials do not display singularity as a function of the thermodynamical variables. In any case, the transition is accompanied by the formation of nuclear clusters. In fact one can expect that at sufficiently low temperature, inside the spinodal region, nuclear matter is composed of nuclei of different sizes, light fragments (tritons, helium-3 and alpha particles) and nucleons. This phase has been described on the basis of the liquid drop model [250] and the relativistic Thomas-Fermi scheme [251]. In the low density limit a virial expansion has been also applied [252]. The detailed theoretical description of this phase is quite relevant mainly for supernova simulations. A microscopic theory of the corresponding EoS, at the same level of accuracy as for the homogeneous matter case, is still missing.

Finally, it has to be mentioned that at even lower temperature the clusters should undergo a liquid-solid phase transition, with the formation of a Coulomb crystal. This transition is even less known and no consensus exists on its general properties like the solidification energy or latent heath. A discussion on this subject is outside the scope of the present review.

10. Conclusions

The excursus we tried to perform on the properties of the peculiar matter, that can be called "nuclear medium", surely does not make justice of the impressive progress that has taken place both at phenomenological and theoretical level. The continuous and vivid interest on the subject is due to the extremely wide realm of phenomena and physical systems, on the Earth and in the Universe, where the nuclear medium plays a central role.

The continuous interplay between theoretical developments on one hand and laboratory experiments and astrophysical observations on the other hand is the main driving force that makes possible progress in this exciting field. As we tried to illustrate, our knowledge on the properties of the nuclear medium has widened and sharpened in many respects. Many physical parameters start to be known with a certain accuracy not only at saturation density but also at lower and higher density, and, in general, the Equation of State has been severely constrained. Taking the risk of being too schematic, let us try to summarize tentatively our knowledge of those properties of the

nuclear medium that we touched in this review.

1. *Equation of State.* The constraints that has been obtained from the data on heavy ion collisions and from the analysis of astrophysical observations on Neutron Stars are complementary between each others, since the nuclear matter asymmetry that is involved is quite different in the two cases. However, it is a challenge for the theory to be able to describe the nuclear medium in both physical conditions. If one takes together the two sets of data, one can get a severe test for the different microscopic theories. Although these constraints have to be confirmed and further analyzed, one can expect that in the near future new data and new results will put under serious exam all existing microscopic theories.

2. *Incompressibility.* The value of the symmetric matter incompressibility near saturation seems now to be constrained to an interval approximately between 210 and 250 MeV. Microscopic theories are in fair agreements with these values. More difficult is to put constraints on the incompressibility at higher density, since its value is determined by the details of the density dependence of the pressure. Astrophysical observations should test in principle the incompressibility of very asymmetric nuclear matter, but the uncertainty on the structure of neutron stars inner core hinders the progress in this direction.

3. *Symmetry energy.* The symmetry energy at saturation can be considered constrained in a narrow interval, essentially 30 ± 1 MeV. All microscopic theories agree with these values. Indirect hints about the density dependence of the symmetry energy come from both heavy ion collision data and astrophysical observation on neutron star phenomenology. The data analysis does not allow to get any sound conclusion, and discrepancies among different groups on the interpretation of the data are present. Microscopic theories agree at subsaturation density and up to 2-3 times saturation density, but disagreements appear at higher density. Correlations between symmetry energy at sub-saturation density and nuclear structure properties have been found. These can be of great help in clarifying many open questions in the field.

4. *Transport coefficients.* Several macroscopic phenomena that occur in neutron stars are determined by transport properties of the nuclear medium. The prediction of the damping of some of the possible overall oscillations of neutron stars requires the calculation of the shear and bulk viscosity. The study of cooling evolution of neutron stars needs the knowledge of the thermal properties of the nuclear medium in different physical conditions. In principle these transport coefficients require only standard techniques based on the Fermi Liquid theory. What is needed presently is a consistent scheme that is able to describe both the mechanical properties, like the EoS, of the nuclear medium and its transport properties. Progresses in this direction have been done and one can be confident that in the near future a coherent picture of the nuclear medium will be possible on the basis of microscopic many-body theory, at least for not too high density.

5. *Low energy excitations.* The elementary excitations of the nuclear medium are relevant for its thermal properties and for many phenomena occurring in neutron stars,

like emission and propagation of neutrinos. They are also a guidance to the low energy excitations in nuclei. They can be studied within the Landau theory of Fermi liquids. The fundamental physical parameters that are needed are the so called "Landau parameters" that fix the effective nucleon-nucleon interaction in the vicinity of the Fermi surface. The microscopic determination of these parameters is a difficult theoretical problem, that has been approached with a variety of techniques. Both in symmetric and pure neutron matter their values are not firmly established. The phenomenology on nuclei excitations give only indications on some of them, since the physical conditions are quite different and finite size effects, like the presence of a surface, are essential.

6. *Nuclei and finite size effects.* The connection between the nuclear medium properties and the structure of nuclei is of course not simple. However, since a long time, the Energy Density Functional method has been developed also to describe the ground state of nuclei and their elementary excitations. This method is the most suited to establish a link between nuclear structure and the nuclear medium properties. Indeed the main assumption that can be taken within this method is to divide the functional to be minimized into a bulk and a surface part and identify the bulk part with the EoS of nuclear matter. Of course, besides these two building blocks, the spin-orbit and Coulomb interaction must be included. This is a theory that is semi-microscopic in character, since all finite size effects are assumed to be included in an effective way in surface terms, to be determined phenomenologically. However, the physical interpretation of the different terms can provide hints on the values of the parameters that fix the non-bulk parts of the functional. If the functionals is treated completely phenomenological and the number and complexity of the surface terms (i.e. containing density gradients) are increased, the accuracy of these functionals can be excellent throughout the mass table. The semi-microscopic and the purely phenomenological approach are complementary, and substantial refinements and increase of accuracy are expected to occur in the future.

7. *Pairing and superfluidity.* The pairing correlation is of paramount relevance both in the physics of neutron stars and in nuclear structure. Substantial progress has been made in the theoretical determination of the effective pairing interaction in neutron matter and in neutron star matter for the different superfluid channels. Due to the extreme sensitivity of the pairing gap to the strength of the effective interaction, the various pairing gaps are still uncertain, but their overall trends as a function of density can be considered established, at least for not too high density. In nuclei it is not yet established to what extent the bare nucleon-nucleon interaction, taken as pairing interaction, is able to reproduce the experimental pairing gaps. However, a substantial fraction can surely come from the bare interaction, while the remaining part is a matter of debates.

8. *Transition to quark matter.* Neutron stars could be the only place in the Universe where macroscopic portion of quark matter is present in stable conditions. Massive neutron stars are indeed expected to have so high density baryonic matter in their interior that a transition to the deconfined phase could be possible. This is of course not firmly established, but progress in this field seems to be rapid. The maximum mass

of observed neutron stars, with a fairly good degree of confidence, has increased in the last few years, up to a value close to 2 $M_{\odot}$. This result, if confirmed, would put definite constraints not only on the nuclear medium EoS but also on the possible quark matter EoS. This shows the interplay between the "traditional" nuclear physics and the theory of the QCD matter in the physics of neutron stars. Further exciting and fundamental progresses are expected in the near future in this field.

This schematic list surely does not exhaust all the facets of the properties of the nuclear medium, but we hope to have given at least some ideas of the state of the art in the field, of what is going on and of the trends that can be expected to develop in the future.

Acknowledgments

We would like the thanks all our collaborators along the years, who appear as co-authors of the papers quoted in this review. To them we would like to express our gratitude and friendship. One of the author (M.B.) would like to acknowledge the illuminating discussions with Prof. P. Schuck on the Thomas-Fermi approximation and Prof. X. Vinas on the Density Functional method.

We acknowledge the support of COMPSTAR, a research and training program of the European Science Foundation.

References

[1] D. Youngblood,H.L. Clark and Y.W. Lui, Phys. Rv. Lett 82, 691 (1999).
[2] W.D. Myers and W.J. Swiatecky, Nucl. Phys. A601, 141 (1996).
[3] J.P. Blaizot, Phys. Rep. 64, 171 (1980).
[4] A.B. Migdal,*Theory of Finite Fermi Systems and Application to Atomic Nuclei*, Wiley Interscience, New York 1967.
[5] A. Bohr and B.R. Mottelson, *Nuclear Structure*, Vol. I, 1974 and Vol. II, 1975, Benjamin (N.Y.).
[6] C.F. von Weisäcker, Z. Phys. 96, 431 (1935).
[7] H.A. Bethe and R.F. Bacher, Rev. Mod. Physics 8, 82 (1936).
[8] P. Ring and P. Schuck, *The nuclear many-body problem* Springer Verlag, Berlin, 1980.
[9] W.D. Myers and W.J. Swiatecki, Nucl. Phys. 81, 1 (1966).
[10] W.D. Myers, Nucl. Phys. A145, 387 (1969).
[11] W.D. Myers and W.J. Swiatecki, Ann. Phys. (N.Y.) 55, 186 (1969).
[12] V.M. Strutinsky , Nucl. Phys. A95, 420 (1967) ; A122, 1 (1968) ; A218, 169 (1974).
[13] P. Danielewicz and J. Lee, Nucl. Phys. A727, 233 (2003).
[14] P. Danielewicz, Nucl. Phys. A818, 36 (2009).
[15] P. Möller, J.R. Nix, W.D. Myers and W.J. Swiatecki, Atomic Data and Nuclear Data Tables 59, 185 (1995).
[16] P. Möller, J.R. Nix and K.-L. Kratz, Atomic Data and Nuclear Data Tables 66, 131 (1996).
[17] W.D Myers and W.J. Swiatecki, Nucl. Phys. A601, 141 (1996).
[18] C.A. Bertulani, arXiv:nucl-th/0607024.
[19] X. Roca-Maza, M. Centelles, F. Salvat and X. Vinas, Phys. Rev. C78, 044332 (2008).
[20] M. Centelles, S.K. Patra, X. Roca-Maza, B.K. Sharma, P.D. Stevenson and X. Vinas, J. Phys. G:Nucl. Part. Phys. 37, 075107 (2010).
[21] N. Chamel, S. Goriely and J.M. Pearson, Nucl. Phys. A812, 72 (2008).

[22] N. Chamel, S. Goriely and J.M. Pearson, Phys. Rev. C80, 065804 (2009).
[23] G. Colo', N. Van Giai, J. Meyer, Bonnaceur and P. Bonche, Phys. Rev. C70, 024307 (2004).
[24] M.M. Sharma, Nucl. Phys. A816, 65 (2009).
[25] L. Trippa, G. Colo' and E. Vigezzi, Phys. Rev. C77, 061304 (2008).
[26] M. Centelles, X. Roca-Maza, X. Vinas and M. Warda, Phys. Rev. Lett. 102, 122502 (2009).
[27] J. Blocki, Y. Boneh, J.R. Nix, J. Randrup, M. Robel, A.J. Sierk and W.J. Swiatecki, Ann. Phys. (N.Y.) 113, 338 (1978).
[28] J. Blocki, J.J. Shi and W.J. Swiatecki, Nucl. Phys. A554, 387 (1993).
[29] C. Jarzynski and W.J. Swiatecki, Nucl. Phys. A552, 1 (1993).
[30] J. Blocki, J. Skalski and W.J. Swiatecki, Nucl. Phys. A594, 137 (1995).
[31] M. Baldo, G.F. Burgio, A. Rapisarda and P. Schuck, Phys. Rev. C58, 2821 (1998).
[32] G.F. Bertsch, P.F. Bortignon and R.A. Broglia, Rev. Mod. Physics 55, 287 (1983).
[33] G.G. Dussel,E.C. Seva and H.M. Sofia, Phys. Rev. C49, 1989 (1994).
[34] J. Aichelin and J. Schaffner-Bielich, arXiv:0812.1341 (nucl-th).
[35] A. Ono, Phys. Rev. C59, 853 (1999).
[36] Ch. Hartnack, R.K. Puri, J. Aichelin, J. Konopka, S.A. Bass, W. Greiner and H. Stöcker, EPJA 1, 151 (1998).
[37] T. Maruyama, K. Niita and A. Iwamoto, Phys. Rev. C53, 297 (1996).
[38] J. Aichelin, Phys. Rep. 202, 233 (1991).
[39] P. Danielewicz, R. Lacey and W. Linch, Science 298, 1592 (2002).
[40] M. Baldo and C. Maieron, J. Phys. G: Nucl. Part. Phys. 34, R1 (2007).
[41] T. Klähn, D. Blaschke, F. Sandin, Ch. Fuchs, A. Faessler, H. Grigorian, G. Ropke and J. Trümper, arXiv:nucl-th/0609067.
[42] C. Fuchs, Progress in Particle and Nuclear Physics 56, 1 (2006)
[43] D. Miskowiec et al., Kaos Collaboration, Phys. Rev. Lett. 72, 3650 (1994).
[44] J. Ritman et al., FOPI collaboration, Z. Phys. A352, 335 (1992).
[45] C. Sturm et al., Kaos Collaboration, Phys. Rev. Lett. 86, 39 (2001).
[46] H.A. Bethe and J.R. Wilson, ApJ 295, 14 (1985).
[47] H.-Th Janka, K. Langanke, A. Marek, G. Martinez-Pinedo and B. Müller, Phys. Rep. 442, 38 (2007).
[48] J. Nordhaus, A. Burrows, A. Almgren and J. Bell, arXiv:1006.3792 [astro-ph.SR].
[49] N.J. Hammer, H.-Th. Janka and E. Müller, ApJ 714, 1371 (2010).
[50] G. Baym, C. Pethick and P. Sutherland, ApJ 170, 199 (1971).
[51] P. Haensel, A.Y. Potekhin and D.G. Yakovlev, *Neutron Stars* Vol. 1, Springer 2007.
[52] J.R. Oppenheimer and G.M. Volkoff, Phys. Rev. 55, 374 (1939).
[53] R.C. Tolman, Phys. Rev. 55, 364 (1939)
[54] D.G. Yakovlev, *Exotic States of Nuclear Matter*, pp. 191, World Scientific 2008, Eds. U. Lombardo, M. Baldo, F. Burgio and H.-J. Schulze.
[55] F. Özel, G. Baym and T. Güver, arXiv:1002.3153 [astro-ph.HE].
[56] A.W. Steiner, J.M. Lattimer and E.F. Brown, arXiv:1005.0811 [astro-ph.HE].
[57] A. Akmal, V.R. Pandharipande and D.G. Ravenhall, Phys. Rev. C58, 1804 (1998).
[58] H.-J. Schulze, A. Polls, A. Ramos and I. Vidana, Phys. Rev. C73, 058801 (2006).
[59] R.A. Hulse and J.H. Taylor, ApJ 195, L51 (1975).
[60] I. Vidana, D. Lagoteta, C. Provisencia, A. Polls and I. Bombaci, arXiv:1006.5660 [nucl-th].
[61] M. Baldo, G.F. Burgio, P. Sahu, A. B. Santra and H.-J. Schulze, Physics Letters B526, 19 (2002).
[62] M. Baldo, G.F. Burgio, P. Sahu, and H.-J. Schulze, Phys. Rev. C66, 025802 (2002).
[63] M. Baldo, M. Buballa, G.F. Burgio, F. Neumann, M. Oertel, and H.-J. Schulze, Physics Letters B562, 153 (2003).
[64] C. Maieron, M. Baldo, G.F. Burgio, and H.-J. Schulze, Phys. Rev. D70, 043010 (2004).
[65] M. Baldo, G.F. Burgio, P. Castorina, S. Plumari, and D. Zappala', Phys. Rev. D78, 063009 (2008).
[66] M. Alford, M. Braby, M. Paris and S. Reddy, ApJ 629, 969 (2005).

[67] M. Alford, D. Blaschke, A. Drago, T. Klahn, G. Pagliara and J. Schaffner-Bielich, Nature 445, E7 (2007).
[68] P.B. Demorest, T. Pennucci, S.M. Ransom, M.S.E. Roberts and J.W.T. Hessels, Nature 467, 1081 (2010).
[69] F. Özel, D. Psaltis, S. Ransom, P. Demorest and M. Alford, arXiv:1010.5790 [astro-ph.HE].
[70] R. Machleidt and I. Slaus, J. Phys. G: Nucl. Part. Phys. 27, R69 (2001).
[71] R. Machleidt, Phys. Rev. C63 024001 (2001).
[72] F. Mandl and G. Shaw, *Quantum Field Theory*, John Wiley and Sons 1995.
[73] A. Li, G.F. Burgio, U. Lombardo and W. Zuo, Phys. Rev. C74, 055801 (2006).
[74] H. Heiselberg and M. Hjorth-Jensen, Astrophys. J. 525, L45 (1999).
[75] E.N.E. van Dalen, Ch. Fuchs and A. Faessler, Phys. Rev. C72, 065803 (2005).
[76] M. Baldo, *Nuclear Methods and the Nuclear Equation of State*, International Review of Nuclear Physics Vol. 8, pp 1, World Scientific 1999, M. Baldo ed.
[77] M. Baldo, I. Bombaci and G.F. Burgio, Astronomy and Astrophysics 328, 274 (1997).
[78] X.R. Zhou, G.F. Burgio, U. Lombardo, H.-J. Schulze and W. Zuo, Phys. Rev. C 69 (2004) 018801.
[79] Z.H. Li, U. Lombardo, H.-J. Schulze, W. Zuo, L.W. Chen and H.R. Ma, Phys. Rev. C74, 047304 (2006).
[80] P. Grange', A. Leujeune, M. Martzolff and J.-F. Mathiot, Phys. Rev. C40, 1040 (1989).
[81] W. Zuo, A. Leujeune, U. Lombardo and J.-F. Mathiot, Nucl. Phys. A706, 418 (2002).
[82] W. Zuo, A. Leujeune, U. Lombardo and J.-F. Mathiot, Eur. Phys. J. A14, 469 (2002).
[83] M. Baldo and Alaa Eldeen Shaban, Phys. Lett. B661, 373 (2008).
[84] J. Navarro, R. Guardiola and I. Moliner, *Introduction to Modern Methods of Quantum Many-Body Theory and their Applications*, Eds. A. Fabrocini, S. Fantoni and E. Krotscheck, World Scientific 2002, Series on Advances in Many-Body Theory, Vol. 7.
[85] V. R. Pandharipande and R.B. Wiringa, Rev. Mod. Phys. 51, 821 (1979).
[86] R. Machleidt, *Advances in Nuclear Physics* Vol. 19 pp. 189, Plenum Press 1989.
[87] R. Brockmann and R. Machleidt, *Nuclear Methods and the Nuclear Equation of State*, International Review of Nuclear Physics Vol. 8, pp 121, World Scientific 1999, M. Baldo ed.
[88] G.E. Brown, W. Weise, G. Baym and J. Speth, Comm. Nucl. Part. Phys. 17, 39 (1987).
[89] T. Gross–Boelting, Ch. Fuchs and A. Faessler, Nucl. Phys. A648, 105 (1999).
[90] S.K. Bogner, R.J. Furnstall and A. Schwenk, Prog. Part. Nucl. Phys. 65, 94 (2010).
[91] D.R. Entem and R. Machleidt, Phys. Lett. B524, 93 (2003).
[92] S. Weinberg, Phys. Lett. B251, 288 (1990).
[93] S. Weinberg, Nucl. Phys. B363, 3 (1991).
[94] S. Weinberg, Phys. Lett. B295, 114 (1992).
[95] J.W. Holt, N. Kaiser and W. Weise, Phys. Rev. C81, 024002 (2010).
[96] R. Machleidt, P. Liu, D.R. Entem and E. Ruiz Arriola, Phys. Rev. C81, 024001 (2010).
[97] V.A. Khodel and E.E. Saperstein, Phys. Rep. 92, 183 (1982).
[98] G. Baym and C. Pethick, *Landau Fermi-Liquid theory*, John Wiley and Sons (N.Y.) 1991.
[99] M. Gell-Mann and L. Low, 1951 Phys. Rev. 84, 350 (1951).
[100] P. Nozieres, *Le Probleme a N Corps*, Dunod, Paris 1963.
[101] L.P. Kadanoff and G. Baym, *Quantum Statistical Mechanics*, W.A. Benjamin, N.Y. 1962.
[102] C. Mahaux, P.F. Bortignon, R.A. Broglia and C.H. Dasso, Phys. Rep. 120, 1 (1985).
[103] J.W. Negele and H. Orland, *Quantum Many-Particle Systems*,Addison-Wesely 1988.
[104] J.P. Jeukenne, A. Lejeunne and C. Mahaux, Phys. Rep 25, 83 (1976).
[105] G. A. Brooker and J. Sykes, Phys. Rev. Lett. 21, 279 (1968).
[106] H. Hojgaard Jensen, H. Smith and J.W. Wilkins, Phys. Lett. A27, 532 (1968).
[107] H. Hojgaard Jensen, H. Smith and J.W. Wilkins, Phys. Rev. 185, 323 (1969).
[108] A.A. Abrikosov and I.M. Khalaktikov, Sov. Phys. JETP 5, 887 (1987).
[109] O. Benhar and M. Valli, Phys. Rev. Lett. 99, 232501 (2007).
[110] O. Benhar, A. Polls, M. Valli and I. Vidana, Phys. Rev. C81, 024305 (2010).

[111] H.F. Zhang, U. Lombardo and W. Zuo, arXiv:1006.2656 [astro-ph.SR].
[112] N. Sandulescu, Phys. Rev. C70, 025801 (2004).
[113] C. Monrozeau, J. Margueron and N. Sandulescu, Phys. Rev. C75, 065807 (2007).
[114] M.G. Alford, S. Mahmoodifar and K. Schwenzer, arXiv:1005.3769 [nucl-th].
[115] P. Haensel, K.P. Levenfish and D.G. Yaklovev, Astronomy and Astrophysics 357, 1157 (2000).
[116] T.K. Jha, H. Mishra and V. Sreekanth, arXiv:1002.4253 [hep-ph].
[117] E. Khan, N. Sandulescu and N. Van Giai, Phys. Rev. C71, 042801 (2005).
[118] M. Baldo and C. Ducoin, Phys. Rev. C79, 035801 (2009).
[119] M. Baldo and C. Ducoin, in preparation.
[120] S. Babu and G.E. Brown, Ann. Phys. 78, 1 (1973).
[121] S.-O. Bäckman, G.E. Brown and J.A. Niskanen, Phys. Rep. 124, 1 (1985).
[122] T.L. Ainsworth, J. Wambach and D. Pines, Phys. Lett. B222, 173 (1989).
[123] U. Lombardo and H.-J. Schulze, in *Physics of Neutron Star Interiors*, pp. 30, Lecture Notes in Physics vol. 578, Eds. D. Blaschke, N. K. Glendenning, and A. Sedrakian (Springer, 2001)
[124] A. Schwenk, G.E. Brown and B. Friman, Nucl. Phys. A703, 745 (2002).
[125] J. Carlson, S.-Y. Chang, V.R. Pandharipande andK.E. Schmidt, Phys. Rev. Lett. 91, 050401 (2003).
[126] G.E. Astrakharchik, J. Boronat, J. Casulleras and S. Giorgini, Phys. Rev. Lett. 93, 200404 (2004).
[127] A. Bulgac, J.E. Drut and P. Magierski, Phys. Rev. Lett. 96, 090404 (2006).
[128] A. Bulgac, J.E. Drut and P. Magierski, Phys. Rev. Lett. 99, 120401 (2007).
[129] B. Friedman and V.R. Pandharipande, Nucl. Phys. 361 A, 501 (1981).
[130] J. Carlson, J. Morales, V.R. Pandharipande and D.G. Ravenhall, Phys. Rev. C 68, 025802 (2003).
[131] A. Schwenk and C.J. Pethick, Phys. Rev. Lett. 95, 160401 (2005).
[132] R.B. Wiringa, V.G.J. Stoks and R. Schiavilla, Phys. Rev. **C 51**, 38 (1995).
[133] M. Baldo and C. Maieron, Phys. Rev. C77, 015801 (2008).
[134] A. Schwenk and C.J. Pethick, Phys. Rev. Lett. 95, 160401 (2005).
[135] M. Baldo, G. Giansiracusa, U. Lombardo and H.Q. Song, Phys. Lett. B473, 1 (2000).
[136] M. Baldo, A. Fiasconaro, G. Giansiracusa, U. Lombardo and H.Q. Song, Phys. Rev. C65, 017303 (2001).
[137] A. Gezerlis and J. Carlson, Phys. Rev. C77, 032801 (2008).
[138] H.S. Xu et al., Phys. Rev. Lett. 85, 716 (2000).
[139] M.B. Tsang, W.A. Friedman,C.K. Gelbke, W.G. Lynch, G. Verde and H.S. Xu, Phys. Rev. Lett. 86, 5023 (2001).
[140] S.R. Souza, M.B. Tsang, R. Donangelo, W.G. Lynch and A.W. Steiner, Phys. Rev. C78, 014605 (2008).
[141] L. Shi and P. Danielewicz, Phys. Rev. C68, 064604 (2003).
[142] Lie-Wen Chen, Che Min Ko and Bao-An Li, Phys. Rev. Lett. 94, 032701 (2005).
[143] M. Baldo, C. Maieron, P. Schuck and X. Vinas, Nucl. Phys. A736, 241 (2004).
[144] Bao-An Li, Lie-Wen Chen and Che Ming Ko, Phys. Rep. 464, 113 (2008).
[145] M.A. Alpar, Astrophys. J. 213, 527 (1977).
[146] M.A. Alpar, S.A. Langer and J.A. Sauls, Astrophys. J. 282, 533 (1984).
[147] J. Bardeen, L.N. Cooper and J.R. Schrieffer, Phys. Rev. 108, 1175 (1957).
[148] U. Lombardo and H.-J. Schulze, "Superfluidity in neutron star matter", in *Physics of Neutron Star Interior*, edited by D. Blaschke, N. Glendenning and A. Sedrakian, pp. 30 (Berlin: Springer) 2001.
[149] M. Baldo and A. Grasso, Phys. Lett. B485, 115 (2000).
[150] M. Baldo and A. Grasso, Phys. At. Nuclei, 64, 611 (2001).
[151] L.G. Cao, U. Lombardo and P. Schuck, Phys. Rev. C74, 064901 (2006).
[152] P. Bozek, Phys. Rev. C65, 034327 (2002).
[153] P. Bozek and P. Czerski, Phys. Rev. C66, 027301 (2002).
[154] A. Gezerlis and J. Carlson, Phys. Rev. C81, 025803 (2010).

[155] S. Gandolfi, A.Yu. Illarionov, S. Fantoni, F. Pedereiva and K.E. Schmidt, Phys. Rev. Lett. 101, 132501 (2008).
[156] M. Baldo and H.-J. Schulze, Phys. Rev. C 75, 025802 (2007).
[157] A. Schwenk and B. Friman, Phys. Rev. Lett. 92, 082501 (2002).
[158] D.G. Yakovlev and C.J. Pethick, "Neutron Star Cooling", *Annu. Rev. Astron. Astrophys.* 42, 169 (2004).
[159] See e.g. N.H. March, Self-consistent Fields in Atoms, Pergamon Press, 1975.
[160] A. Bhagwat, X. Vinas, M. Centelles, P. Schuck and R. Wyss, arXiv: 0911.4648 [nucl-th].
[161] B.G. Carlson, J. Dobaczweski, K. Mizuyama and J. Toivanen, Phys. Rev. C77, 064307 (2008).
[162] J. Dobaczweski, arXiv:1009.0899 [nucl-th].
[163] W. Kohn and L.J. Sham, Phys. Rev. A140, 1133 (1965).
[164] R.O. Jones and O. Gunnarsson, Rev. Mod. Phys. 61, 689 (1989).
[165] H. Eschrig, The Fundamentals of Density Functional Theory (B. G. Teubner, Stuttgart, 1996).
[166] A. E. Mattsson, Science 298, 759 (2002).
[167] J.P. Perdew and K.Schmidt, Density Functional Theory and Its Applications to Material, V. Van Doren et al. Eds. CP577 (American Institute of Physicas, Melville NY, 2001).
[168] Jianmin Tao, J.P. Perdew, V.N. Staroverov and G.F. Scuseria, Phys. Rev. Lett. 91, 146401 (2003).
[169] Jianmin Tao and J.P. Perdew, Phys. Rev. Lett. 95, 196403 (2005).
[170] P. Bonche, S. Koonin and J.W. Negele, Phys. Rev. C13, 1226 (1976).
[171] A.S. Umar, M.R. Strayer, P.-G. Reinhard, K. T.R. Davies and J.-S. Lee, Phys. Rev. C40, 706 (1989).
[172] S.A. Fayans et al. Nucl. Phys. 676, 49 (2000).
[173] M. Baldo, P. Schuck and X. Vinas, Phys. Lett. B663, 390 (2008).
[174] M. Baldo, L. Robledo, P. Schuck and X. Vinas and P. Schuck, J. Phys. G.:Nucl. Part. Phys. 37, 064015 (2010).
[175] P. Hohenberg and W. Kohn, Phys. Rev. 136, 864 (1964).
[176] J.F. Berger, M. Girod and D.Gogny, Comput. Phys. Commun. 63, 365 (1991); Nucl. Phys. A502, 85c (1989).
[177] A. Bohr, B.R. Mottelson and D. Pines, Phys. Rev. 110, 936 (1958).
[178] F. Barranco, R.A. Broglia, H. Esbensen and E. Vigezzi, Phys. Lett. B390, 13 (1997).
[179] F. Barranco, R.A. Broglia, G. Colo', et al., Eur. Phys. J. A21, 57 (2004).
[180] A. Pastore, F. Barranco, R.A. Broglia and E. Vigezzi, Phys. Rev. C78, 024315 (2008).
[181] S.S. Pankratov, M. Baldo, U. Lombardo, E.E. Saperstein and M.V. Zverev, Nucl. Phys. A765, 61 (2006).
[182] S.S. Pankratov, M. Baldo, U. Lombardo, E.E. Saperstein and M.V. Zverev, Nucl. Phys. A811, 127 (2008).
[183] S.S. Pankratov, M. Baldo, M.V. Zverev, U. Lombardo, E.E. Saperstein and S.V. Tolokonnikov, JETP Lett. 90, 560 (2009)
[184] T. Duguet and T. Lesinski T, Eur. Phys. J. (Special Topics) A156, 207 (2008)
[185] K. Hebeler, T. Duguet, T. Lesinski and A. Schwenk, arXiv:0904.3152v1 [nucl-th].
[186] M. Baldo, U. Lombardo, E.E. Saperstein and M.V. Zverev, Nucl. Phys. A628, 503 (1998).
[187] M. Baldo, U. Lombardo, E.E. Saperstein, M.V. and Zverev, Phys. Lett. B459, 437 (1999)
[188] M. Farine M and P. Schuck, Phys. Lett. B459, 444 (1999)
[189] M. Baldo, M. Farine, U. Lombardo, E.E. Saperstein, P. Schuck and M.V. Zverev, Eur. Phys. J. A18, 17 (2003)
[190] M. Baldo, U. Lombardo, S.S. Pankratov and E.E. Saperstein, J. Phys. G:Nucl. Part. Phys. 37, 064016 (2010).
[191] M. Baldo, U. Lombardo, E.E. Saperstein and M.V. Zverev, Phys. Rep. 391, 261 (2004).
[192] E.E. Saperstein, S.S. Pankratov, M.V. Zverev, M. Baldo and U. Lombardo, Phys. At. Nucl. 72, 1167 (2009).
[193] S.S. Pankratov, E.E. Saperstein, M.V. Zverev, M. Baldo and U. Lombardo, Phys. Rev. C79,

024309 (2009)
[194] N. Pillet, N. Sandulescu and P. Schuck, Phys. Rev. C76, 024310 (2007).
[195] P.-G. Reinhard, M. Rufa, J. Maruhn, W. Greiner and J. Friedrich, Z. Phys. **A323** (1986) 13.
[196] G.A. Lalazissis, J. Köning and P. Ring, Phys. Rev. C55, 540 (1997).
[197] R.J. Furstahl, B.D. Serot and H.B. Tang, Nucl. Phys. A598, 539 (1996) ; Nucl. Phys. A615, 441 (1997).
[198] B.G. Todd and J. Pikarewicz, Phys. Rev. C67, 044317 (2003).
[199] J.P. Blaizot, J.F. Berger, J. Dechargé and M. Girod, Nucl. Phys. A591, 435 (1995).
[200] M. Beiner, H. Flocard, Nguyen Van Giai and P. Quentin, Nucl. Phys. A238, 29 (1975).
[201] J. Bartel. P. Quentin, M. Brack, C. Guet and H.B. Hakansson, Nucl. Phys. A386, 183 (1982).
[202] E. Chabanat, P. Bonche, P. Haensel, J. Mayer and R. Schaeffer, Nucl. Phys. A635, 231 (1998).
[203] M. Rayet, M. Arnould, F. Tondeur and G. Paulus, Astron. Astrophys. 116, 183 (1982).
[204] Nguyen Van Giai and H. Sagawa, Phys. Lett. B106, 381 (1981).
[205] D. Vautherin and D.M. Brink, Phys. Rev. C5, 626 (1972).
[206] B. Alex Brown, Phys. Rev. Lett. 85, 5296 (2000).
[207] R. Michaels, P.A. Souder and G.M. Urcioli, Lead Radius Experiment PREX proposal, http://hallaweb.jlab.org/parity/prex/
[208] A.E. Dieperink, Y. Dewulf, D. Van Neck, M. Waroquier and V. Rodin, Phys. Rev. C68, 064307 (2003).
[209] A. Trzcinka, J. Jastrzolski, P. Lubrik, F.J. Hartmann, R. Schmidt, T. von Egidy and B. Klos, Phys. Rev. Lett. 87, 082501 (2001).
[210] P.-G. Reinhard and W. Nazariewicz, arXiv:1002.4140 [nucl-th].
[211] M. Baldo, E.E. Saperstein and S.V. Tolokonnikov, Phys. Rev. C76, 025803 (2007).
[212] J. Negele and D. Vautherin, Nucl. Phys. A207, 298 (1973).
[213] M. Baldo, E.E. Saperstein and S.V. Tolokonnikov, Eur. Phys. J. A32, 97 (2007).
[214] S.B. Rüster, M. Hempel and J. Schaffner-Bielich, Phys. Rev. C73, 035804 (2006).
[215] G.L. Israel, T. Belloni, L. Stella, Y. Rephaeli, D.E. Gruber, P. Casella, S. Dall' Osso, N. Rea, M. Persic and R.E. Rothschild, Astrophys. J. 628, L53 (2005).
[216] D. Altamirano, M. Linares, A. Patruno, N. Degenaar, R. Wijnands, M. Klein-Wolt, M. van der Klis, C. Markwardt and J. Swank, arXiv:0908.4039 [astro-ph.HE].
[217] D. Altamirano, A. Watts, M. Linares, C.B. Markwardt, T. Strohmayer and A. Patruno, arXiv:1005.5299 [astro-ph.HE].
[218] A.L. Watts and T.E. Strohmayer, Astrophys. J. 637, L117 (2006).
[219] A.W. Steiner and A.L. Watts, Phys. Rev. Lett. 103, 181101 (2009).
[220] B. Friedman and V.R. Pandharipande, Nucl. Phys. A361, 502 (1981).
[221] M. Baldo and L.S. Ferreira, Phys. Rev. C59, 682 (1999).
[222] C. Bloch and C. De Dominicis, Nucl. Phys. 7, 459 (1958) ; Nucl. Phys. 10, 181 (1959) ; Nucl. Phys. 10, 509 (1959).
[223] B. ter Haar and R. Malfliet, Phys. Rev. Lett. 56, 1237 (1986) ; Phys. Rep. 149, 207 (1987).
[224] H. Huber, F. Weber and M.K. Weigel, Phys. Rev. C57, 3484 (1999).
[225] G. Baym, Phys. Rev. 127, 1391 (1962).
[226] A. Rios, A. Polls, A. Ramos and H. Müther, Phys. Rev. C74, 054317 (2006).
[227] A. Rios, A. Polls, A. Ramos and H. Müther, Phys. Rev. C78, 044314 (2008).
[228] M. Colonna, V. Baran, M. Di Toro and H.H. Wolter, Phys. Rev. C78, 064618 (2008).
[229] C. Ducoin, P. Chomaz and F. Gulminelli, Nucl. Phys. A781, 407 (2007).
[230] C. Ducoin, P. Chomaz and F. Gulminelli, Nucl. Phys. A771, 68 (2006).
[231] S. Levit and P. Bonche, Nucl. Phys. A437, 426 (1985).
[232] H. Q. Song and R. K. Su, Phys. Rev. C44, 2505 (1991).
[233] J.B. Natowitz, R. Wada. K. Hagel, T.Keutgen, M. Murray, A. Makeev, L. Qin, P. Smith and C. Hamilton, Phys. Rev. C65, 034618 (2002).
[234] J. Pochdzalla *et al.*, Phys. Rev. Lett. 75, 1040 (1995).

[235] R. Wada et al. , Phys. Rev. C55, 227 (1997).
[236] J. Cibor et al. , Phys. Lett. B473, 29 (2000).
[237] D. Cussol et al. , Nucl. Phys. A561, 298 (1993).
[238] J. Bondorf, R. Donangelo, I.N. Mishustin and H. Schulz, Nucl. Phys. A444, 460 (1985).
[239] J. Bondorf, R. Donangelo, I.N. Mishustin, C. Pethick, H. Schulz, and K. Sneppen, Phys. Lett. B150, 57 (1985) ; Nucl. Phys. A443, 321 (1985).
[240] J. Bondorf, R. Donangelo, H. Schulz and K. Sneppen, Phys. Lett. B162, 30 (1985)
[241] A.S. Botvina et al. , Nucl. Phys. A475, 663 (1987).
[242] D. Gross et al. Prog. Part. Nucl. Phys. 30, 155 (1993), and references therein.
[243] W. A. Friedman, Phys. Rev. Lett. 60, 2125 (1988).
[244] L.P Csernai and J. I. Kapusta, Phys. Rep. 131, 223 (1986), and references therein.
[245] J.P. Bondorf et al. , Phys. Rep. 257, 133 (1995).
[246] J.B. Natowitz, K. Hagel, Y. Ma, M. Murray, L. Qin, R. Wada and J. Wang, Phys. Rev. Lett. 89, 212701 (2002).
[247] M. Baldo, L.S. Ferreira and O. Nicotra, Phys. Rev. C69, 034321 (2004).
[248] S. Fritsch, N. Kaiser and W. Weise, Phys. Lett. B545, 73 (2002).
[249] C. Ducoin, K.H.O. Hasnoaui, P. Chomaz and F. Gulminelli, Phys. Rev. C75, 065805 (2007).
[250] J. Lattimer and F.D. Swesty, Nucl. Phys. A535, 331 (1991).
[251] H. Shen, Phys. Rev. C65, 035802 (2002).
[252] C.J. Horowitz and A. Schwenk, Phys. Lett. B638, 153 (2006).

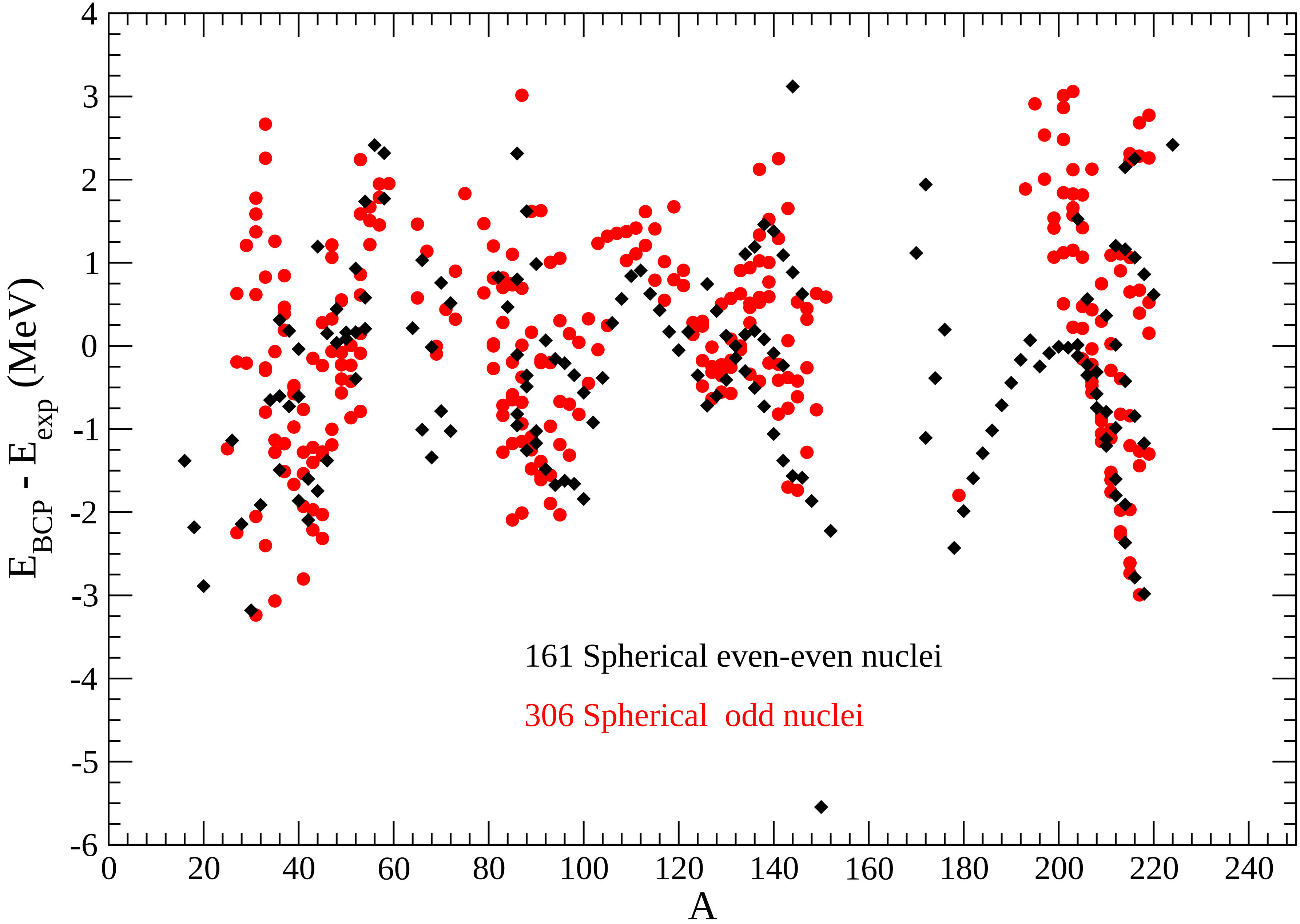

161 Spherical even-even nuclei
306 Spherical odd nuclei
$E_{BCP} - E_{exp}$ (MeV)
A
4
3
2
1
0
-1
-2
-3
-4
-5
-6
0
20
40
60
80
100
120
140
160
180
200
220
240

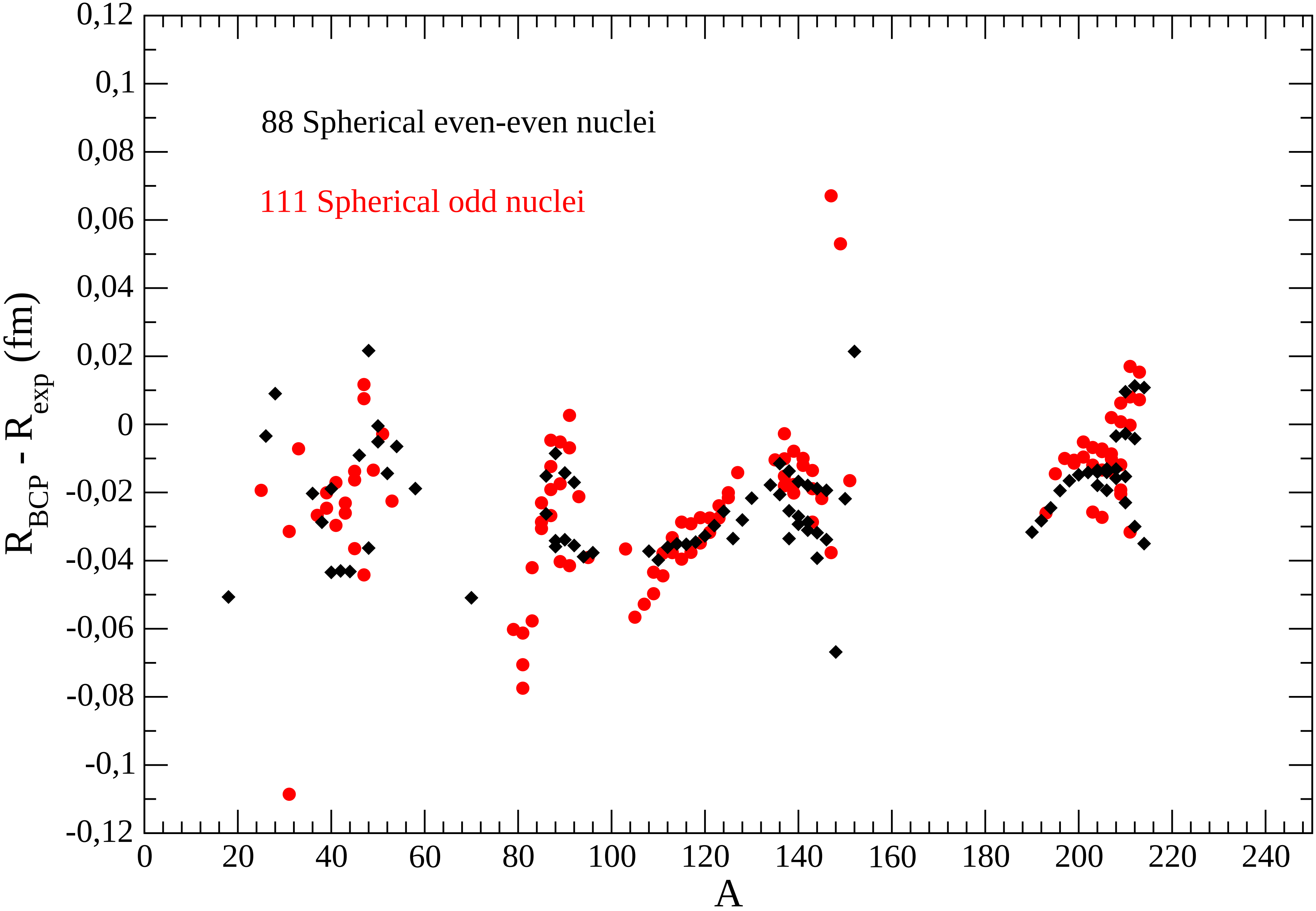

88 Spherical even-even nuclei
111 Spherical odd nuclei
$R_{BCP} - R_{exp}$ (fm)
A
0,12
0,1
0,08
0,06
0,04
0,02
0
-0,02
-0,04
-0,06
-0,08
-0,1
-0,12
0
20
40
60
80
100
120
140
160
180
200
220
240

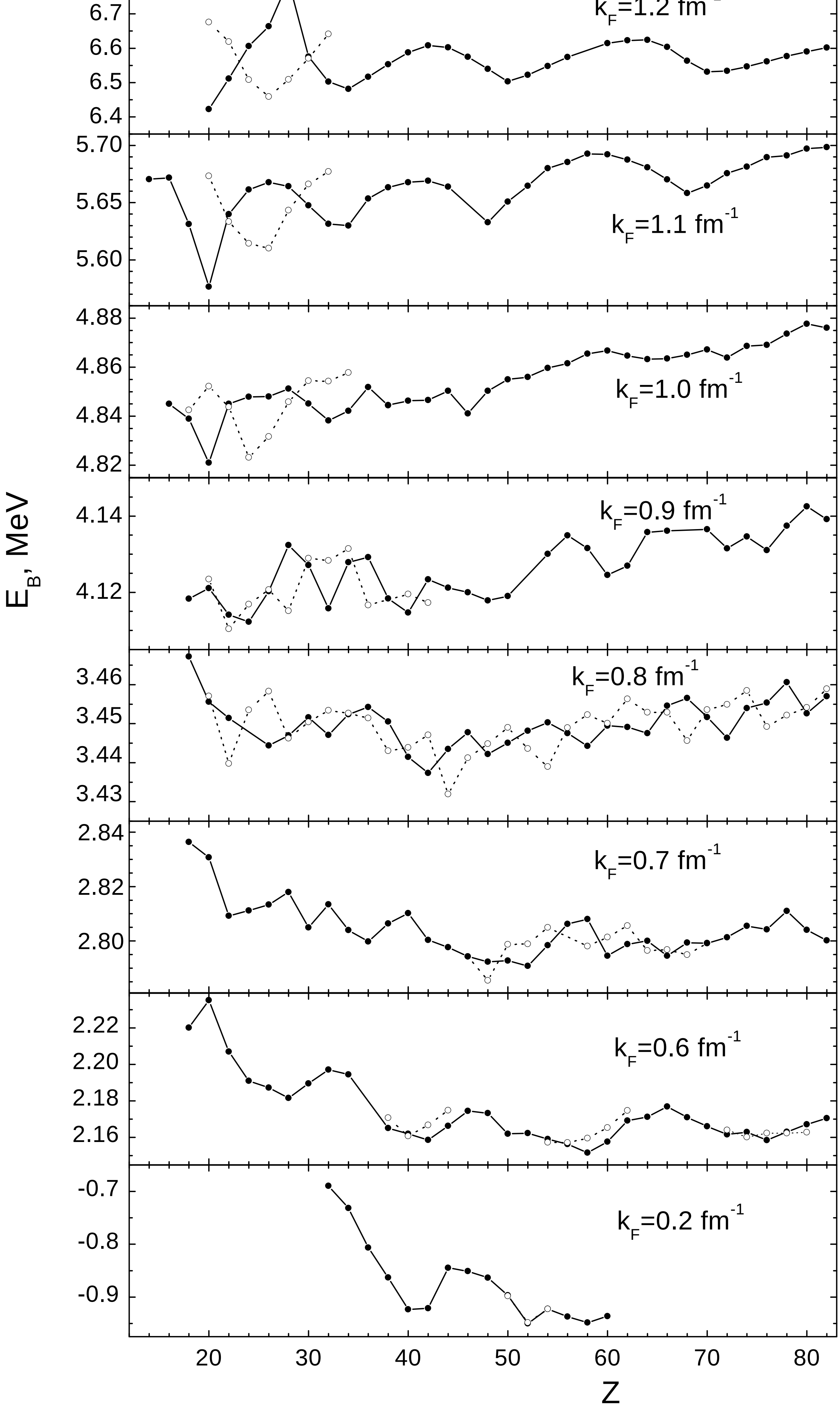

k_F=1.2 fm^{-1}
k_F=1.1 fm^{-1}
k_F=1.0 fm^{-1}
k_F=0.9 fm^{-1}
k_F=0.8 fm^{-1}
k_F=0.7 fm^{-1}
k_F=0.6 fm^{-1}
k_F=0.2 fm^{-1}
E_B, MeV
Z

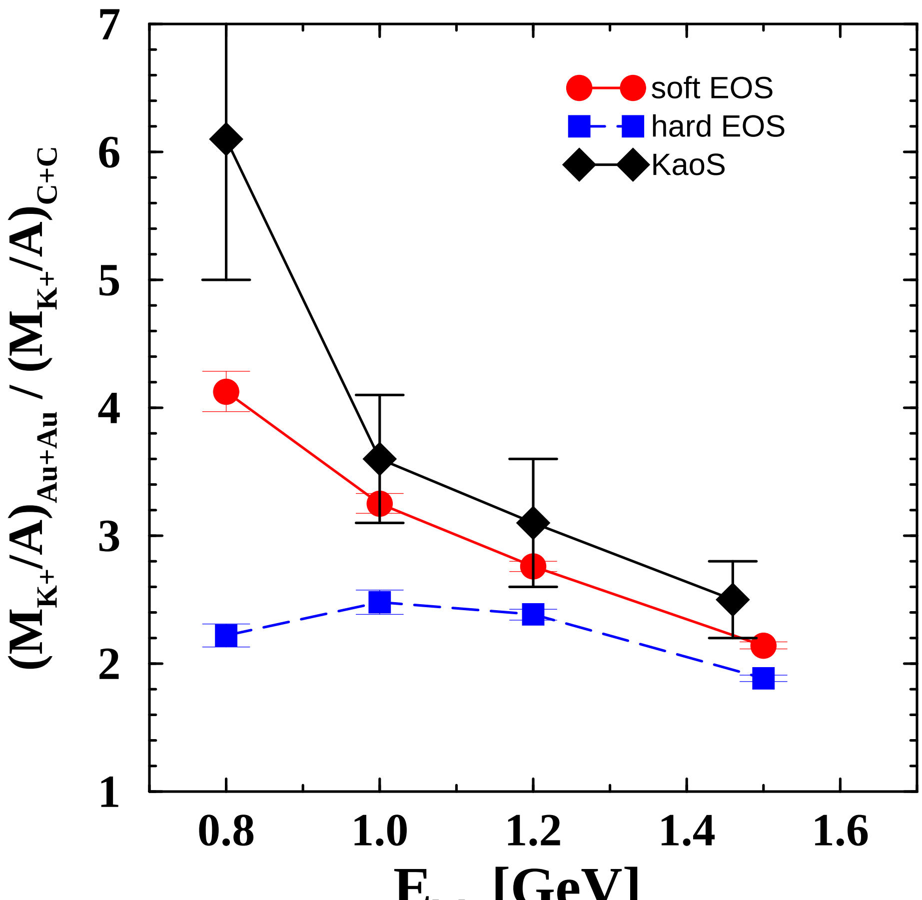

soft EOS
hard EOS
KaoS
$(M_{K^+}/A)_{Au+Au} / (M_{K^+}/A)_{C+C}$
E_{lab} [GeV]
0.8
1.0
1.2
1.4
1.6
1
2
3
4
5
6
7

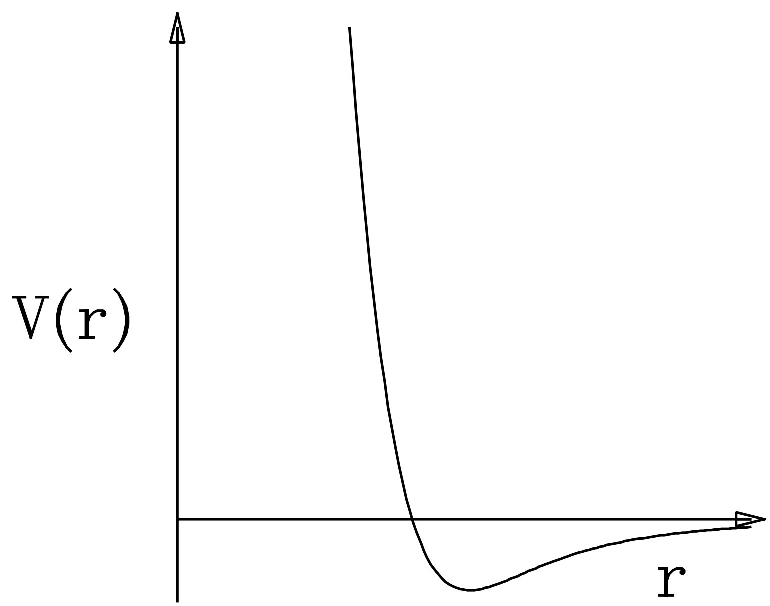
V(r)
r

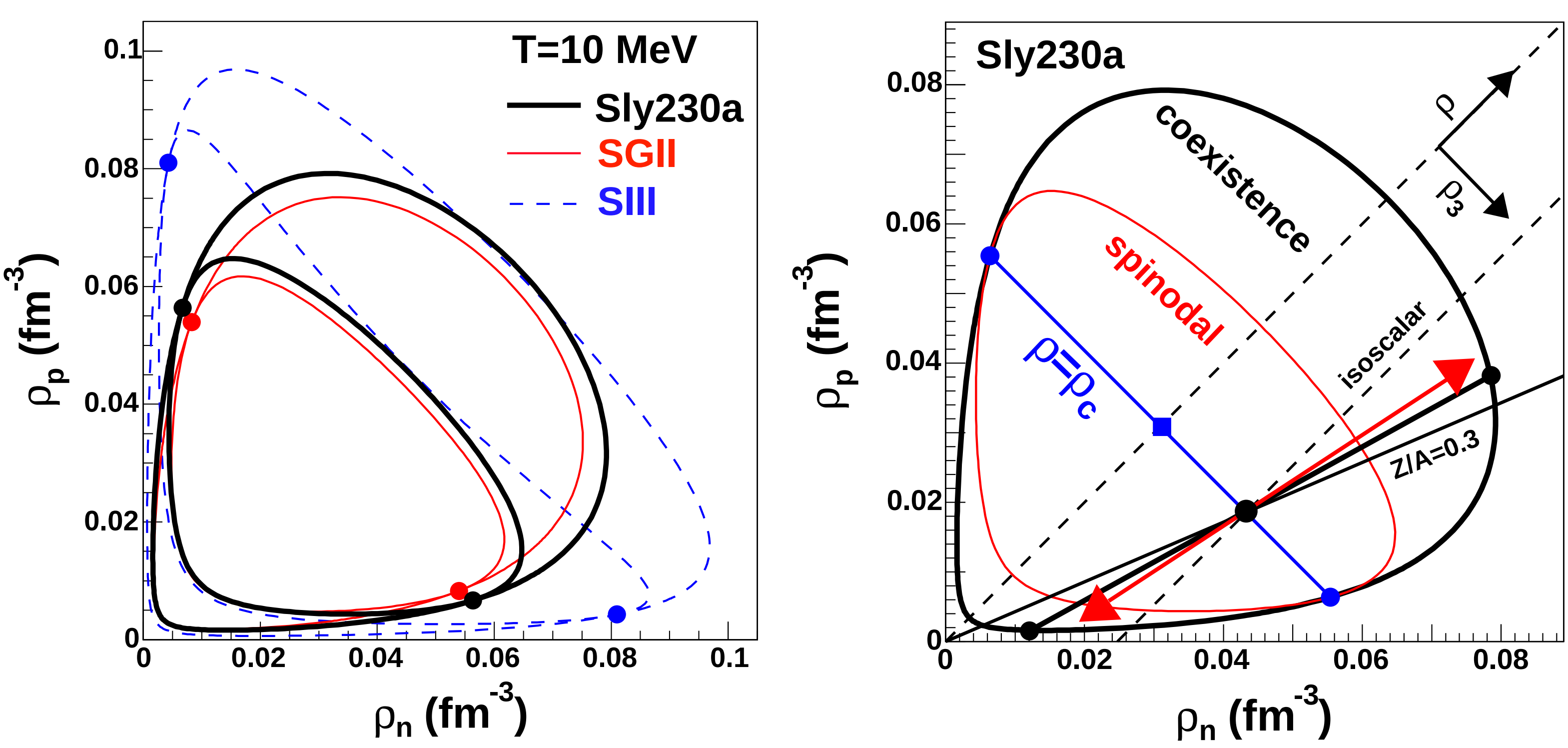

T=10 MeV
Sly230a
SGII
SIII
ρ_p (fm^{-3})
ρ_n (fm^{-3})
Sly230a
coexistence
spinodal
$\rho=\rho_c$
isoscalar
Z/A=0.3
ρ
ρ_3

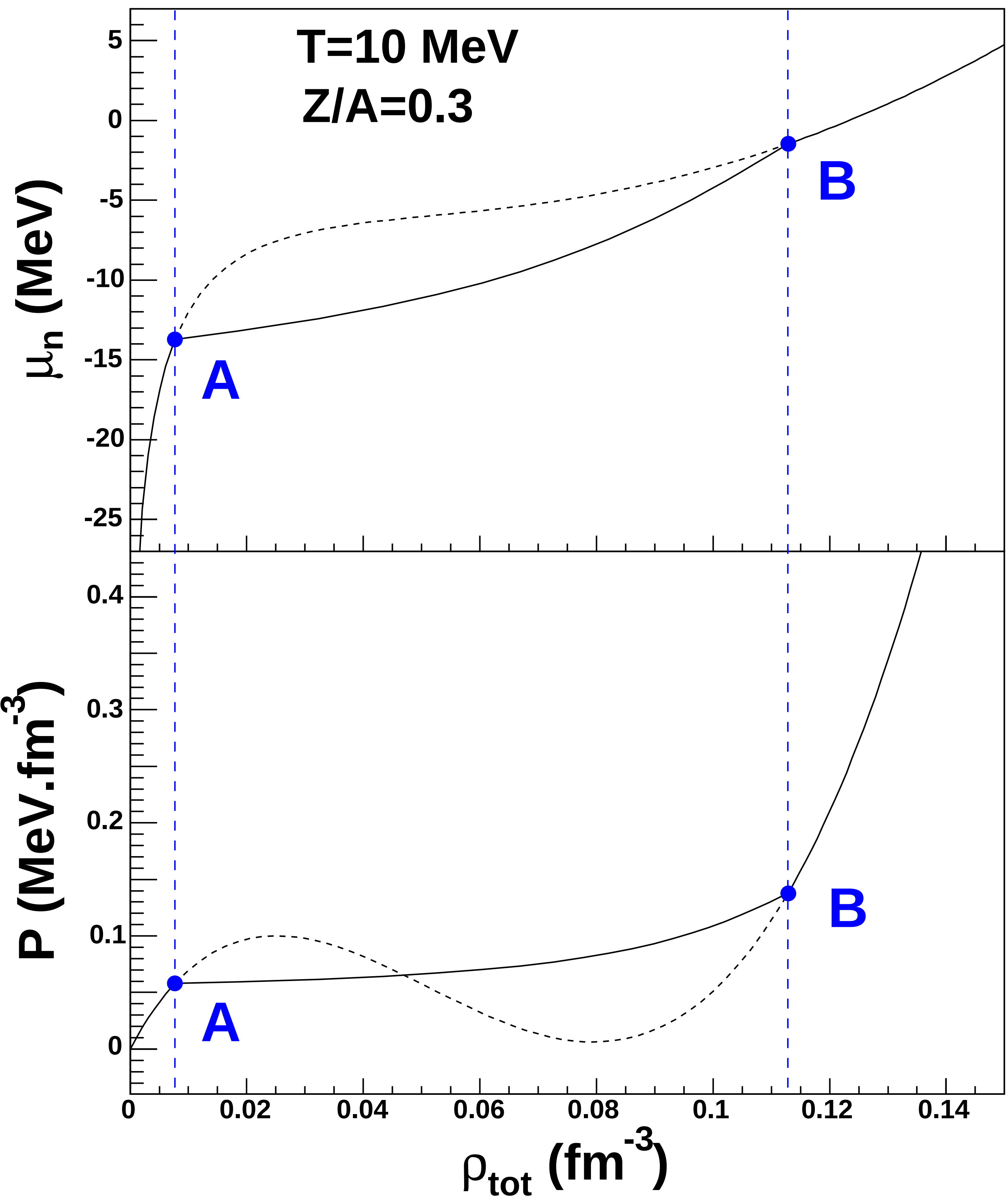

T=10 MeV
Z/A=0.3
A
B
A
B
μ_n (MeV)
P (MeV.fm^{-3})
ρ_{tot} (fm^{-3})
5
0
-5
-10
-15
-20
-25
0.4
0.3
0.2
0.1
0
0
0.02
0.04
0.06
0.08
0.1
0.12
0.14

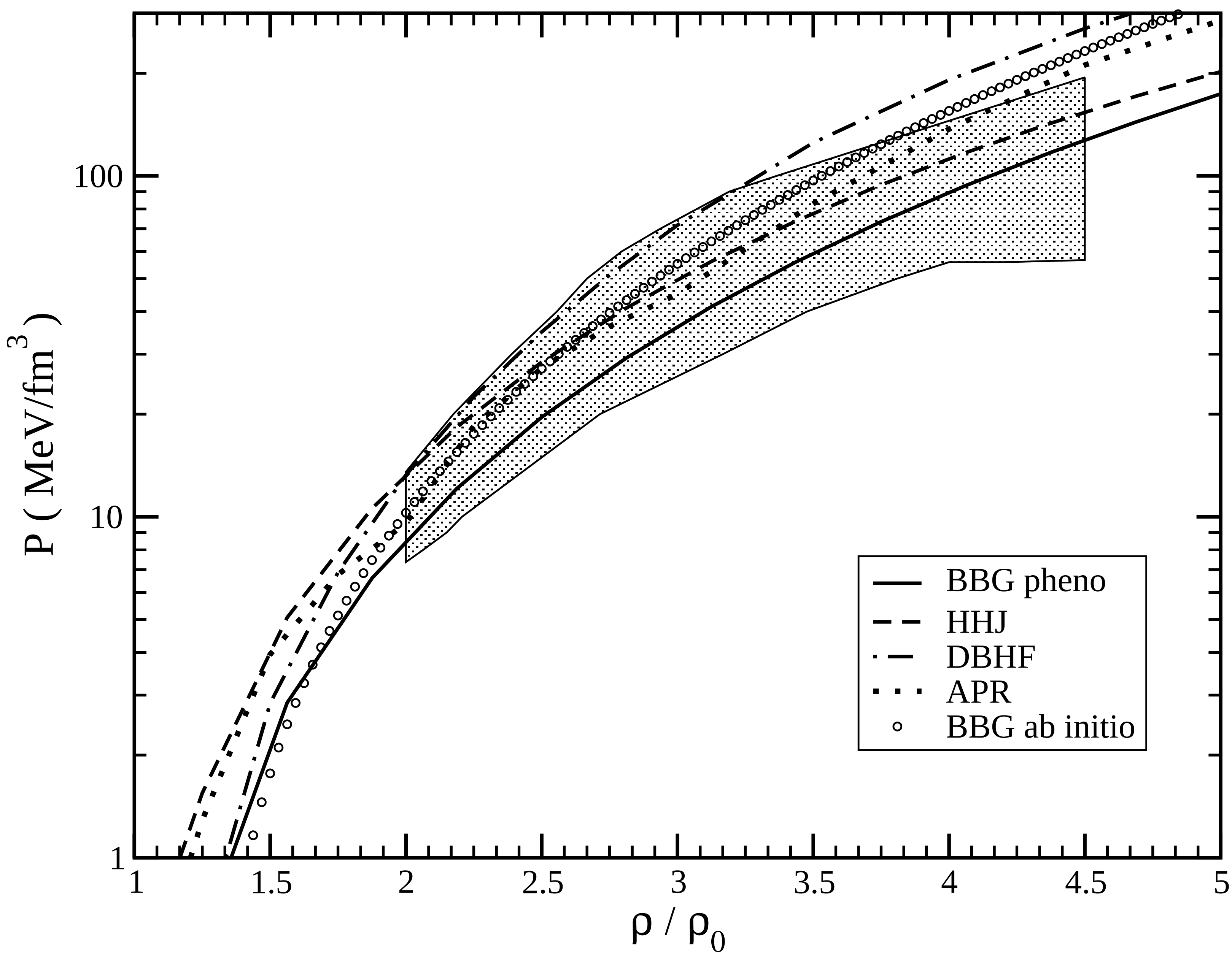

P (MeV/fm^3)
100
10
1
1
1.5
2
2.5
3
3.5
4
4.5
5
ρ / ρ$_0$
BBG pheno
HHJ
DBHF
APR
BBG ab initio

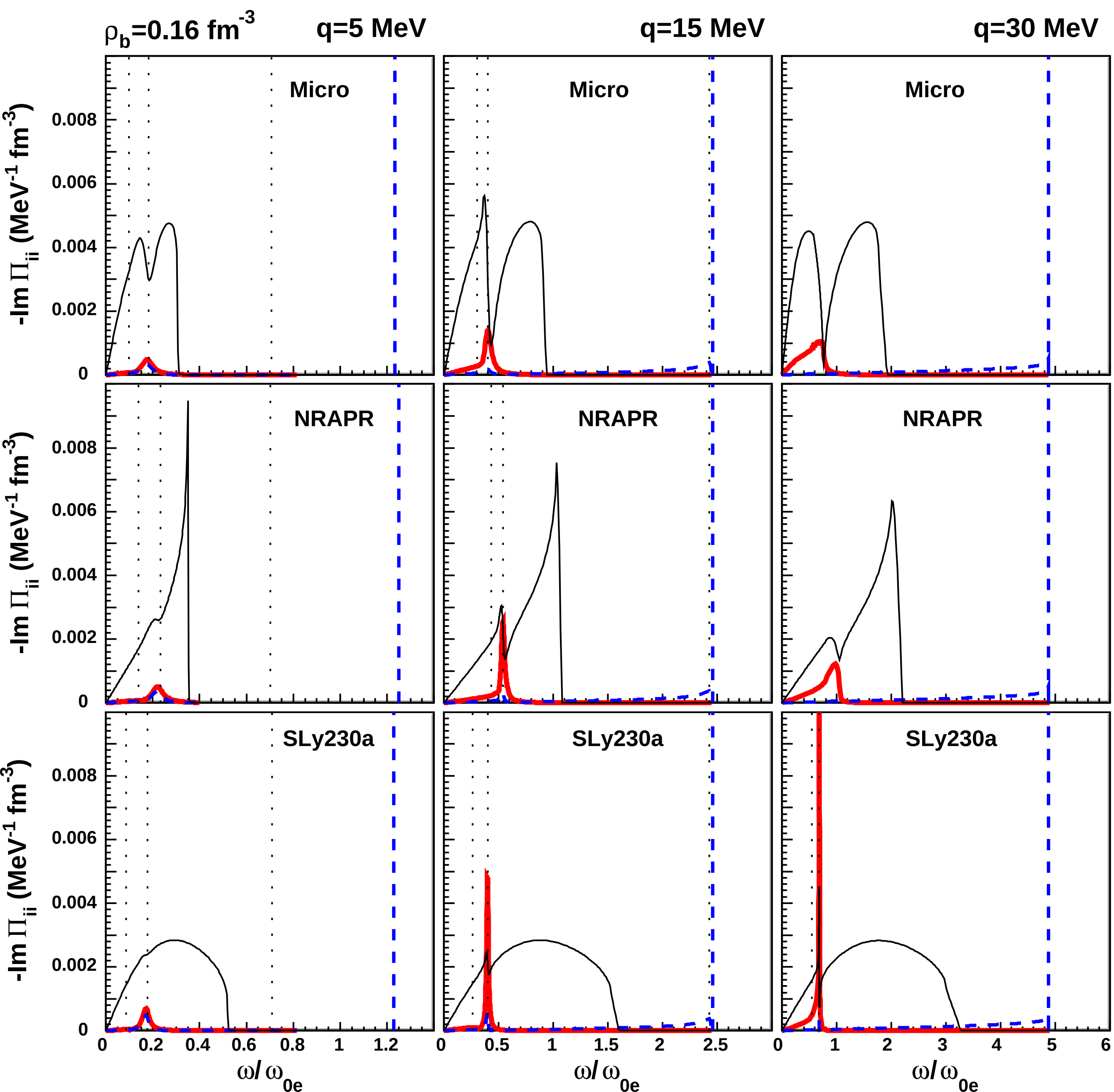

ρ_b=0.16 fm^{-3}
q=5 MeV
q=15 MeV
q=30 MeV
Micro
NRAPR
SLy230a
-Im Π_{ii} (MeV^{-1} fm^{-3})
ω/ω_{0e}

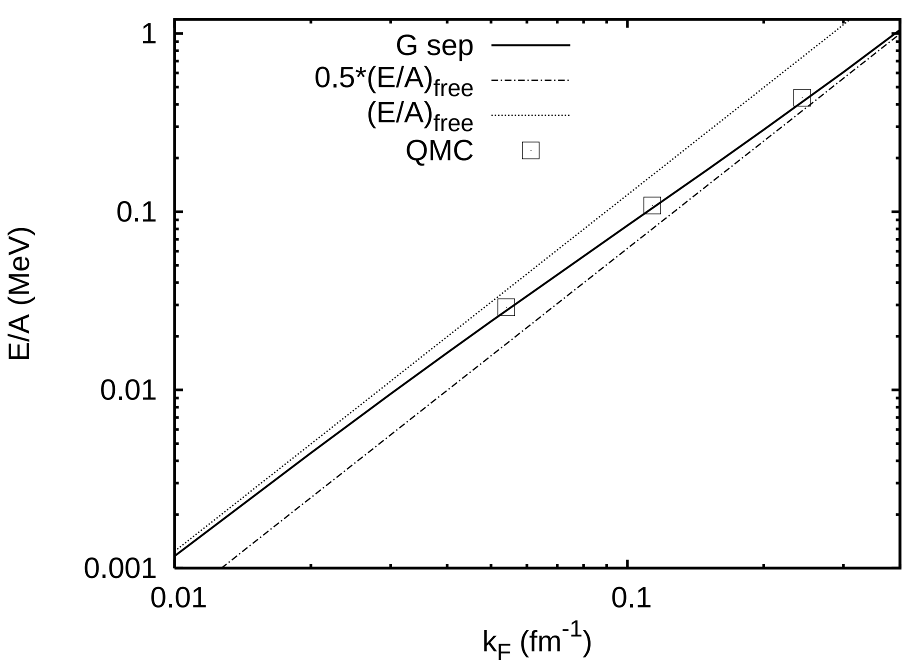
G sep
0.5*(E/A)free
(E/A)free
QMC
1
0.1
0.01
0.001
0.01
0.1
E/A (MeV)
kF (fm-1)

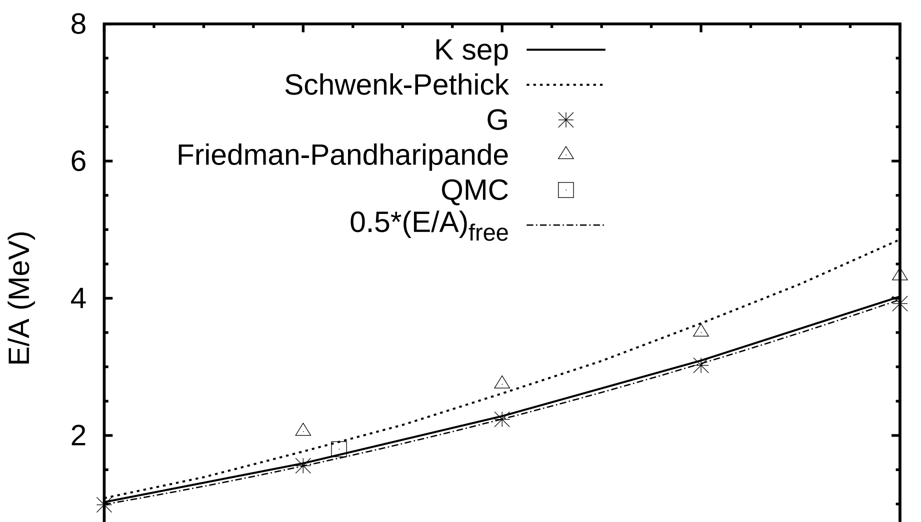

K sep
Schwenk-Pethick
G
Friedman-Pandharipande
QMC
0.5*(E/A)free
E/A (MeV)
k_F (fm^-1)
0
2
4
6
8
0.4
0.5
0.6
0.7
0.8

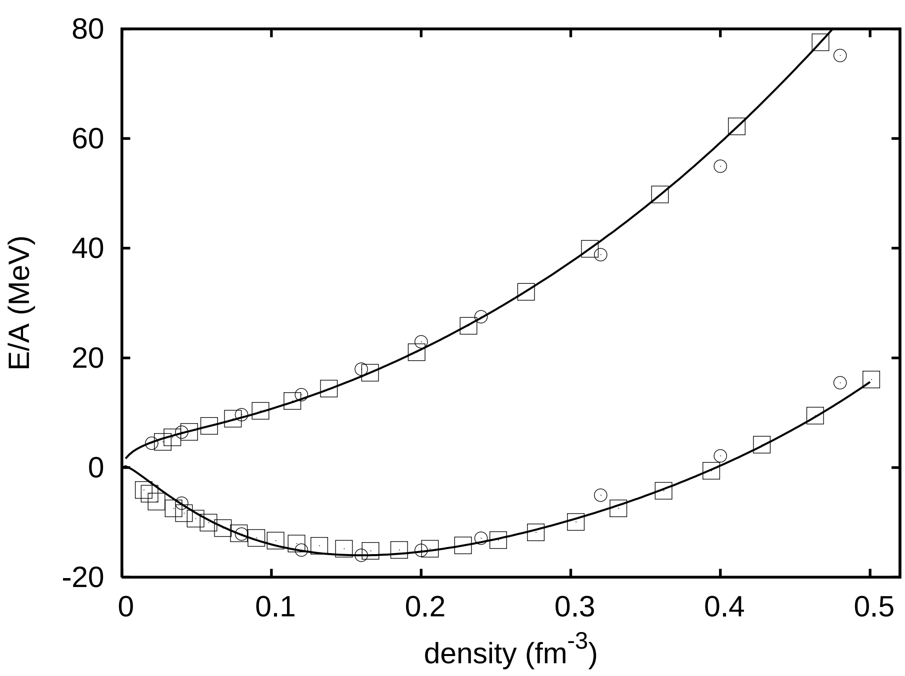
80
60
40
20
0
-20
0
0.1
0.2
0.3
0.4
0.5
E/A (MeV)
density (fm^{-3})

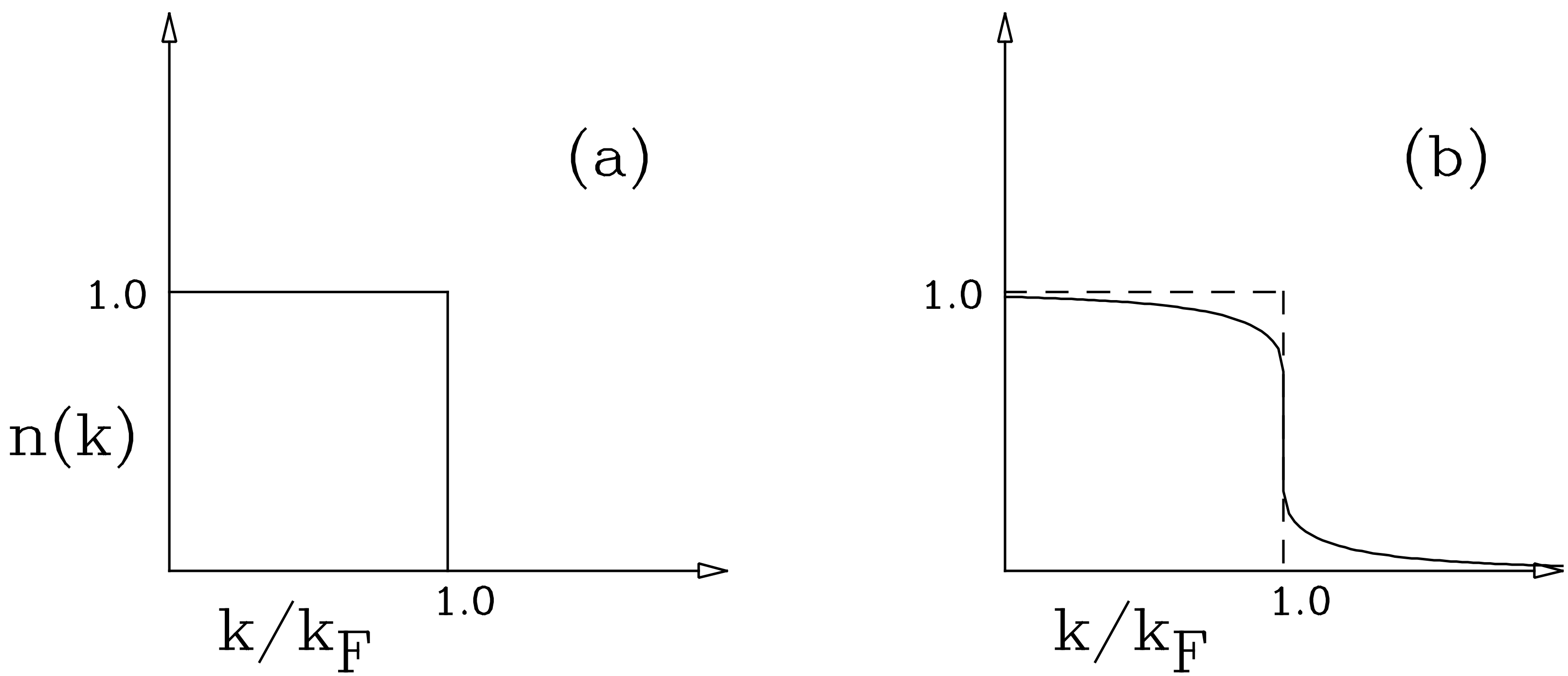

n(k)
1.0
1.0
k/k_F
(a)
1.0
1.0
k/k_F
(b)

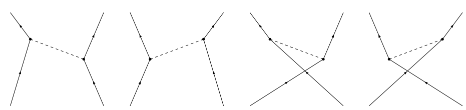

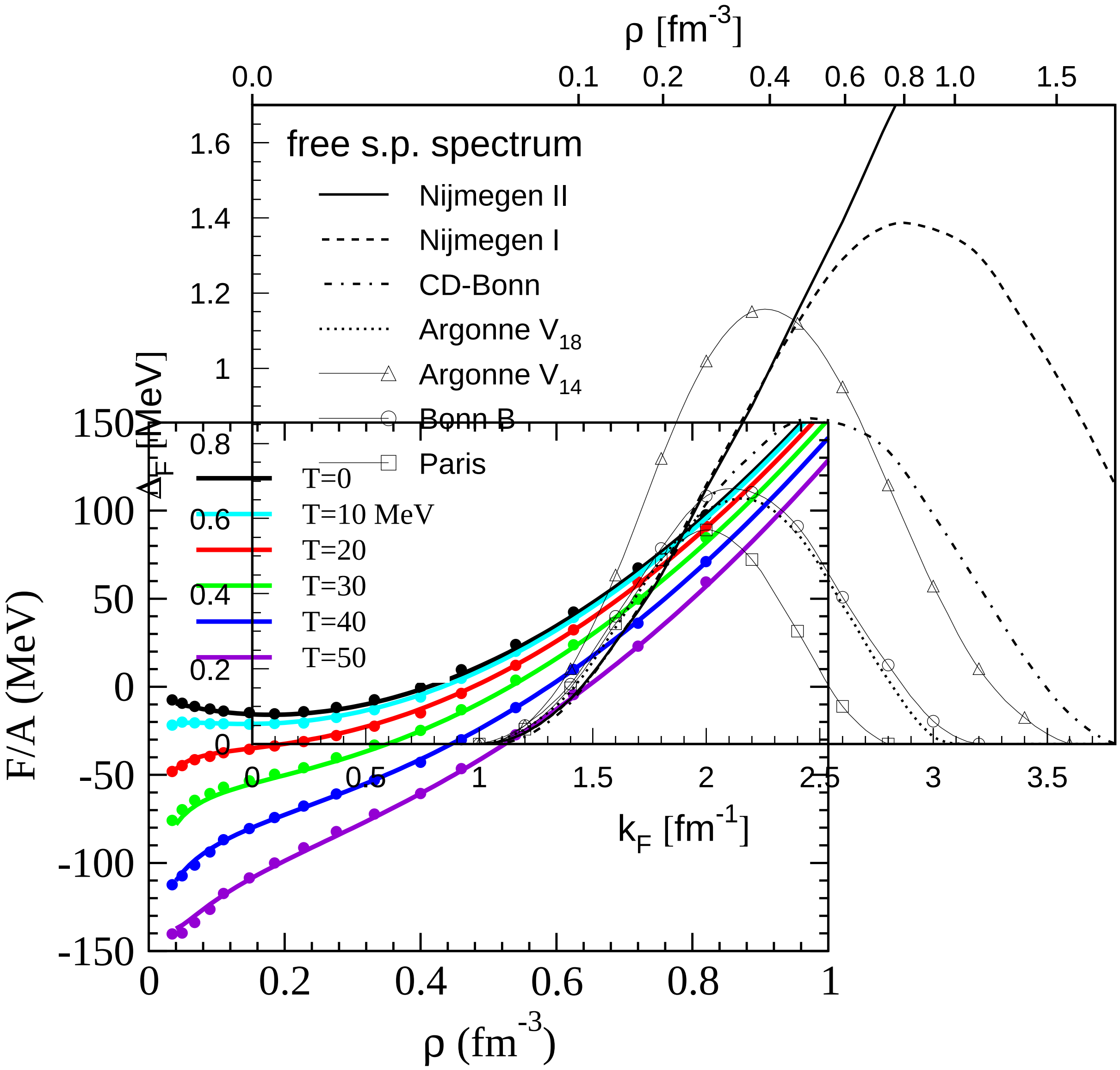

ρ [fm^-3]
0.0
0.1
0.2
0.4
0.6
0.8
1.0
1.5
free s.p. spectrum
Nijmegen II
Nijmegen I
CD-Bonn
Argonne V18
Argonne V14
Bonn B
Paris
Δ_F [MeV]
k_F [fm^-1]
T=0
T=10 MeV
T=20
T=30
T=40
T=50
F/A (MeV)
ρ (fm^-3)

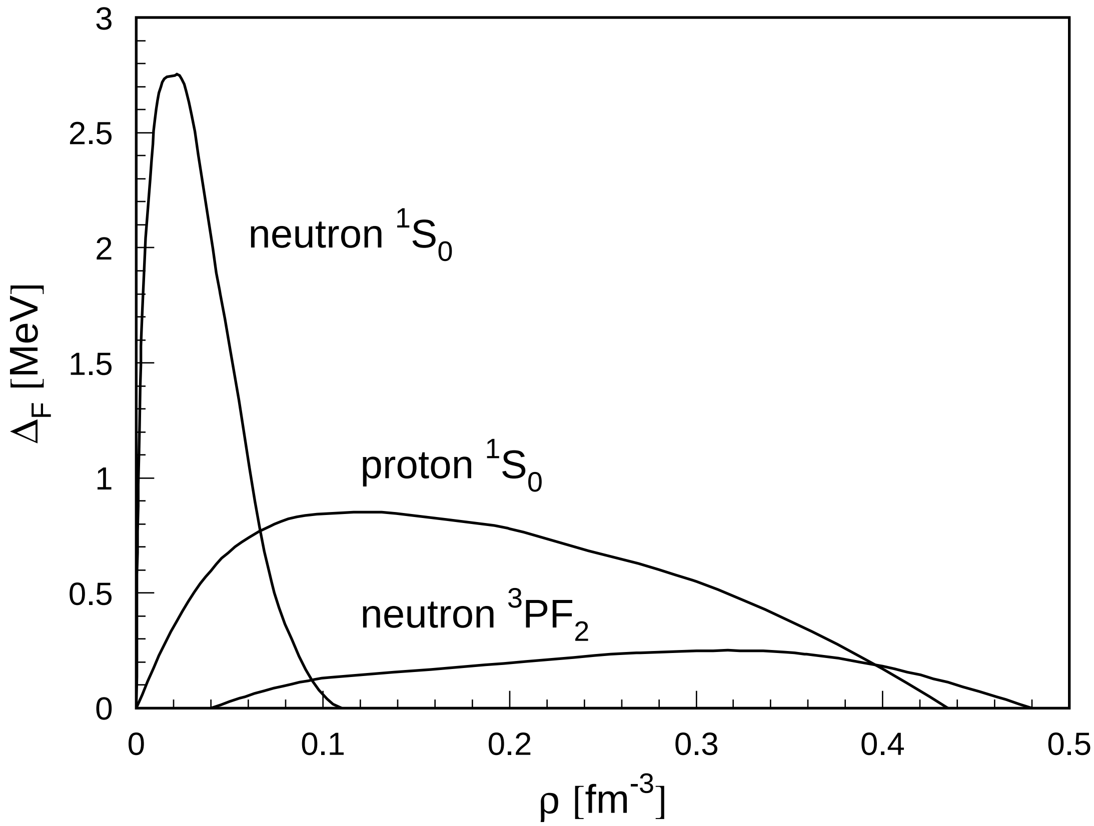

neutron $^1S_0$
proton $^1S_0$
neutron $^3PF_2$
Δ_F [MeV]
ρ [fm^{-3}]
0
0.5
1
1.5
2
2.5
3
0
0.1
0.2
0.3
0.4
0.5

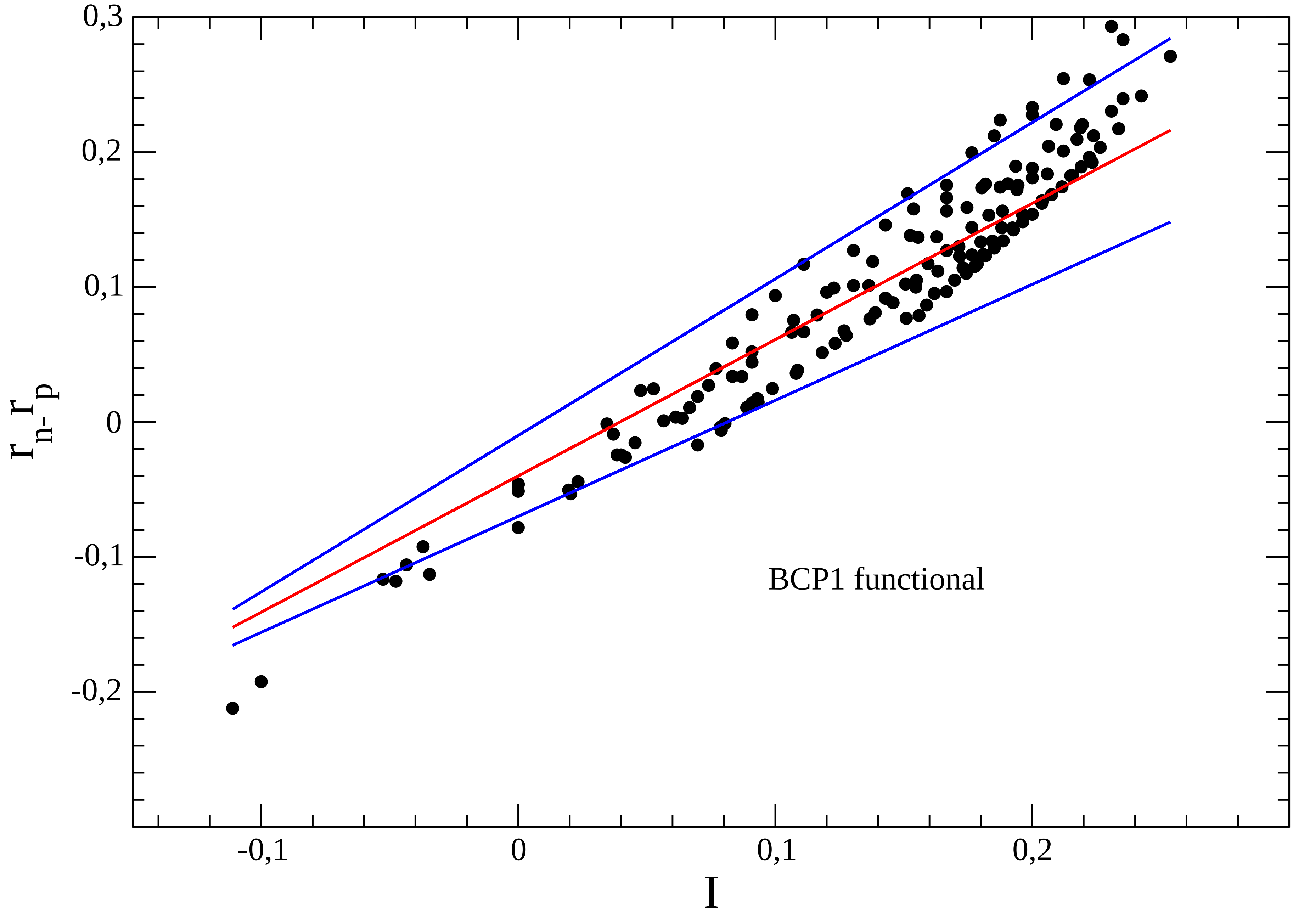

0,3
0,2
0,1
0
-0,1
-0,2
$r_n - r_p$
-0,1
0
0,1
0,2
I
BCP1 functional

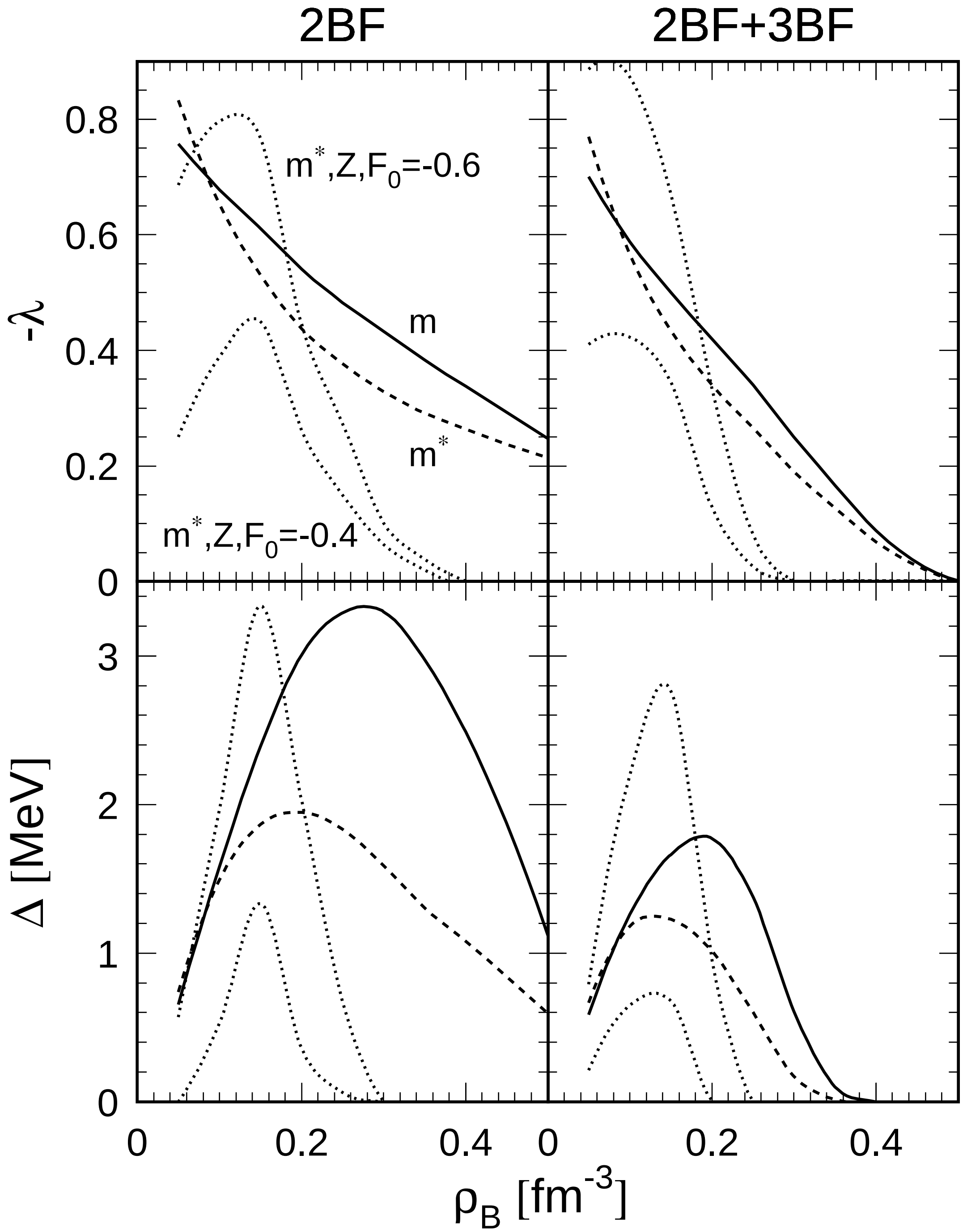

2BF
2BF+3BF
0.8
0.6
0.4
0.2
0
-λ
m*,Z,F0=-0.6
m
m*
m*,Z,F0=-0.4
3
2
1
0
Δ [MeV]
0
0.2
0.4
0
0.2
0.4
ρB [fm-3]

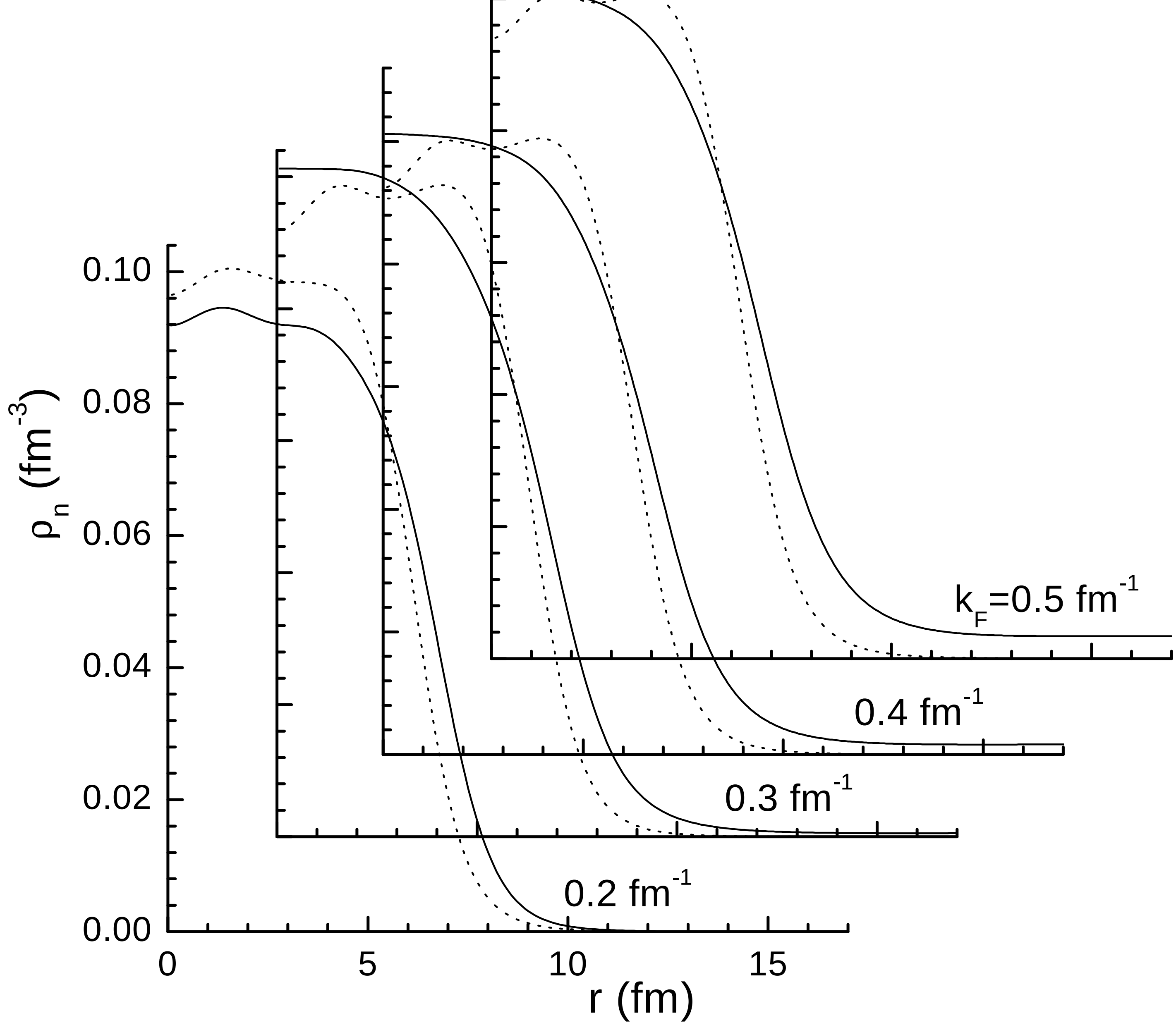

k_F=0.5 fm^{-1}
0.4 fm^{-1}
0.3 fm^{-1}
0.2 fm^{-1}
0.00
0.02
0.04
0.06
0.08
0.10
ρ_n (fm^{-3})
0
5
10
15
r (fm)

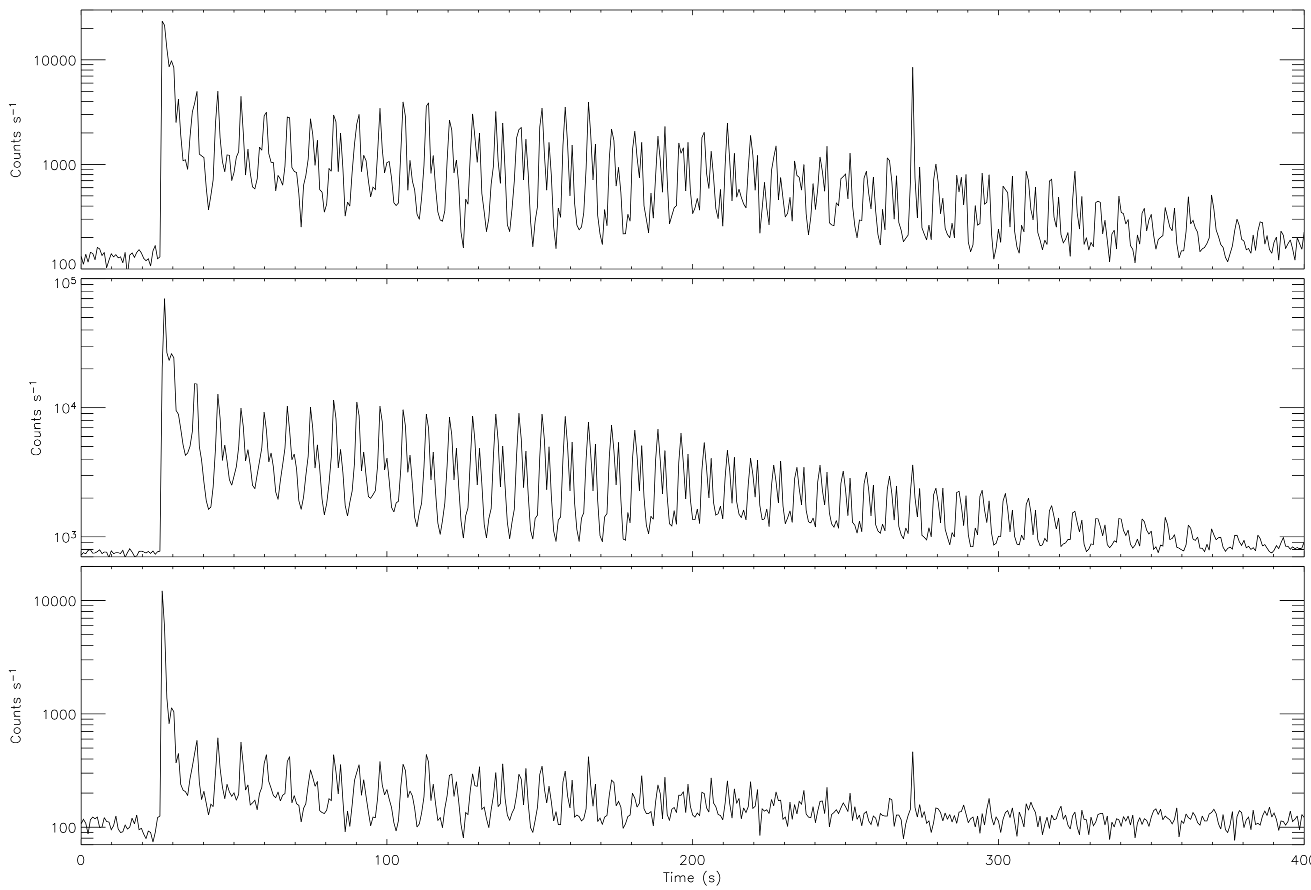
Counts s^{-1}
10000
1000
100
10^5
10^4
10^3
0
100
200
300
400
Time (s)

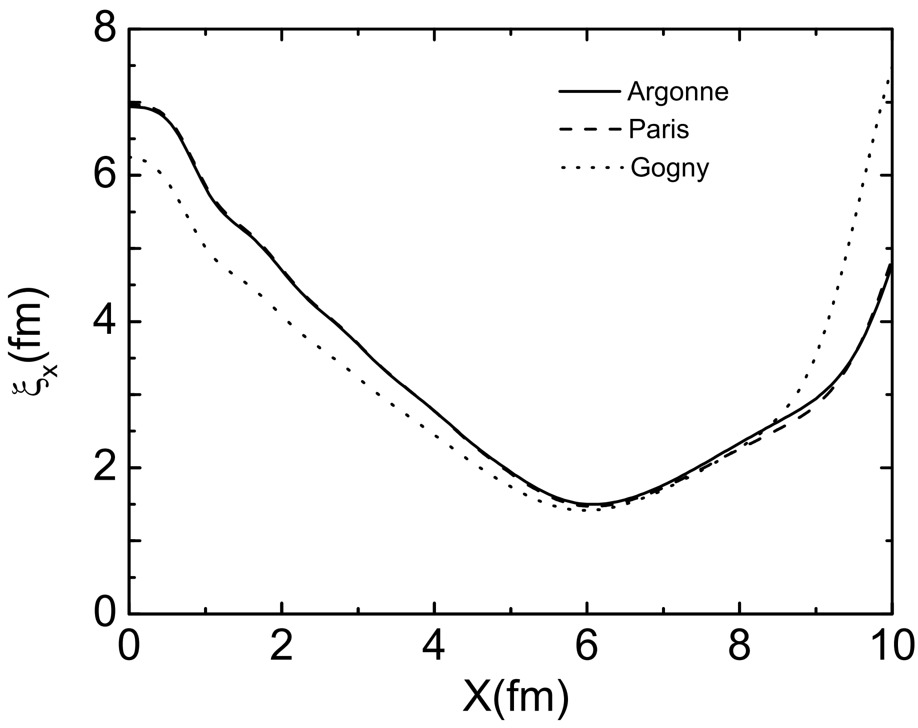
Argonne
Paris
Gogny
ξ_x(fm)
X(fm)
0
2
4
6
8
10

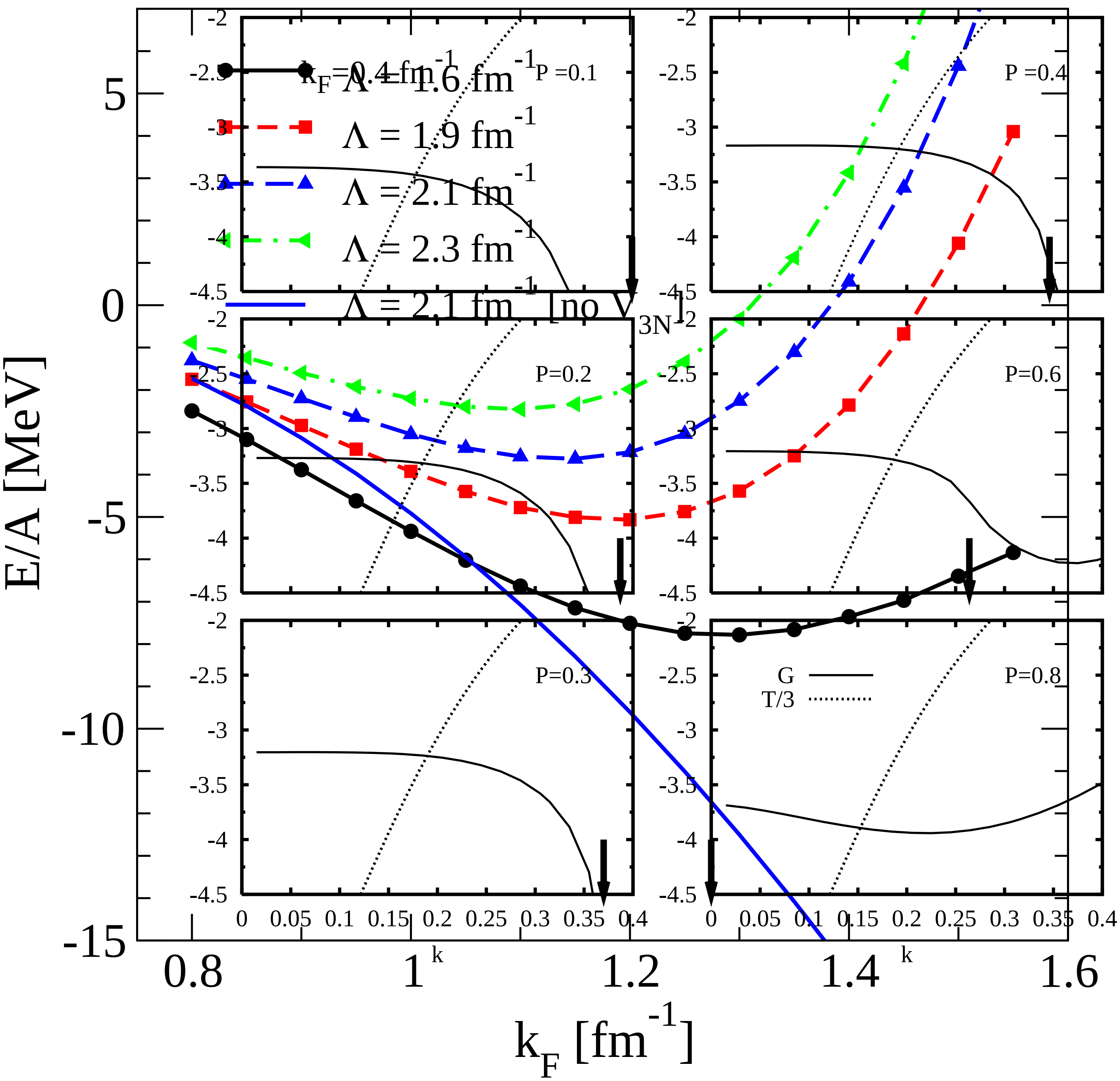

E/A [MeV]
k_F [fm^{-1}]
Λ = 1.6 fm^{-1}
Λ = 1.9 fm^{-1}
Λ = 2.1 fm^{-1}
Λ = 2.3 fm^{-1}
Λ = 2.1 fm^{-1} [no V_{3N}]
k_F=0.4 fm^{-1}
P =0.1
P=0.2
P=0.3
P =0.4
P=0.6
P=0.8
G
T/3
k

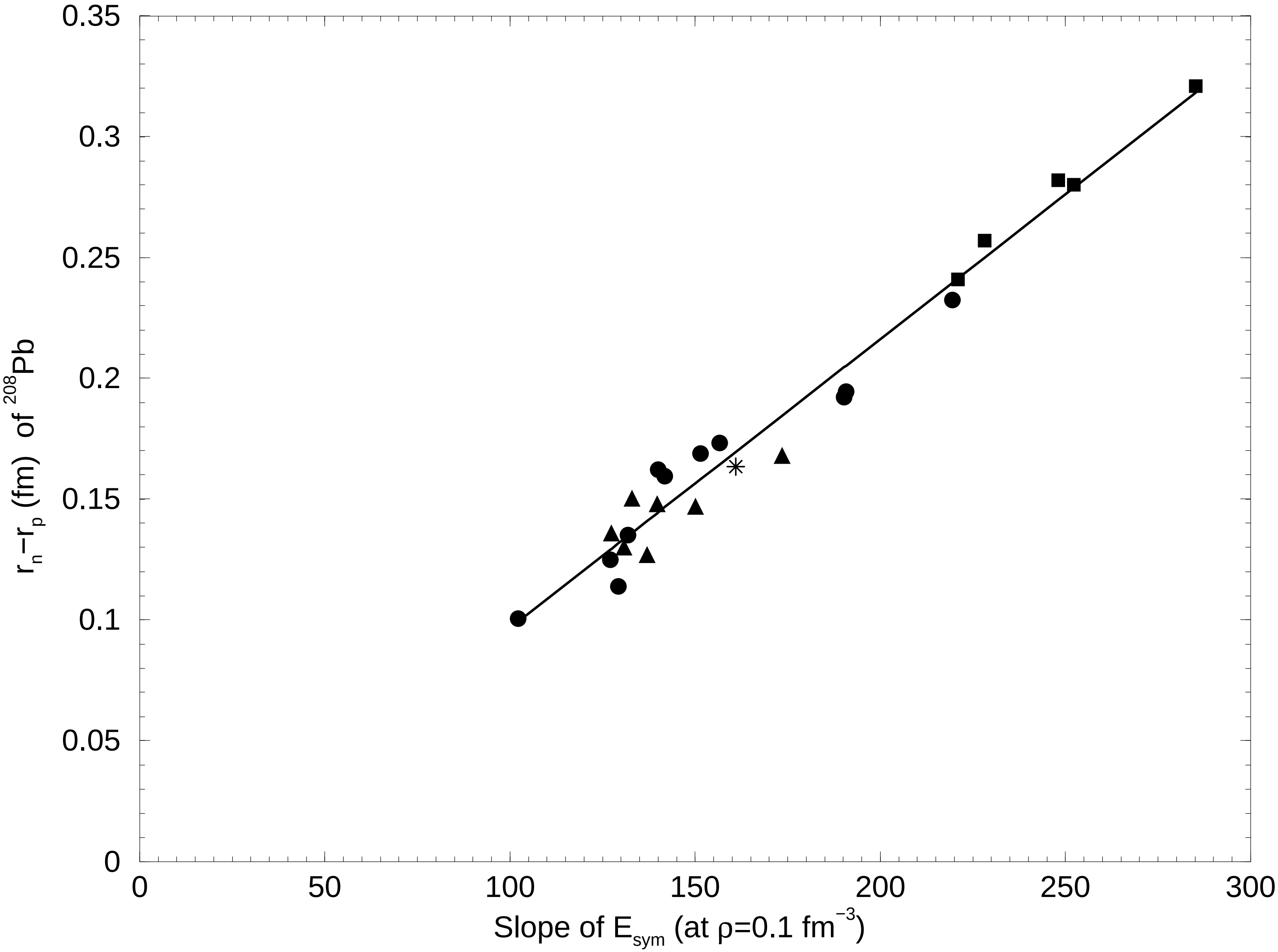

0.35
0.3
0.25
0.2
0.15
0.1
0.05
0
0
50
100
150
200
250
300
$r_n - r_p$ (fm) of ^{208}Pb
Slope of E_{sym} (at ρ=0.1 fm^{-3})

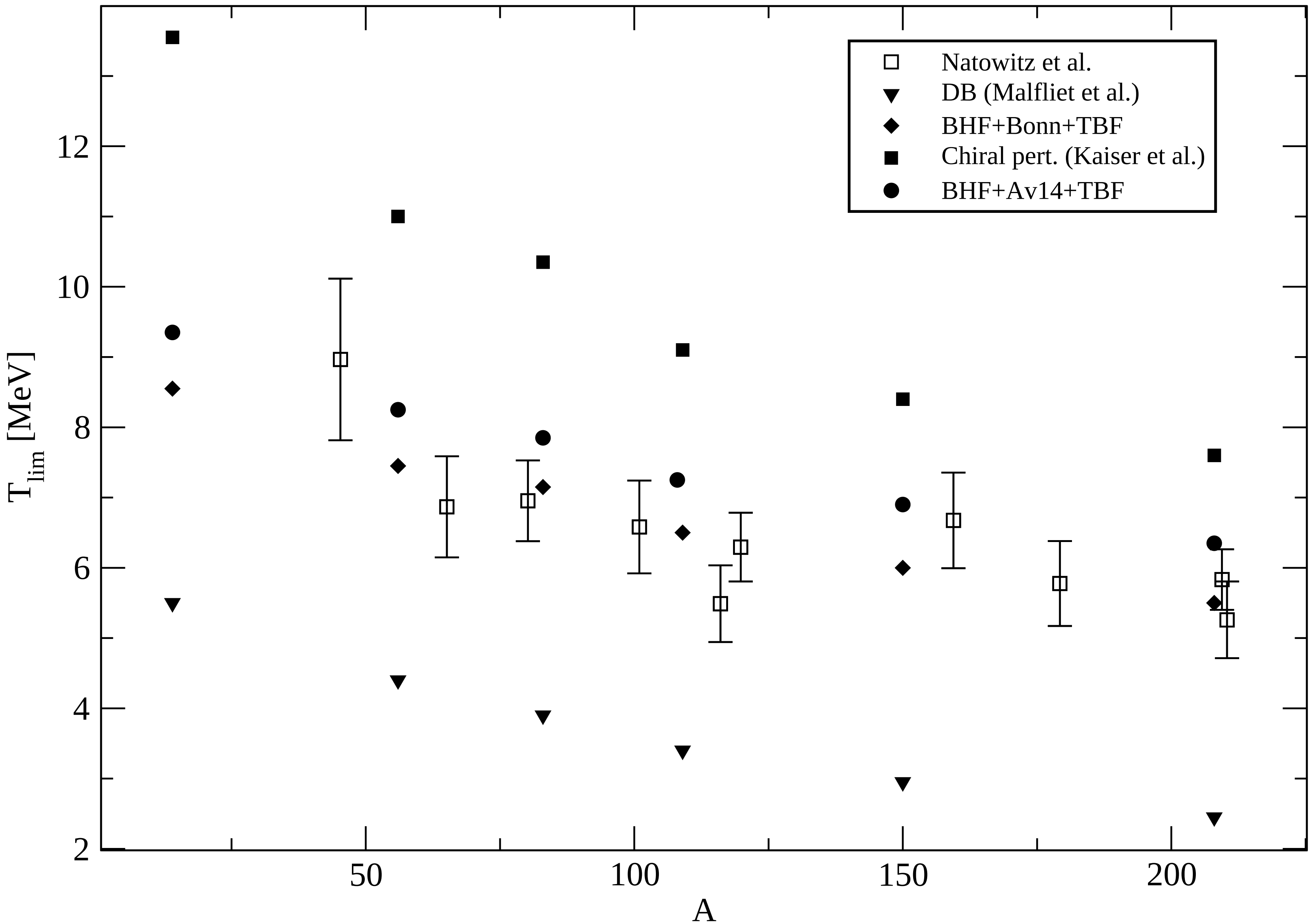

Natowitz et al.
DB (Malfliet et al.)
BHF+Bonn+TBF
Chiral pert. (Kaiser et al.)
BHF+Av14+TBF
T_{lim} [MeV]
A
2
4
6
8
10
12
50
100
150
200

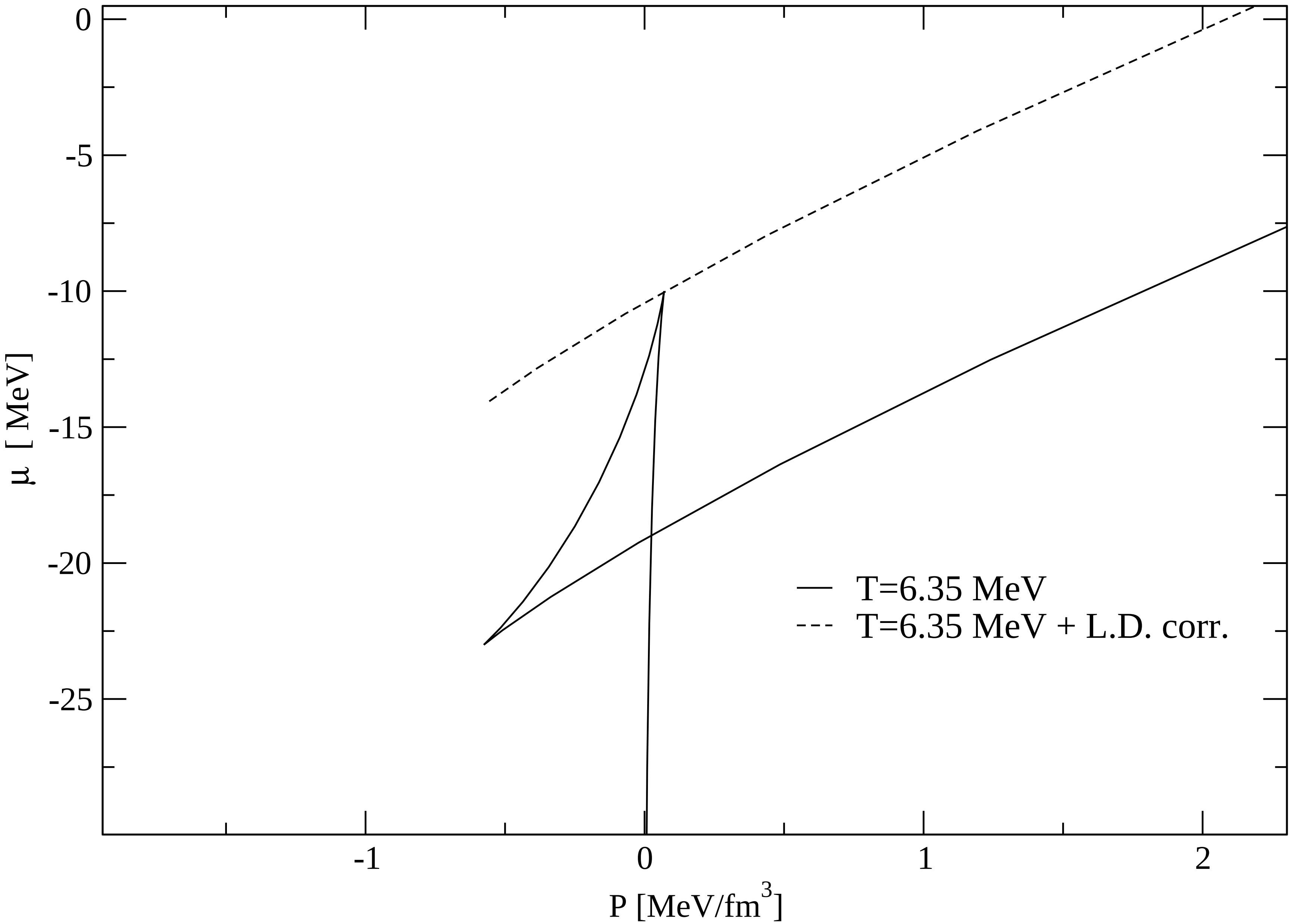

0
-5
-10
-15
-20
-25
μ [MeV]
-1
0
1
2
P [MeV/fm^3]
T=6.35 MeV
T=6.35 MeV + L.D. corr.